

Synthesis and Evaluation of CO₂ Thickeners Designed with Molecular Modeling

Semi-Annual Report

Start Date: Sept. 1, 2005

End Date: Feb. 28, 2006

Dr. Robert M. Enick
Dr. Eric J. Beckman
Chemical and Petroleum Engineering
University of Pittsburgh

Dr. Andrew Hamilton
Chemistry
Yale University

Date Issued: May 1 2006

DE-FG26-04NT-15533

Dr. Robert M. Enick and Dr. Eric J. Beckman
Department of Chemical and Petroleum Engineering
University of Pittsburgh
1249 Benedum Engineering Hall
Pittsburgh, PA 15261

Dr. Andrew Hamilton
Chemistry Department
Yale University
2250 Prospect Ave.
PO Box 208107
New Haven, CT
06520-8107

Disclaimer

This report was prepared as an account of work sponsored by an agency of the United States Government. Neither the United States Government nor any agency therefore, nor any of their employees, makes any warranty, express or implied, or assumes any legal liability or responsibility for the accuracy, completeness, or usefulness of any information, apparatus, product or process disclosed, or represents that its use would not infringe privately owned rights. Reference herein to any specific commercial product, process or service by trade name, trademark, manufacturer, or otherwise does not necessarily constitute or imply its endorsement, recommendation, or favoring by the United States Government or any agency thereof. The views and opinions of authors expressed herein do not necessarily state or reflect those of the United States Government or any agency thereof.

Abstract

The objective of this research is to use molecular modeling techniques, coupled with our prior experimental results, to design, synthesize and evaluate inexpensive, non-fluorous carbon dioxide thickening agents. The first type of thickener to be considered is *associating polymers*. Typically, these thickeners are copolymers that contain a highly CO₂-philic monomer, and a small concentration of a CO₂-phobic associating monomer. Yale University will be solely responsible for the synthesis of a second type of thickener; *small, hydrogen bonding compounds*. These molecules have a core that contains one or more hydrogen-bonding groups, such as urea or amide groups. Non-fluorous, CO₂-philic functional groups will be attached to the hydrogen bonding core of the compound to impart CO₂ stability and macromolecular stability to the linear “stack” of these compounds. The third type of compound under investigation is *CO₂-soluble surfactants*. These surfactants contain conventional ionic head groups and composed of CO₂-philic oligomers (short polymers) or small compounds (sugar acetates) previously identified by our research team. Mobility reduction could occur as these surfactant solutions contacted reservoir brine during CO₂ injection, or via the self-assembly of surfactants into viscosity-enhancing cylindrical micelles.

This report thoroughly documents the synthesis and characterization of the first series of non-fluorous, ionic, highly CO₂-soluble surfactants that has been reported. Specific tails include oligo(vinyl acetate), sugar acetates, and oligo(propylene oxide). The surfactants with vinyl acetate tails were particularly promising. The report also includes preliminary foam stability test results conducted in a high pressure view cell. Several of the surfactants, most notably those with oligomeric vinyl acetate tails, yielded the most stable foams. Our subsequent work will investigate the ability of these surfactant solutions to generate stable foams in a brine-saturated sandstone core with our colleague Reid Grigg at New Mexico Tech PRRC.

Table of Contents

Executive Summary	v
Preface	vi
Oxygenated Hydrocarbon-Based and Hydrocarbon-Based CO ₂ Soluble Surfactants	1
Conclusions and Research Significance	167
Plans for the Next Reporting Period	169
Milestones, Decision Points	170
Significant Accomplishments	172
Technology Transfer	173

Executive Summary

The objectives of this work are to design, synthesize, and evaluate hydrocarbon-based or oxygenated hydrocarbon-based CO₂ soluble surfactants. These surfactants would be able to form stable water-in-CO₂ microemulsions with polar microenvironments capable of dissolving polar species in the bulk non-polar CO₂ solvent, or to form metal precursors which can be reduced to nanoparticles in the presence of stabilizing ligands, or to generate foams in-situ for enhanced oil recovery application.

Several oxygenated hydrocarbons, including acetylated sugars, poly(propylene glycol), oligo(vinyl acetate), and highly branched methylated hydrocarbons were used generate CO₂-soluble ionic surfactants. Surfactants with vinyl acetate tails yielded the most promising results, exhibiting levels of CO₂ solubility comparable to those associated with fluorinated ionic surfactants. For example, a sodium sulfate with single, oligomeric vinyl acetate (VAc) tails consisting of 10 VAc repeat units was 7 wt% soluble in CO₂ at 25 °C and 48 MPa. Upon introduction of water to these systems, only surfactants with the oligomeric vinyl acetate tails exhibited spectroscopic evidence of a polar environment that was capable of solubilizing the methyl orange into CO₂-rich phase.

Silver bis(3,5,5-trimethyl-1-hexyl) sulfosuccinate, Ag-AOT-TMH, was synthesized from hydrocarbon-based ionic surfactant of sodium bis(3,5,5-trimethyl-1-hexyl) sulfosuccinate, Na-AOT-TMH through ion exchange. Ag-AOT-TMH exhibits 1.2 wt% solubility in dense CO₂ at 40 °C and 52 MPa. Silver nanoparticles were produced by reducing the supercritical CO₂ solution containing 0.06 wt% Ag-AOT-TMH and 0.5 wt% perfluorooctanethiol (stabilizing ligand) using a reducing agent of NaBH₄. Iso-stearic acid, a short, stubby compound with branched, methylated tails, as a hydrocarbon-based nonionic surfactant, has been shown to have high

solubility in carbon dioxide. The solvation of the tails by carbon dioxide has made isostearic acid sterically stabilize metallic nanoparticles as a ligand.

The stability of CO₂-water emulsion formed by ionic and nonionic surfactants was studied in CO₂ at 22 °C and 34.5 MPa for 0.01-1.0 wt% surfactant mixed with equivalent volumes of CO₂ and water. Emulsion stability was monitored by observing the rate of collapse of the white, opaque middle-phase emulsion between the transparent CO₂ and water phases and the steady-state volume of the emulsion. It was found that at surfactant concentration of 0.01 wt%, oligo(vinyl acetate)₁₀ sodium sulfate displayed the best emulsion, taking over 450 minutes to collapse.

TABLE OF CONTENTS

PREFACE	xvii
1.0 INTRODUCTION	1
2.0 BACKGROUND	3
2.1 Properties of Supercritical/Liquid CO ₂	3
2.2 Surfactants	6
2.3 CO ₂ -Soluble Surfactants	8
2.4 Fluorinated and Silicone-Based CO ₂ Soluble Surfactants	10
2.5 Oxygenated Hydrocarbon and Hydrocarbon-based CO ₂ Soluble Surfactants.....	14
2.5.1 Design of Oxygenated Hydrocarbon and Hydrocarbon-based CO ₂ Soluble Surfactants.....	14
2.5.2 Oxygenated Hydrocarbon and Hydrocarbon-based CO ₂ -philic Functionalities.....	16
2.6 Micelles and Microemulsions	20
2.7 Applications of Surfactants in Carbon Dioxide	23
2.7.1 Nanoparticle Formation.....	24
2.7.2 CO ₂ in Enhanced Oil Recovery.....	26
3.0 RESEARCH OBJECTIVES AND OUR APPROACH	35
3.1 Research Objectives.....	35
3.1.1 CO ₂ Soluble Surfactants for Nanoparticle Synthesis and Stabilization	35
3.1.2 CO ₂ Soluble Surfactants for Generating in-Situ EOR Foams.....	36
3.2 Our Approach.....	37

4.0 OXYGENATED HYDROCARBON-BASED IONIC SURFACTANTS	38
4.1 Ionic Surfactants with Peracetyl Gluconic Tails	38
4.1.1 Materials	38
4.1.2 Characterizations	38
4.1.3 Synthesis	39
4.1.4 Phase Behavior of Peracetyl Gluconic-Based Ionic Surfactants.....	43
4.1.4.1 Experimental Apparatus.....	43
4.1.4.2 Phase Behavior Results	47
4.1.5 Dye Solubilization and Spectroscopic Measurements	51
4.1.5.1 Experimental Apparatus	52
4.1.5.2 Spectroscopic Results.....	53
4.2 Ionic Surfactants with PPG Tails.....	54
4.2.1 Materials.....	54
4.2.2 Synthesis.....	54
4.2.3 Phase Behavior Results.....	60
4.2.4 Spectroscopic Results	61
4.3 Ionic Surfactants with Oligo(vinyl acetate) Tails	62
4.3.1 Materials	62
4.3.2 Synthesis	62
4.3.3 Phase Behavior Results	67
4.3.4 Spectroscopic Results	70
4.4 Discussions	73

4.4.1 Modeling Results	73
4.4.2 Water Solubility Values of Three Acetate Functionalized Surfactants	74
4.4.3 Effects of the Addition of Water in Surfactants/CO ₂ Systems	75
4.4.4 Formation of the Reverse Micelles	76
5.0 PREPARATION OF SILVER NANOPARTICLES VIA CO₂-SOLUBLE HYDROCARBON-BASED METAL PRECURSOR	77
.....	
5.1 Materials.....	77
5.2 Synthesis of a CO ₂ -Soluble Hydrocarbon-based Silver Precursor	78
5.3 Phase Behavior Study	81
5.3.1 Experimental Apparatus.....	81
5.3.2 Phase Behavior Results	81
5.4 Silver Nanoparticle Formation	82
5.4.1 Experimental Apparatus.....	82
5.4.2 Nanoparticle Formation Results	83
5.5 Non-Fluorous Thiols Results	86
5.6 Conclusions	88
6.0 STABLE DISPERSION OF SILVER NANOPARTICLES IN CARBON DIOXIDE WITH HYDROCARBON-BASED LIGANDS	89
6.1 Stable Dispersion of Nanoparticles in Carbon Dioxide with Ligands.....	89
6.2 Experimental Apparatus	91
6.3 Phase Behavior Results	91
7.0 STABILITY OF CO₂-WATER EMULSIONS STABILIZED WITH CO₂-SOLUBLE SURFACTANTS	93

7.1 Introduction	93
7.2 Experiments	98
7.3 Results and Discussions	100
7.4 Conclusions	105
8.0 NONIONIC SURFACTANTS	106
8.1 Effect of Alkyl Chain Length	106
8.2 Effect of Ethylene Oxide and Propylene Oxide	107
9.0 CONCLUSIONS	109
10.0 FUTURE WORK	111
APPENDIX A. SPECTRA OF SURFACTANTS IN CHAPTER 4	112
APPENDIX B. SPECTRA OF SURFACTANTS IN CHAPTER 5	137
BIBLIOGRAPHY	142

LIST OF TABLES

Table 2.1	Comparison of density, viscosity, and diffusivity of gases, supercritical fluids, and liquids	4
Table 4.1	W and W ^{corr} for the PGESS surfactant in water and CO ₂ mixture at different weight percents and temperature	49
Table 4.2	Experimental Data for PVAc-OH Oligomers from ¹ H NMR at [AIBN]/[VAc]=0.1%.....	66
Table 4.3	W and W ^{corr} for sodium bis(vinyl acetate)8 sulfosuccinate in water and CO ₂ mixture at different weight percents and 22 °C	70
Table 4.4	Interaction energies for several different dimers related to the CO ₂ /H ₂ O surfactant systems	74
Table 4.5	Water solubility values of three acetate functionalized surfactants	75
Table B.1	Soil analysis results of Ag-AOT-TMH.....	141

LIST OF FIGURES

Figure 2.1	Pressure-temperature diagram for pure CO ₂ , showing the solid, liquid, gas, and supercritical regions	4
Figure 2.2	Example of a basic surfactant structure Viscosity of CO ₂ as Function of Temperature and Pressure.....	7
Figure 2.3	Structure of AOT (Aerosol-OT, sodium bis(2-ethyl-1-hexyl) sulfosuccinate)...	8
Figure 2.4	Example of a CO ₂ -soluble surfactant structure	9
Figure 2.5	Structures of fluorinated and silicones CO ₂ -philic functionalities.....	11
Figure 2.6	Oxygenated hydrocarbon-based and hydrocarbon-based CO ₂ -philic groups	16
Figure 2.7	Two point interaction between CO ₂ and acetate	17
Figure 2.8	Cloud point pressure at ~ 5 wt% polymer concentration and 25 °C for binary mixture of CO ₂ with poly(methyl acrylate) (PMA), poly(lactide) (PLA), poly(vinyl acetate) (PVAc), poly(dimethyl siloxane) (PDMS), and poly(fluoroalkyl acrylate) (PFA) as a function of number of repeat units based on Mw.....	19
Figure 2.9	Representation of a micelle and a reverse micelle	21
Figure 2.10	Working temperature and pressure for CO ₂ flooding as a function of oil average molecular weight	29
Figure 2.11	Viscosity of CO ₂ as function of temperature and pressure	31
Figure 2.12	CO ₂ flooding in EOR: (a) CO ₂ “fingering” (b) ideal case	32
Figure 4.1	Structures of peracetyl gluconic-based ionic surfactants.....	39
Figure 4.2	Reaction scheme for preparation of peracetyl gluconic ethyl sodium sulfate	40
Figure 4.3	Schematic apparatus for solubility/phase behavior measurements	43
Figure 4.4	Variable volume view D. B. Robinson cell with magnetic mixer	44

Figure 4.5	Phase diagram for surfactant/CO ₂ system (P-x diagram).....	46
Figure 4.6	Phase diagram for liquid surfactant/CO ₂ system (P-x diagram)	46
Figure 4.7	Phase behavior of peracetyl gluconic-CH ₂ CH ₂ -OSO ₃ Na/CO ₂ mixtures. Insoluble at W = 0; 25 °C, W =10 (◆); 40 °C, W=10 (o).....	48
Figure 4.8	Phase behavior of peracetyl gluconic-COONa/CO ₂ mixtures at 40 °C. W=0 (o); W=10 (●).....	50
Figure 4.9	Phase behavior of peracetyl gluconic-COONH ₄ /CO ₂ mixtures at 40 °C. W =0 (o); W =10 (●).....	51
Figure 4.10	Structures of peracetyl gluconic-based ionic surfactants	55
Figure 4.11	Reaction scheme for the synthesis of PPGMBE (Mn=340) sodium sulfate	56
Figure 4.12	Reaction scheme for the synthesis of sodium bis(PPGMBE 340) sulfosuccinate	57
Figure 4.13	Phase behavior of PPGMBE surfactants/CO ₂ mixtures at 40 °C	61
Figure 4.14	Structures of oligo(vinyl acetate)-based ionic surfactants	63
Figure 4.15	Reaction scheme for the synthesis of oligo(vinyl acetate) sodium sulfate.....	64
Figure 4.16	Phase behavior of PVAc-OSO ₃ Na/CO ₂ mixtures.....	68
Figure 4.17	Phase behavior of sodium bis(vinyl acetate) ₈ sulfosuccinate/CO ₂ mixtures at 25 °C. W = 0 (Δ); W = 10 (◆); W = 50 (●).....	69
Figure 4.18	UV-vis absorption spectra of methyl orange in 0.15 wt% twin tailed sodium bis(vinyl acetate) ₈ sulfosuccinate based water-in-CO ₂ reverse microemulsions with different loading of water at 34.5 MPa and 25 °C.....	72
Figure 4.19	Two different binding modes for the isopropyl acetate/H ₂ O system. (white = H, gray = C, red = O).....	73
Figure 5.1	Structures of sodium bis(3,5,5-trimethyl-1-hexyl) sulfosuccinate (AOT-TMH) and silver precursor, silver bis(3,5,5-trimethyl-1-hexyl) sulfosuccinate (Ag- AOT-TMH).....	78
Figure 5.2	Synthesis of Ag-AOT-TMH (a) anhydrous THF, RT, 24 h; (b) NaHSO ₃ , ⁱ PrOH-H ₂ O, 80 °C, 24 h; (c) AgNO ₃ , ethanol-H ₂ O, RT.....	79

Figure 5.3	Phase behavior of AOT-TMH and Ag-AOT-TMH at 40 °C.....	82
Figure 5.4	TEM Image of silver nanoparticles formed by reducing CO ₂ solution containing Ag-AOT-TMH and fluorinated thiol stabilizing ligands using NaBH ₄ as reducing agent.....	84
Figure 5.5	Size distribution of silver nanoparticles synthesized in CO ₂ . P = 28.6 MPa, t = 40 °C, [Ag-AOT-TMH] = 0.06 wt%, [Fluorinated Thiol] = 0.5 wt%.....	85
Figure 5.6	EDS measurement of the silver nanoparticles.....	85
Figure 5.7	Structures of silicone-based and PEG-based thiols investigated in this study....	86
Figure 5.8	Phase behavior of 4-tert-butylbenzenethiol at 22 °C.....	87
Figure 5.9	Phase behavior of tert-nonyl mercaptan at 22 °C.....	87
Figure 6.1	Structure of iso-stearic acid, Mn = 284 g/mol.....	91
Figure 6.2	Phase behavior of iso-stearic acid/CO ₂ mixture at 22 °C.....	92
Figure 7.1	Structures of ionic surfactants with oxygenated hydrocarbon CO ₂ -philic tails...	97
Figure 7.2	Structures of nonionic surfactants.....	98
Figure 7.3	Foam stability of peracetyl gluconic-based ionic surfactants at concentration of 0.01 wt% in CO ₂ , 22 °C and 34.5 MPa.....	101
Figure 7.4	Foam stability of PPGMBE-based ionic surfactants at concentration of 0.01 wt% in CO ₂ , 22 °C and 34.5 MPa	102
Figure 7.5	Foam stability of oligo(vinyl acetate)-based ionic surfactants at concentration of 0.01 wt% in CO ₂ , 22 °C and 34.5 MPa	103
Figure 7.6	Foam stability of OVAc10-OSO ₃ Na and Chaser CD 1045 at concentration of 0.01 wt% in CO ₂ , 22 °C and 34.5 MPa	104
Figure 7.7	Foam stability of iso-stearic acid and PPG-PEG-PPG nonionic surfactants at concentration of 0.01 wt% in CO ₂ , 22 °C and 34.5 MPa	105
Figure 8.1	Structures of PBE-14 and PSE-15.....	106
Figure 8.2	Phase behavior of PBE-14, PSE-15/CO ₂ mixtures at 22 °C.....	107

Figure 8.3	Structures of Vanwet9N9, LS-54, TD-23 and TD-29.....	108
Figure 8.4	Phase behavior of Vanwet9N9, LS-54, TD-23 and TD-29/CO ₂ mixtures at 22 °C.....	108
Figure A.1	Mass spectrum of peracetyl gluconic ethyl sodium sulfate.....	112
Figure A.2	Mass spectrum of peracetyl gluconic sodium carboxylate.....	113
Figure A.3	Mass spectrum of peracetyl gluconic ammonium carboxylate.....	114
Figure A.4	Phase behavior of peracetyl gluconic-CH ₂ CH ₂ -OSO ₃ Na/CO ₂ mixtures. Insoluble at W = 0; 25 °C, W =10 (●); 40 °C, W=10 (▲). (Surfactant concentration in mM)	115
Figure A.5	Phase behavior of peracetyl gluconic-COONa/CO ₂ mixtures at 40 °C. W=0 (o); W=10 (●). (Surfactant concentration in mM)	115
Figure A.6	Phase behavior of peracetyl gluconic-COONH ₄ /CO ₂ mixtures at 40 °C. W =0 (o); W =10 (●). Surfactant concentration in mM. (Surfactant concentration in mM).....	116
Figure A.7	Mass spectrum of PPGMBE 340 sodium sulfate.....	117
Figure A.8	FTIR spectrum of PPGMBE 340.....	118
Figure A.9	FTIR spectrum of PPGMBE 340 diester.....	119
Figure A.10	Mass spectra of sodium bis(PPGMBE 340) sulfosuccinate.....	120
Figure A.11	Phase behavior of PPGMBE surfactants/CO ₂ mixtures at 40 °C. (Surfactant concentration in mM)	121
Figure A.12	FTIR spectrum of OVAc6-OH.....	122
Figure A.13	¹ H-NMR spectrum of OVAc6-OH.....	123
Figure A.14	FTIR spectrum of OVAc8-OH.....	124
Figure A.15	¹ H-NMR spectrum of OVAc8-OH.....	125
Figure A.16	FTIR spectrum of OVAc10-OH.....	126

Figure A.17	¹ H-NMR spectrum of OVAc10-OH.....	127
Figure A.18	FTIR spectrum of OVAc17-OH.....	128
Figure A.19	¹ H-NMR spectrum of OVAc17-OH.....	129
Figure A.20	¹ H-NMR spectrum of OVAc6-OSO ₃ Na.....	130
Figure A.21	¹ H-NMR spectrum of OVAc10-OSO ₃ Na.....	131
Figure A.22	¹ H-NMR spectrum of OVAc17-OSO ₃ Na.....	132
Figure A.23	FTIR spectrum of OVAc8 diester.....	133
Figure A.24	¹ H-NMR spectrum of OVAc8 diester.....	134
Figure A.25	Phase behavior of PVAc-OSO ₃ Na/CO ₂ mixtures. (Surfactant concentration in mM)	135
Figure A.26.	Phase behavior of sodium bis(vinyl acetate) ₈ sulfosuccinate/CO ₂ mixtures at 25 °C	136
Figure B.1	FTIR spectrum of diester of AOT-TMH.....	137
Figure B.2	¹ H-NMR spectrum of diester of AOT-TMH.....	138
Figure B.3	¹ H-NMR spectrum for AOT-TMH.....	139
Figure B.4	Phase behavior of AOT-TMH and Ag-AOT-TMH at 40 °C. (Surfactant concentration in mM).....	140

PREFACE

I want to express my gratitude to Dr. Enick, my Ph.D. advisor, for his enlightening guidance, resourceful suggestions and endless encouragement throughout my studies at the University of Pittsburgh. I would also like to thank my committee members: Dr. Beckman, Dr. Johnson, and Dr. Fulay for serving as my doctoral committee and for their helpful comments and suggestions. Thanks our collaborators of Dr. Vijay Potluri and Dr. Andrew Hamilton at Yale University for their assistance of the synthesis of acetylated sugar-based surfactants and Dr. Chandler McLeod, Dr. Junchen Liu, Dr. Philip Bell and Dr. Christopher Roberts at Auburn University for carrying out the UV-vis analysis, silver nanoparticle synthesis and stabilization in CO₂. I would like to thank the financial support for this project from the US Department of Energy.

I am very grateful to the faculty, staff and friends in the chemical engineering department. Special thanks to all my friends for their moral support and the fun times we shared together. Especially, I want to thank Lei Hong, Jianying Zhang, Xiaoqiang Shen, Yang Wang, and Deepak Tapriyal for their discussion and assistance. I also want to thank two undergraduates of Wenling Yu and Kerry Leonard for their help of phase behavior study and foam stability study.

Finally, I would like to dedicate this work to my parents and my family. I would like to express my deep gratitude to my husband, Deliang Shi, for his constant support, encouragement, understanding and love, and to my parents for their unlimited love, and continuous support from overseas.

1.0 INTRODUCTION

Supercritical carbon dioxide (sc-CO₂) is a potential alternative to organic solvents in many chemical processes because of its abundance, low cost, non-toxicity, non-flammability and easily accessible critical conditions ($P_c = 7.38$ MPa, $T_c = 31.1$ °C). Unfortunately, sc-CO₂ is a feeble solvent. Although it can solubilize low-molecular weight, volatile compounds at pressures below 10 MPa, polar and high-molecular weight materials are usually poorly soluble at tractable pressures. One strategy for enhancing the capabilities of CO₂ as a green solvent has been the identification of additives, such as surfactants,[1, 2] dispersants,[3, 4] chelating agents,[5, 6] thickeners[7] and polymers,[4, 8] that are designed to exhibit favorable thermodynamic interactions with CO₂. With regards to surfactants, nearly all conventional hydrocarbon-based ionic surfactants are essentially insoluble in sc-CO₂; however, because ionic head groups are CO₂-phobic and hydrocarbon surfactant tails are not designed for favorable interactions with dense CO₂. [9]

A number of groups began a search for CO₂-philic materials that would be soluble in CO₂ at moderate pressures. Beckman and Desimone's groups have shown experimentally that fluoralkyls,[10] fluorethers,[11] fluoracrylates,[12] and silicones [13, 14] are miscible with CO₂ at moderate pressures, while conventional alkyl functional polymers and oligomers are nearly insoluble. Ionic surfactants with CO₂-solubility of 1

wt% or more have been developed by incorporating highly CO₂-philic fluorinated tails or silicone-based tails. For example, perfluoropolyether (PFPE) sodium and ammonium carboxylates with average molecular weights of 2500, 5000, and 7500 were soluble in supercritical CO₂ at 40 °C and pressures below 17 MPa.[11] Fluoroalkyl-tailed sulfosuccinate surfactants, such as di-CF₃, di-CF₄, and di-CF₆ stabilized microemulsions at CO₂ bottle pressure (5.7 MPa) at 15 °C, with a W value ([water]/[surfactant]) of 10.[15] Silicone-based ionic surfactants, such as PDMS-based AOT analogue can dissolve in CO₂ at 65 °C and pressures below 31 MPa.[16, 17] Although these surfactants have been used successfully in supercritical fluid research such as emulsion polymerization, dispersion polymerization, and extraction, the environmental and biological persistence of these expensive fluororous and silicone-based surfactants (approaching \$1/gram) has impeded their use in commercial applications, especially for large-scale applications in which the surfactant will be lost to the environment, such as enhanced oil recovery (EOR). Less expensive, biodegradable, CO₂-soluble surfactants composed of carbon, hydrogen, and oxygen would hasten the practical applications of CO₂ as a processing solvent.

2.0 BACKGROUND

2.1 PROPERTIES OF SUPERCRITICAL/LIQUID CO₂

A supercritical fluid (SCF) is a substance elevated above its critical temperature (T_c) and pressure (P_c). The critical temperature is defined as the temperature above which a pure, gaseous compound cannot be liquefied regardless of the pressure applied. The critical pressure is then defined as the vapor pressure of the gas at the critical temperature. The temperature and pressure at which the gas and liquid phases become identical is the critical point. In the supercritical region, only one phase exists; the supercritical fluid, as it is termed, is neither a gas nor a liquid and is best described as intermediate to the two extremes. A comparison of typical values for density, viscosity, and diffusivity of gases, supercritical fluids, and liquids is presented in Table 2.1.[18] Supercritical fluids have a density close to liquids, a viscosity close to gases, and a high diffusivity, which retain the solvent power common to liquids as well as the transport properties common to gases.

As carbon dioxide is the most commonly used SCF, the pressure-temperature phase diagram for carbon dioxide is presented in Figure 2.1 to illustrate the differences between the gas, liquid, and supercritical states. The critical point is marked at the end of the gas-liquid equilibrium curve, and the supercritical fluid region is indicated by the shaded area. CO₂ attains its supercritical state at near-ambient temperature ($T_c=31\text{ }^\circ\text{C}$)

and relatively moderate pressure ($P_c=7.4$ MPa). Supercritical CO_2 (sc- CO_2), like all other supercritical fluids, offers many mass transfer advantages over conventional organic solvents due to its gas-like diffusivity, low viscosity, and negligible surface tension.

Table 2.1. Comparison of density, viscosity, and diffusivity of gases, supercritical fluids, and liquids.[18]

Property	Gas	Supercritical Fluid	Liquid
Density (g/ml)	0.001	0.1 – 1	1
Viscosity (cp)	0.01	0.05-0.1	0.5-1
Diffusivity (mm^2/s)	1-10	0.01-0.1	0.001

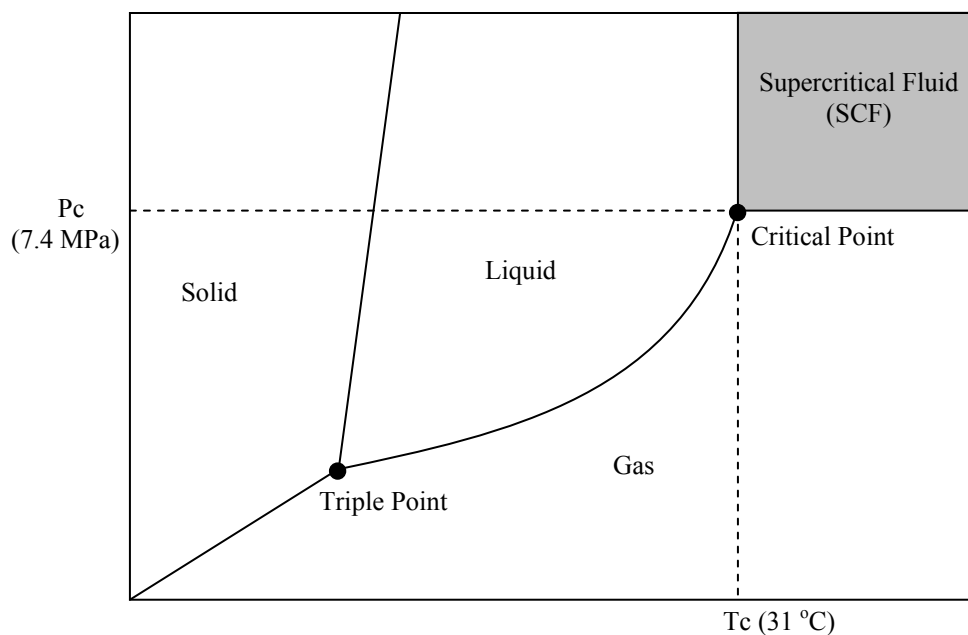


Figure 2.1. Pressure-temperature diagram for pure CO_2 , showing the solid, liquid, gas, and supercritical regions.

Supercritical CO₂ has many properties that make it an interesting solvent; it is abundant, inexpensive, nontoxic, and nonflammable. It has been proposed as a green alternative to traditional organic solvents because it is not regulated as a volatile organic chemical (VOC). Moreover, supercritical fluids have a tunable solvent power, which increases as a function of increasing density.[19] As a result, the solvent power of supercritical CO₂ can be easily tuned simply by adjusting the operating temperature and/or pressure, which in turn affects the density of the supercritical CO₂. In addition to the tunable solvent power, a number of other physical properties such as dielectric constant, viscosity, and diffusivity change significantly near the critical point.[20, 21] One interesting characteristic of supercritical fluids is the extremely low surface tension possessed as a result of the gas-like transport properties of viscosity and diffusivity.[22] This imparts supercritical fluids the ability to easily penetrate very small surface areas and contributes to their attractiveness for extraction of solutes from porous media.[21] A particularly attractive advantage of using supercritical CO₂ is that the solvent can be removed by simply decompression. It is worth noting that liquid CO₂ can sometimes be used in the place of sc-CO₂ in certain procedures. Near the critical point, liquid CO₂ has many of the similar properties of the supercritical fluid and can be achieved at milder conditions. Overall, CO₂ has a great potential to be a valuable process solvent.

There is one major drawback to supercritical/liquid CO₂ as a solvent. CO₂ has an extremely low polarizability/volume ratio (a parameter to estimate solvent power) and hence is a somewhat feeble solvent for many polar and nonpolar compounds, although it can dissolve many small molecules.[23] It was once believed that CO₂ had solvent properties similar to those of hexane based on solubility parameters calculations, but in

fact, Mcfann et al. have shown that the quadrupole moment of CO₂ serves to inflate the calculated solubility parameter by 20%.[24, 25] Consequently, using the solubility parameter as a sole determination of solubility could be misleading. The polarizability/volume has been suggested as a better parameter on which to estimate the solvent power of CO₂, but the polarizability/volume of CO₂ indicates that it is a weak solvent.[25] Other properties of CO₂ include low polarizability and electron accepting capacity, since CO₂ is a Lewis acid and can participate in Lewis acid: Lewis base interactions. Fourier transform infrared (FTIR) spectroscopy has been used to show that CO₂ interacts with polymers containing electron-donating functional groups[26] and Lewis bases.[27] Specific interactions resulting from quadrupole-dipole interactions between CO₂ and certain polymers are also believed to influence solubility.[28, 29] O'Neill et al. suggest that cohesive energy density (CED), reflected by surface tension, of a polymer determines solubility in CO₂.[30]

2.2 SURFACTANTS

A surfactant (surface active agent) is an amphiphilic molecule containing both hydrophilic head group and lipophilic tail group. Typically, the hydrophilic head contains groups like water such as sulfonates, sulfates, and phosphonates while the lipophilic or hydrophobic tail group consists of a hydrocarbon chain. Figure 2.2 represents the structure of a common surfactant consists of a hydrophilic head group and a hydrophobic tail group.

The polar or ionic portion is solvated by water as a result of strong dipole-dipole or ion-dipole interactions. It is therefore said to be hydrophilic, and often simply called the head group. The hydrocarbon chain of the surfactant is typically called hydrophobic because of the hydrocarbon section's minimal interaction with the water in an aqueous environment. Furthermore, the strong attractions between water molecules, arising from dispersion forces and hydrogen bonding, act to force the hydrocarbon out of the water. Since the nonpolar, hydrophobic part is usually an elongated alkyl chain, it is often simply called the tail. The balanced properties of both the hydrophilic and hydrophobic portions of surfactants combine to give the unique properties commonly associated with surface active agents.

Surfactants can be classified according to the charge present in the hydrophilic portion of the molecule (after dissociation in aqueous solution): anionic, cationic, nonionic, and amphoteric surfactants. Typically, these four kinds of surfactants are composed of similar lipophilic or hydrophobic tail group, such as a long hydrocarbon chain, however with different hydrophilic head groups.

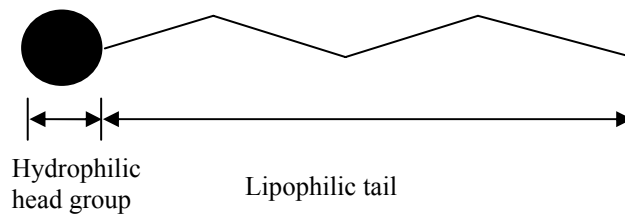


Figure 2.2 Example of a basic surfactant structure

AOT (Aerosol-OT, bis(2-ethyl-1-hexyl) sodium sulfosuccinate), as an anionic surfactant, has been extensively utilized and investigated in numerous alkane solvents for the formation of reverse micelles due to its ability to disperse large amount of water. The structure of AOT is shown in Figure 2.3. The rich phase behavior of AOT, and its ability to form microemulsions, is often attributed to its twin hydrocarbon tails which impart a cone-like structure and encourage the molecule to pack into spherical aggregations.

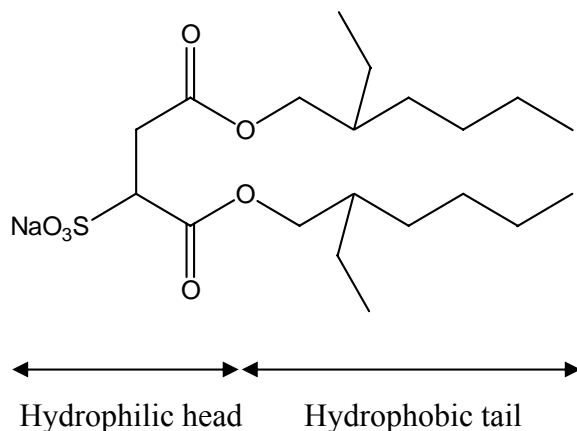


Figure 2.3. Structure of AOT (Aerosol-OT, sodium bis(2-ethyl-1-hexyl) sulfosuccinate)

2.3 CO₂-SOLUBLE SURFACTANTS

Sc-CO₂ is a feeble solvent, although it can solubilize low-molecular weight, volatile compounds at pressures below 10 MPa, polar and high molecular weight materials are usually poorly soluble at tractable pressures. One strategy to broaden the range of applications of CO₂ as a green solvent has been the identification of additives, such as

surfactants,[1, 2] dispersants,[3, 4] chelating agents,[5, 6] thickeners[7] and polymers,[4, 8] that are designed to exhibit favorable thermodynamic interactions with CO₂. With regards to surfactants, nearly all conventional hydrocarbon-based ionic surfactants are essentially insoluble and could not form microemulsions in sc-CO₂; however, because ionic head groups are CO₂-phobic and hydrocarbon surfactant tails are not designed for favorable interactions with dense CO₂. [9] A CO₂-soluble surfactant would be amphiphilic, like a traditional surfactant, but instead of hydrophilic and lipophilic segments, it would contain CO₂-philic and CO₂-phobic segments. Once the CO₂-philic portion of the surfactant has been identified, the CO₂-phobic segment can be chosen from conventional hydrophilic or lipophilic groups. The structure of a CO₂-soluble surfactant is presented in Figure 2.4.

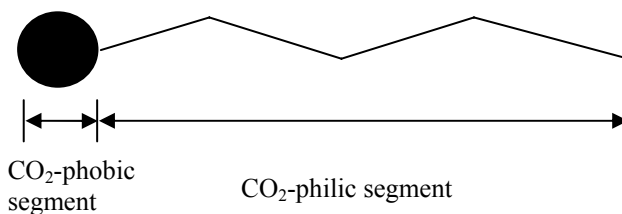


Figure 2.4. Example of a CO₂-soluble surfactant structure

Development of CO₂-philic surfactants has been a target of researchers for many years. Functional CO₂-soluble surfactants would allow the feeble solvent nature of CO₂ to be enhanced by the formation of a microemulsion with a polar water domain which can favorably dissolve polar solutes and high molecular weight molecules. The concept of a nm-scale water pool dispersed in CO₂ find applications in a variety of reaction chemistry and material synthesis.[31-34]

2.4 FLUORINATED AND SILICONE-BASED CO₂ SOLUBLE SURFACTANTS

Preliminary studies by Consani and Smith have shown that most conventional surfactants are insoluble in CO₂. They studied over 130 commercially available surfactants, among which only a few nonionic exhibited reasonable solubility in CO₂ [9]. Focus was then being given to fluorinated and silicone compounds as effective CO₂-philic agents. Followed the finding by Iezzi et al. that fluorocarbons and CO₂ are compatible,[35] Beckman and Desimone's groups have shown experimentally that fluoalkyls,[10] fluoethers,[11] fluoacrylates,[12] and silicones [13, 14] are miscible with CO₂ at moderate pressures, while conventional alkyl functional polymers and oligomers are nearly insoluble. The fluorinated and silicon chains represent low cohesive energy density groups thereby promoting low solubility and low polarizability, which are more characteristic of carbon dioxide's properties. The structures of fluorinated and silicone CO₂-philes are shown in Figure 2.5, and these molecules have been used in the design and synthesis of surfactants for applications in CO₂. Ionic surfactants with CO₂-solubility of 1 wt% or more have been developed by incorporating highly CO₂-philic fluorinated tails or silicone-based tails.

Fluoroalkyls: Fluorocarbon-Based Ionic surfactants

Based on the fact that the fluorocarbons and CO₂ are compatible, Hoefling et al. designed the first effective fluoro-surfactants for CO₂, the pioneering work demonstrating solubility of a fluorinated analogue to AOT in CO₂. [10] Harrison et al. reported the first water-in-CO₂ (w/c) microemulsion using a double chain hybrid surfactant comprising of separate fluororocarbon and hydrocarbon chains: (C₇F₁₅)(C₇H₁₅)CHOSO₃⁻Na⁺ or F7H7. Water up W of 32 could be stabilized in w/c microemulsion at 35 °C, 26.2 MPa, and surfactant concentration of 1.9 wt%. [36] In 1997, Eastoe et al. launched a study of fluoroalkyl analogues to AOT. Twelve different linear chain fluoroalkyl AOT analogues were investigated, of which nine stabilized w/c microemulsions at 15 °C and CO₂ bottle pressure (5.7 MPa), with a W value of 10; these were di-HCF₄, di-HCF₆, di-CF₃, di-CF₄, di-CF₆, di-CF₄H, di-CF₆H, di-CF₄GLU and the cobalt salt of Co-HCF₄. [37]

Fluoroethers: PFPE-Based Ionic Surfactants

In 1993, perfluoropolyether (PFPE) sodium and ammonium carboxylates with average molecular weights of 2500, 5000, and 7500, were reported to be soluble in liquid CO₂ up to 10 wt% at 40 °C and pressures below 17 MPa. [11] However, these high molecular weight polymers were not effective for stabilizing w/c microemulsions. Later, Johnston et al. formed w/c microemulsion with a PFPE ammonium carboxylate (PFPE-COO⁻NH₄⁺) surfactant of only 740 M_w. [38] Success with this class was attributed to the chemical structure itself. PFPE constitutes an extremely CO₂-philic tail group, accentuated by the presence of pendant fluoromethyl groups, which tend to increase the volume at the interface on the CO₂ side and thus favor curvature around water.

Fluoroacrylates: PFOA Block Copolymer Nonionic Surfactants

Fluorinated acrylate polymer, poly(1,1-dihydroperfluorooctylacrylate) or PFOA, was obtained from homopolymerization in sc-CO₂ at 60 °C and 20.7 MPa, with molecular weight of 270,000.[12] Small angle neutron and scattering (SANS) investigations of dilute solutions of PFOA in CO₂, over a wide range of temperatures and pressures, provided clear evidence for favorable interaction between PFOA and CO₂. [39] PFOA contains a lipophilic, acrylic backbone, and a CO₂-philic segment, rendering it amphiphilic, thus it can be used as a surfactant without modification. McClain et al used PFOA as the CO₂-philic segment of a nonionic surfactant, where PFOA was copolymerized with a CO₂-insoluble polystyrene (PS) segment to form a block copolymer of PFOA-b-PS. The micelles formed by PFOA-b-PS were used to solubilize CO₂-phobic hydrocarbon oligomers.[40] Copolymers composed of PFOA and poly(ethylene oxide) (PEO) were also able to form micelles in CO₂, in which small amount of water was able to be stabilized.[41]

Silicones: PDMS

For applications in CO₂, silicones are generally considered less effective than their fluorinated counterparts. Solubility of poly(dimethyl siloxane) (PDMS) in CO₂ was first reported in 1996. At a level of 4 wt%, PDMS (M_n~13,000) is soluble in CO₂ at 35 °C and 27.7 MPa.[30] Block copolymer surfactants consisting of CO₂-philic PDMS and CO₂-phobic poly(methacrylic acid) (PMA) or poly(acrylic acid) (PAA) were used to form water-in-CO₂ (w/c) and CO₂-in-water (c/w) emulsions.[17] Recently, Fink's research in

silicone-based ionic surfactants pointed that a PDMS-based AOT analogue can dissolve in CO₂ at 65 °C and pressure below 31 MPa up to 1 wt%.[16]

Although these surfactants have been used successfully in supercritical CO₂ research, the environmental and biological persistence of these expensive fluorinated and silicone-based surfactants (approaching \$1/gram) has impeded their use in commercial applications, especially for large-scale applications in which the surfactant will be lost to the environment, such as enhanced oil recovery (EOR). The development of CO₂-soluble surfactants, which are composed of carbon, hydrogen, and oxygen, biodegradable and less expensive, would hasten the applications of CO₂, as they could represent significant advantages over the biological persistent and high-cost fluorinated or silicone counterparts.

2.5 OXYGENATED HYDROCARBON AND HYDROCARBON-BASED CO₂ SOLUBLE SURFACTANTS

2.5.1 Design of Oxygenated Hydrocarbon and Hydrocarbon-Based CO₂ Soluble Surfactants

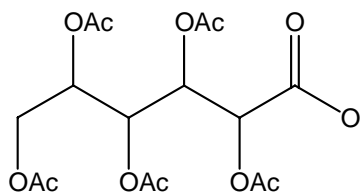
Experimental results from several research groups have shown that the incorporation of CO₂-philic functionalities into the structures of surfactants, dispersants, and chelating agents has greatly enhanced their solubility, making it possible to use CO₂ for polymerization [4, 8], metal extraction [5, 6] and other more sustainable processes. It must be noted that combining a CO₂-philic tail to a conventional head group does not

ensure the resultant surfactant will also exhibit CO₂-solubility, or that will be effective in the proposed application if it is solubility. CO₂ solubility is a necessary but insufficient property of the candidate surfactant. The interactions between the tail and CO₂ must be strong enough to impart CO₂-philicity to a compound that contains a CO₂-phobic segment.

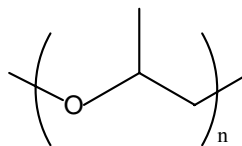
The characteristic of hydrocarbons most commonly associated with enhanced CO₂-solubility is the presence of polymer side chains [42] or a high degree of branching [43]. This enhanced solubility is usually attributed to the increased polymer free volume and the diminished intermolecular interactions [43]. Recently, Stone and Johnston found that the interaction between CO₂ and CH₂ is about the same as CO₂ and CF₂. [44] A level of 1 wt% surfactant soluble in CO₂, which would typically be needed for microemulsions, requires a moderate high, yet reasonable pressure. Clearly, solubility is a key factor that governs whether a surfactant will lead to water-in-CO₂ microemulsions. An additional factor, steric force, which plays an important role in designing hydrocarbon surfactants for w/c microemulsions, has been described recently. Stubby tails enhance the formation of w/c microemulsions as they raise surfactant solubility in CO₂ by weakening interactions between tails, weaken interactions between droplets, favor curvature of the interface bending toward water, and reduce the interfacial tension. [44-46] Ryoo and Johnston achieved about 1 wt% water, significant protein solubilities, and the presence of microemulsions as detected with dynamic light scattering formed by a methylated branched hydrocarbon nonionic surfactant. Furthermore, this study shows that the surfactant lowers the water-CO₂ interfacial tension significantly, which is an important requirement for forming microemulsions. [46]

2.5.2 Oxygenated Hydrocarbon and Hydrocarbon-Based CO₂-Philic Functionalities

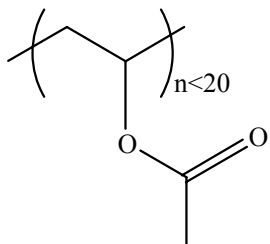
Several oxygenated hydrocarbon and hydrocarbon-based groups previously shown to exhibit CO₂-philicity include acetylated sugars, poly (propylene oxide), acetate-rich compounds, and short alkyl group with t-butyl tip. These CO₂-philes are illustrated in Figure 2.6.



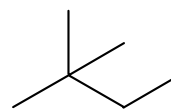
(a) per-acetylated glucose (Ac=COCH₃)



(b) Poly(propylene oxide)



(c) Oligo(vinyl acetate)



(d) Short alkyl group with tert-butyl tip

Figure 2.6. Oxygenated hydrocarbon-based and hydrocarbon-based CO₂-philic groups

Per-acetylated sugars

The replacement of the proton of every hydroxyl group (-OH) with an acetate group (-OCOCH₃) can dramatically enhance the CO₂-philicity of sugar molecules. Acetylated sugars, such as per-acetylated glucose and galactose,[47] sorbitol,[48] maltose[49] and cyclodextrins,[50] have been shown to dissolve in CO₂ at low pressures up to 10-50 wt%. The high degree of CO₂ solubility has been attributed to a favorable two-point interaction between CO₂ and the accessible acetate side chain, a Lewis acid–Lewis base interaction between the C of the CO₂ and the O of the acetate carbonyl, and a weak, complimentary hydrogen bond between the O of the CO₂ and a proton on the methyl group of the acetate,[51, 52] as shown in Figure 2.7.

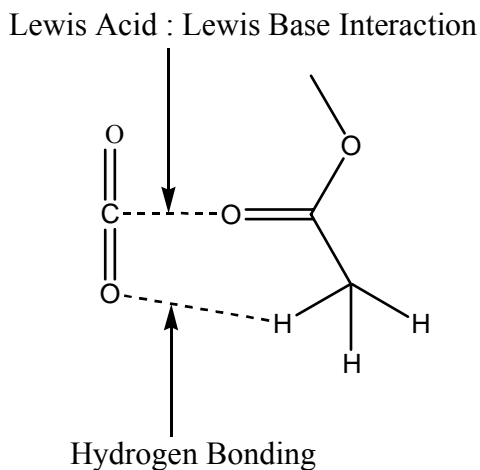


Figure 2.7. Two point interaction between CO₂ and acetate

Poly(propylene oxide) (PPO)

Low molecular weight PPO (M_n<2000) is quite CO₂-soluble at moderate temperature,[30] and higher MW PPO (>2000) is also soluble in CO₂ at elevated

temperatures.[53] The solubility of the PPO oligomers has been attributed to the Lewis acid–Lewis base interaction between the carbon in CO₂ and the ether oxygen in poly(propylene oxide),[54] and the lower surface tension caused by the pendent methyl group on each monomer unit favoring solvation by CO₂. [30] The lowering of the interfacial tension at the water-CO₂ interface, emulsion formation and solubilities of block copolymers containing PPO segment were reported.[30, 55] PPO has been used as a CO₂-philic segment in di-block and tri-block nonionic surfactants along with hydrophilic blocks of poly(ethylene oxide) (PEO).[56-59] For example, the tri-block nonionic surfactant, (PO)₁₅(EO)₁₀(PO)₁₅, composed of two CO₂-philic propylene oxide oligomers, and a single hydrophilic ethylene oxide oligomers, exhibit CO₂ solubility up to 0.6 wt% below 30 MPa at 25 °C.[59] Other CO₂ soluble nonionic triblock surfactants include those contain an alkyl group, an ethylene oxide block and a propylene oxide block, such as C₁₂H₂₅-(EO)₃(PO)₆-OH, which is 1 wt% soluble in CO₂ at 35–45 °C and pressures below 10-15 MPa.[57]

Poly(vinyl acetate)

McHugh and coworkers were the first to note that poly(vinyl acetate) demonstrated remarkable solubility in dense CO₂. [29] Recently, poly(vinyl acetate) has been identified as the most CO₂ soluble, high molecular weight, oxygenated hydrocarbon-based homopolymer composed of solely of carbon, hydrogen and oxygen; however, only short oligomers of PVAc, n<20 are likely to be soluble in CO₂ at pressure below moderate pressure (35 MPa), as shown in Figure 2.8.[53] The interactions between poly(vinyl acetate) and CO₂ are similar to those of per-acetylated sugars and CO₂.

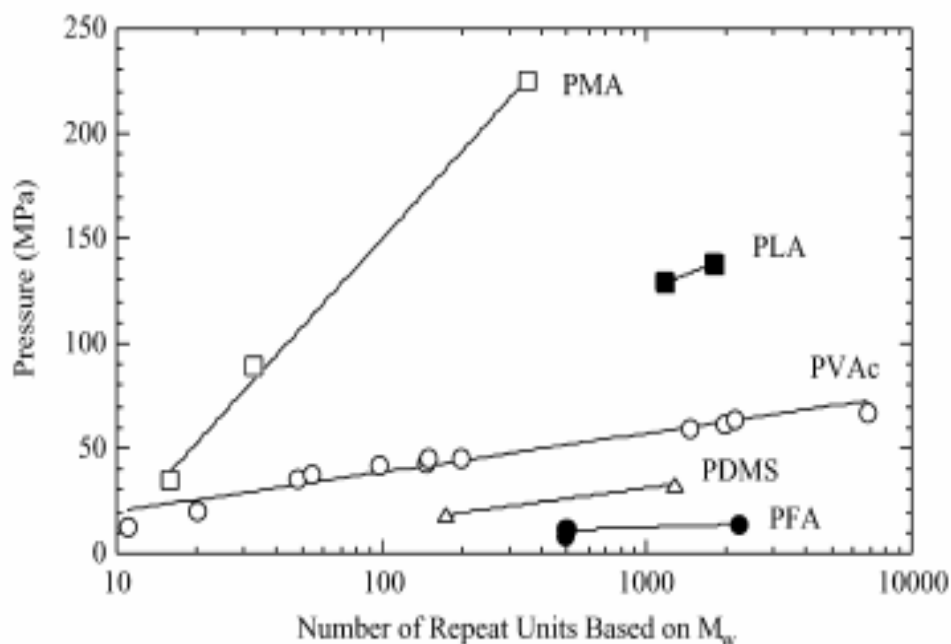


Figure 2.8. Cloud point pressure at ~ 5 wt% polymer concentration and 25 °C for binary mixture of CO₂ with poly(methyl acrylate) (PMA), poly(lactide) (PLA), poly(vinyl acetate) (PVAc), poly(dimethyl siloxane) (PDMS), and poly(fluoroalkyl acrylate) (PFA) as a function of number of repeat units based on M_w. [53]

Short Alkyl Chain with t-Butyl Tip

Recently, Eastoe and Johnston [60-62] described two branched hydrocarbon-based ionic surfactants, sodium bis(2,4,4-trimethyl-1-pentyl) sulfosuccinate and sodium bis(3,5,5-trimethyl-1-hexyl) sulfosuccinate, that exhibit CO₂ solubility. These twin tailed sodium succinates are similar in structure to the CO₂-insoluble surfactant AOT, sodium bis(2-ethyl-1-hexyl) sulfosuccinate, but they contain trimethyl pentyl or trimethyl hexyl tails and are referred to as AOT-TMP and AOT-TMH, respectively. This is illustrated as the “short alkyl chain with t-butyl tip” in Figure 2.6. AOT-TMH has been reported 0.1

wt% solubility in CO₂ at 40 °C, 50 °C, and 80 °C at 34.5 MPa, 31MPa, and 29 MPa, respectively.[62] Even though there are no specific sites for strong CO₂-alkyl interactions in this system, the favored solvation of the branched tail surfactants by CO₂ may be attributable to the surface energy of the pendant methyl groups being much lower than that of the CH₂ groups of linear tails.[30] Further, it was found the high degree of chain tip methylation do form water-in-carbon dioxide (w/c) reverse micelles [61].

2.6 MICELLES AND MICROEMULSIONS

Surfactants reduce interfacial tension and aid in the solubilization of hydrophobic compounds into hydrophilic solvents, or vice versa. A micelle or a microemulsion droplet is an aggregation of surfactant molecules, which can only form when the surfactant concentration is greater than the critical micellar concentration (CMC). Depending on the nature of the continuous phase, the micelles formed are termed oil-in-water (o/w, for a bulk water phase with dispersed organic phase) or water-in-oil (w/o, for a bulk organic phase with dispersed water phase). Water-in-CO₂ microemulsion (w/c) is formed for bulk CO₂ with dispersed water phase. The structure of typical oil-in-water (o/w) micelle is shown in Figure 2.9 a, in which the hydrophilic segment interacts with the aqueous phase and the lipophilic segment is oriented to interact with the organic phase. The opposite structure of water-in-oil (w/o), or water-in-CO₂ (w/c), called reverse micelle, is also formed whereby the lipophilic tail interacts with the continuous organic phase and the hydrophilic heads are directed to the core of the micelle, thus interacting with the aqueous phase, as shown in Figure 2.9 b. Micelles can exist in different shapes, including spherical, cylindrical, hexagonal, or lamellar.

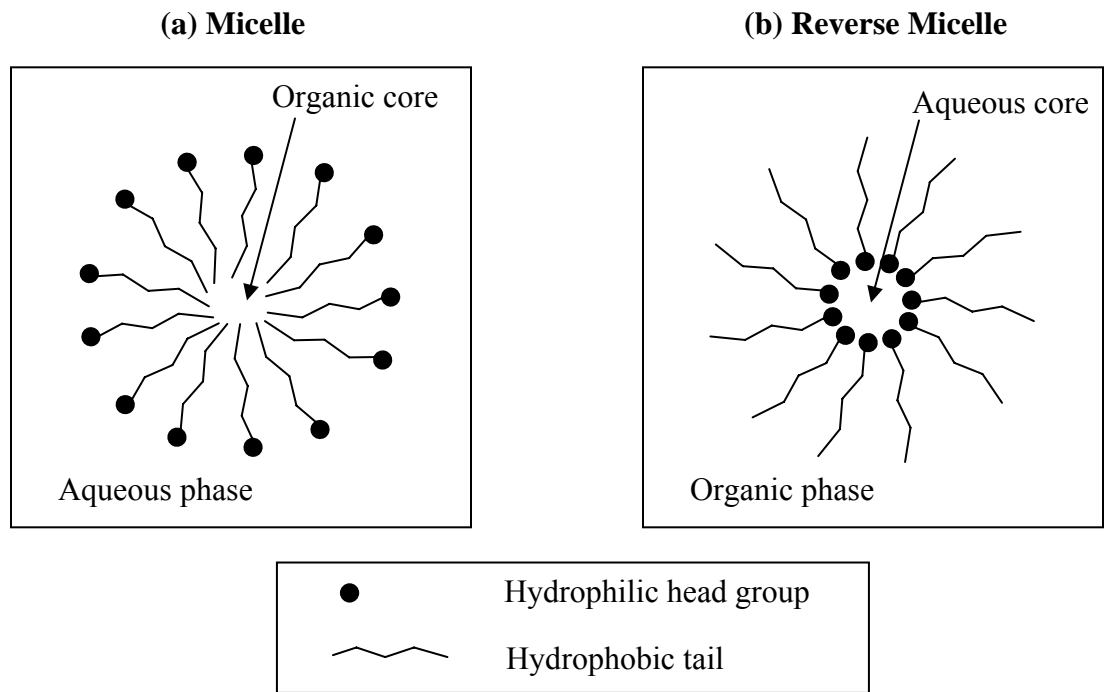


Figure 2.9. Representation of a micelle and a reverse micelle.

System containing micelles is referred to as emulsion, which is a dispersion of one liquid in another. Microemulsions are special kind of emulsions, which are thermodynamically stable and optically transparent, with the dispersed liquid droplets dimensions less than 100 nm. It has been long established that hydrophilic-hydrophobic balance plays a crucial role in the formation and stability of colloidal dispersions and self-assembly structures. An important efficiency factor for a surfactant to form water-in-CO₂ microemulsion is the water uptake W , defined as the molar ratio of water loading to the surfactant, which is highly dependent on the surfactant type and nature of the CO₂-philic chains, as well as CO₂ pressure and temperature. Another measure of efficiency is the minimum pressure that requires keeping the dispersion a stable single transparent

phase. Above this pressure the surfactant is able to stabilize w/c microemulsion, whereas below this pressure a phase separation occurs.

The formation of microemulsions in a scf continuous phase was first reported by Smith and co-workers using AOT in sub- and supercritical alkanes.[63] Since then, interest in surfactant/scf has grown steadily and produced a wide variety of research aimed at characterizing and applying these systems.[63-65] The most commonly used alkanes to form the scf continuous phase have been ethane and propane.[64] However, interest in using more environmentally benign solvents in chemical processes has pushed the forefront of surfactant/scf systems and formation of microemulsions to include CO₂ as the continuous phase.[61, 62, 66]

One interesting feature in the formation of water-in-CO₂ microemulsions is the creation of a nanosized water pool in a bulk CO₂ phase. The concept of a nano-scale water pool dispersed in CO₂ is particularly interesting in that there is tremendous potential for chemical applications. For example, the low viscosity (high diffusivity) of a scf makes scf-based microemulsions particularly attractive as separation media. Also, water pools formed in CO₂ find applications in a variety of reaction chemistry and material synthesis. The advantages of using sc-CO₂ to carry out these processes lies in one's ability to achieve more specific or selective control over separation and/or reactivity via the tunable solvent property. By changing the system pressure, one can selectively tune droplet-droplet interactions, thereby directly influencing the chemistry that takes place within the water domain.

Characterizations of Microemulsions

Various probing techniques such as FTIR, UV-vis, X-band electron parametric resonance (EPR), and time-resolved fluorescence depolarization have been used to characterize the nature of the PFPE/CO₂ reverse micelles. EPR identified the micelle as having a bulk-like water core able to solvate ionic species while time-resolved fluorescence depolarization revealed an anisotropic/nonspherical reverse micelle.[67] FTIR and UV-vis spectroscopy by Johnston and coworkers[68, 69] showed that the w/c microemulsion consists of regions of “bulk” hydrogen bonded water, “interfacial” water, and “free” water dissolved in sc-CO₂. The UV-vis spectroscopic studies using methyl orange as a probe indicated that the PFPE/sc-CO₂/water reverse micelle cores have a polar environment as seen in dry PFPE reverse micelles, a bulk-like water region, and an acidic environment resulting from carbonic acid formation. Additionally, Lee et al.[70] observed the interaction strength between the droplets to be larger in water-in-CO₂ relative to water-in-oil microemulsions due to stronger tail-tail interactions resulting from the weak solvation by CO₂. As a result, it is more difficult to overcome droplet interactions to produce stable microemulsions. Lastly, SANS measurements performed by Zielinski et al.[71] show evidence of water-in-CO₂ microemulsion with a droplet radius ranging from 20 to 36 Å.

2.7 APPLICATIONS OF SURFACTANTS IN CARBON DIOXIDE

Carbon dioxide is desirable as a process solvent because of its “green” characteristics and it has been considered as a replacement for organic solvents in numerous technologies, such as the production of nanoparticles, polymer processing, chemical reactions, and extractions due to the development of CO₂ soluble surfactants specifically for each application.

2.7.1 Nanoparticle Formation

There is a growing interest in the preparation of nanoparticles for use as catalysts, pharmaceuticals, sensors, semiconductors, optical materials, and others. Current techniques for producing nanoparticles involve harsh process conditions and do not provide adequate control over particle characteristics. Recently, CO₂ has been extensively investigated as a pressure-tunable reaction medium for the manufacture of nanoparticles. Changes to CO₂ solvent properties through manipulation of the pressure can affect the growth rate of nanoparticles, their final size, and their size distribution, allowing fine control over nanoparticles. Several modes of nanoparticle synthesis have been explored in CO₂.

Nanoparticle Formation in w/c Microemulsions

One method provides for the formation of nanoparticles within w/c microemulsions by reducing metal salts dissolved in the nano aqueous core and has been demonstrated for copper,[33] silver,[33, 72-74] and palladium.[34] This technique employs CO₂-philic perfluoropolyether (PFPE) surfactants in order to form reverse micelles in CO₂ with a water core into which CO₂-phobic polar species (metal salts) can dissolve. Typically, by using this strategy, metallic nanoparticles having diameters from 2–15 nm were synthesized and stabilized in the water-in-CO₂ microemulsions formed by PFPE surfactants. In nanoparticle formation, a metal ion is introduced into a reverse micelle. A reducing agent within the CO₂ continuous phase diffuses into the micelle, reducing the metal ions to form very small metal particles. The inter-micellar exchange of the metal particles solubilized within the core of the micelles allows for the particles growth by the aggregation and coalescence of the very small particles. The particle

growth continues until the particles reach a terminal size determined by the system and where the surfactant aids in stabilization of the particles.

The substitute of oxygenated hydrocarbon-based or hydrocarbon-based surfactants for fluorinated surfactants in the applications of nanoparticle formation in w/c microemulsion would mitigate the problems associated with the environmental and biological persistence associated with fluorinated surfactants. One of the objectives of this study was to design, synthesize, characterize, and evaluate the CO₂ solubility of ionic surfactants with oxygenated hydrocarbon tails composed of acetylated sugar, PPO, or oligo(vinyl acetate). Additionally, these surfactants were examined for their ability to form stable microemulsions with polar microenvironments capable of dissolving polar species in the bulk non-polar CO₂ solvent.

Nanoparticle Formation via Reducing CO₂-Soluble Organometallic Precursors

An alternative technology forgoes the formation of the reverse micelles, and instead employs the reduction of fluorinated, CO₂-soluble organometallic precursors of Ag(1,1,1,5,5,5-hexafluoropentane-2-,4-dione)(tetraglyme) [Ag(hfpd)(tetraglyme)], palladium(II) hexafluoroacetylacetonate [Pd(hfac)₂],[75] and triphenylphosphine gold(I) perfluorooctanoate [TPAuFO].[76] After reduction, the metal atoms aggregate to form nanoparticles which are capped by the CO₂ soluble fluorinated thiols. The thiol binds to the surfaces of nanoparticles, quenches particle growth and provides a steric barrier to aggregation. In this manner, metallic silver, palladium, and gold nanoparticles with a size range of about 1–4 nm were dispersed in supercritical CO₂.

Another method involves reducing CO₂-soluble fluorinated, organometallic precursors, such as Ag(hfpd)(tetraamine), Ag(hfpd)(tetraglyme), and Pd(hfac)₂ in the

absence of stabilizing thiols. Rather, the reduced silver nanoparticles were trapped in porous substrates, such as poly(styrene-divinylbenzene) and silica aerogels,[77] palladium nanoparticles were stabilized in swelled plastics.[78] In each of these cases, CO₂-soluble fluorinated metal complexes were required to make the metal nanoparticles.

The use of hydrocarbon-based or oxygenated hydrocarbon-based precursor complexes in supercritical CO₂ manufacture of metal nanoparticles would mitigate the problems associated with the environmental and biological persistence associated with fluorinated compounds. Platinum, copper, and nickel film were successfully deposited onto polymer substrates or silicon wafer by reducing CO₂-soluble hydrocarbon-based metal precursors, such as dimethyl(cyclooctadiene)platinum(II) [CODPtMe₂],[79] bis(2,2,6,6-tetramethyl-3,5-heptanedionato)copper (II) [Cu(tmhd)₂], and bis(cyclopentadienyl)nickel [NiCp₂].[80] Silver acetylacetonate, [Ag(acac)] was reported as a hydrocarbon-based precursor for the preparation of silver nanocrystals capped with fluorinated ligands of 1H,1H,2H,2H-perfluorooctanethiol.[81, 82] However, these prior reports of metallic nanoparticle synthesis by reducing hydrocarbon-based metal precursors did not contain any CO₂-metal precursor phase behavior data. Our objective was to produce silver nanoparticles capped with non-fluorinated ligands via the reduction of highly CO₂-soluble hydrocarbon-based or oxygenated hydrocarbon-based metal precursors.

2.7.2 CO₂ in Enhanced Oil Recovery

The largest application of CO₂ is in the area of enhanced oil recovery. Carbon dioxide, being available at high purity and in large quantities from natural reservoirs, has been used in enhanced oil recovery for many years.

Enhanced Oil Recovery

In petroleum industry, primary recovery, producing oil under natural reservoir pressure, accounts 5-20% of original oil in place (OOIP). Subsequently, secondary recovery, the injection of water to displace oil, called water flooding, can recover up to 50% of OOIP. Much of the oil still remains behind in place due to inefficiency of these recovery processes. With the increasing demand for petroleum versus limited resources, tertiary recovery methods, referred to as enhanced or improved oil recovery (EOR/IOR) employ fluids other than water to displace additional oil from reservoir. Recent production trends show less than 10% of OOIP comes from EOR processes. EOR processes include hydrocarbon miscible flooding, CO₂ flooding, polymer flooding, surfactant flooding, steam flooding, and immiscible gas injection. Different fluids are injected to displace additional oil from the reservoir, via several mechanisms including solvent extraction to achieve (or approach) miscibility, interfacial-tension (IFT) reduction, improved sweep efficiency, pressure maintenance, oil swelling, and viscosity reduction.[83]

CO₂ as a Flooding Agent in Enhanced Oil Recovery

During a CO₂ flooding, also called miscible displacement, because CO₂ is miscible with light oils under reservoir conditions. CO₂ is injected into the oil-bearing porous media, typically at a depth greater than 2000 ft and reservoir temperature usually between 300 K and 400 K. The working pressure is maintained slightly above the “minimum miscibility pressure” (MMP, approximately 7-30 MPa) as shown in Figure 2.10,[84] thus CO₂ can dynamically develop effective miscibility with oil and displace

the oil left behind by water flooding.[85] As the reservoir fluids are produced from the production well, CO₂ can be easily separated from the oil simply by pressure reduction. Other properties of CO₂ such as low cost, nonflammable, nontoxic, and easy separation from the oil also contribute to make CO₂ flooding an attractive oil recovery procedure.

CO₂ flooding at nearly 70 projects sites in the U.S. produces more than 200,000 barrels per day, which is approximately 3% of the domestic oil production rate. About 1.3 billion standard cubic feet (SCF) of CO₂ is injected into domestic reservoirs each day, the majority of which are located in the Southwest. At typical reservoir conditions, CO₂ is a dense fluid and its utilization corresponds to 3 barrel of liquid CO₂ injected per barrel of oil rejected. Despite the large amount of CO₂ flooding injected into these formations, the recovery efficiency is typically only 10-20% of the OOIP. Further, shallow reservoirs are not amenable to CO₂ flooding because the MMP exceeds the overburden pressure of the formation.

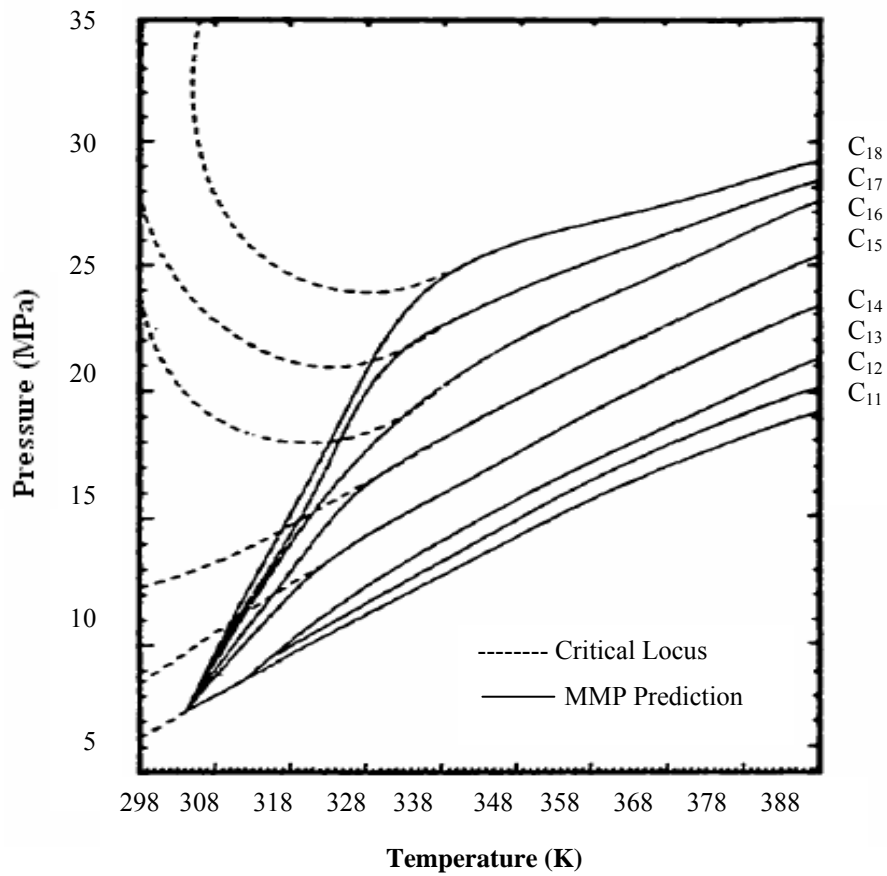


Figure 2.10. Working temperature and pressure for CO₂ flooding as a function of oil average molecular weight.[84]

The foremost disadvantage of CO₂ as an oil displacement fluid is its low viscosity, 0.03-0.1 cp at the reservoir conditions, as shown the shade area in Figure 2.11,[86] which is up to 100 times lower than that of the oil being displaced, varying from 0.1 cp to 50 cp. The low viscosity of CO₂ results in its much higher mobility (defined as permeability/viscosity of that fluid in porous media) compared to that of the oil, because the permeability of CO₂ and oil are comparable in magnitude. This unfavorable high mobility of CO₂ causes CO₂ “fingering” its way towards the production well, bypassing as much as 85% of the oil in the reservoir, which reduces the area sweep efficiency. Figure 2.12 shows the comparison of CO₂ fingering and the ideal case in EOR. Injection is in the lower left hand corner, and production is in the upper right hand corner, the curves show CO₂/oil interface as a function of time

Moreover, the low viscosity of CO₂ also contributes to the low vertical sweep efficiency, especially in stratified reservoirs that include two or more layers. The formation may contain a highly permeable water-rich zone caused by extensive water flooding, while the other layer is low permeability oil-rich zone. The high mobility of CO₂ prefers entering the highly permeable water-rich zone, leaving oil residing in the less permeable zones, which is not contacted by CO₂ and thus not efficiently displaced.

Furthermore, some shallow reservoirs are not amenable to CO₂ flooding because the MMP exceeds the overburden pressure of the formation. In this case, the displacement of oil by CO₂ would be conducted at pressures below the MMP, and the resultant displacement would be categorized as immiscible displacement. Such a process would benefit from a CO₂ thickener to improve sweep efficiency. The displacement

efficiency would also be enhanced if there was a way to reduce the CO₂-oil interfacial tension.

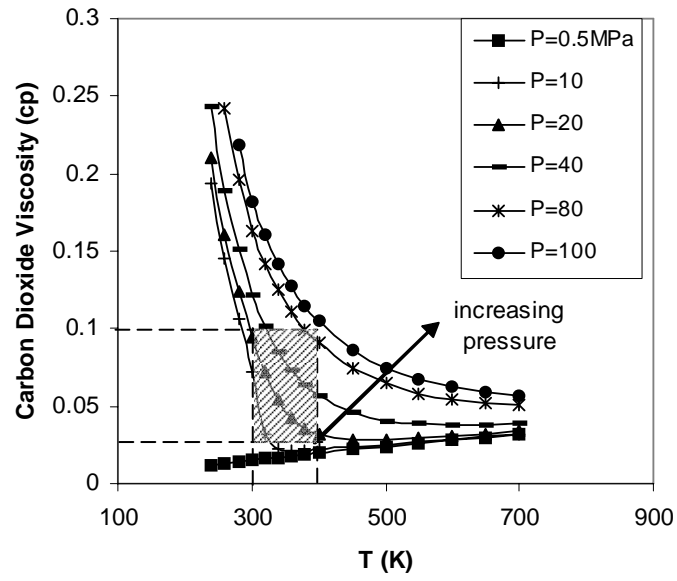


Figure 2.11. Viscosity of CO₂ as function of temperature and pressure.[86]

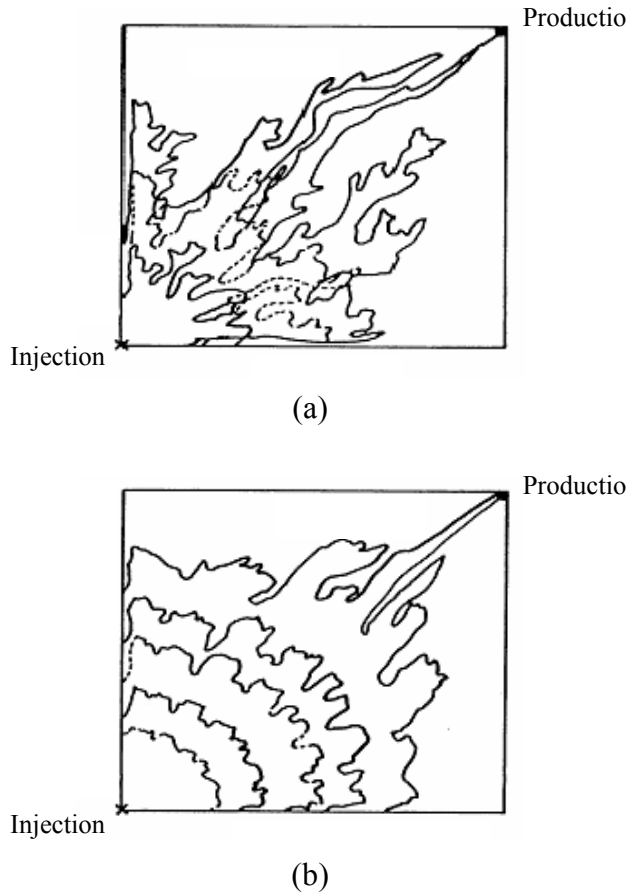


Figure 2.12. CO₂ flooding in EOR: (a) CO₂ “fingering” (b) ideal case.

Mobility Control Technologies to Improve the Efficiency of CO₂ Flooding

The high CO₂ utilization rate and low volumetric sweep efficiency are primarily attributing to the low viscosity and density of dense CO₂ relative to the oil being displaced. For example, the density of CO₂ at reservoir conditions may be 0.45-0.75 g/cm³, while the oil density varies between 0.7-0.9 g/cm³. The viscosity of CO₂, 0.03-1 cp at reservoir conditions, is commonly 2-20 times less than that of the oil being displaced. Although it is not feasible to significantly increase the density of CO₂, it is possible to significantly alter the relative viscosity of CO₂ using several technologies.

Water-Alternating-Gas (WAG) Technology

Currently, the water-alternating-gas (WAG) process remains the most common means of moderating CO₂ mobility.[87] The water slugs act as a blocking agent to impeding CO₂ flow in the porous medium. Alternating slugs of water and CO₂ are injected to improve the mobility of CO₂ by reducing the relative permeability of CO₂. The increased water saturation in the porous media decreases the relative permeability of CO₂; however, the high saturation of water may impede the contact of CO₂ with oil, and gravity segregation of CO₂ and water can impede the effectiveness of this process. The injection of water also extends the time required to inject the desired amount of carbon dioxide. Further, a significant amount of oil can still be left behind during the WAG process; recovery of only 10-20% of the oil is common.

CO₂ Foam Flooding or Surfactant Solution-Alternating-Gas (SAG) Technology

Foam is a dispersion of a gas in a liquid. CO₂ foams have also been studied by both academic groups[42, 88-90] and by industrial researchers.[91, 92] An aqueous surfactant solution is injected into the formation, followed by the CO₂, which is called surfactant-alternating-gas (SAG) process. The in-situ generation of foams results in high phase volume CO₂ foams in which bubbles of the CO₂ are separated by aqueous films. Foams show potential for both mobility control (modest decreases in mobility) and permeability modification (significantly decreases in mobility). Shorter cycles are recommended in the SAG process to obtain a more uniform foam quality. Problems associated with CO₂ foam flooding or SAG process includes corrosion, surfactant adsorption and control of foam mobility within the reservoir for extended periods of time.

CO₂-Soluble Polymeric Thickener Technology

A search for CO₂-soluble polymers or smaller associating compounds capable of directly enhancing the viscosity of dense CO₂ have been conducted by numerous research groups [42, 93]. Subsequently, Enick and co-workers identified the first CO₂ thickener, poly(**fluoroalkylacrylate-styrene**) copolymer, poly FAST, which successfully increased the viscosity of CO₂ by a factor of 10 in porous media at 1 wt%.[7, 94] Poly FAST isn't practical for field use; however due to its expensive and environment persistence.

These examples demonstrate the diversity applications of CO₂ from nanoparticle formation to enhanced oil recovery. Despite difficulties associated with its feeble solvent nature, application of creative engineering solutions can still enable its use, provided that CO₂ soluble surfactants can be specifically designed and synthesized for each application. Such surfactants contain a CO₂-philic segment such as a fluoroether, fluoroacrylate, or silicone-based compound and a CO₂-phobic segment made up of a hydrophilic or lipophilic molecule, depending on the application.

3.0 RESEARCH OBJECTIVES AND APPROACH

3.1 RESEARCH OBJECTIVES

The primary objective of this project is to enhance the performance of petroleum and chemical engineering CO₂-based processes using oxygenated hydrocarbon-based or hydrocarbon-based, novel, inexpensive, biodegradable CO₂ soluble surfactants with tails composed of C, H, and O (other elements may be used in ionic surfactant counterions).

3.1.1 CO₂ Soluble Surfactants for Nanoparticle Synthesis and Stabilization

Our objectives are to design, synthesize, characterize, and evaluate the CO₂ solubility of ionic surfactants with oxygenated hydrocarbon tails composed of acetylated sugar, PPO, or oligo(vinyl acetate). Additionally, these surfactants were examined for their ability to form stable microemulsions with polar microenvironments capable of dissolving polar species in the bulk non-polar CO₂ solvent. Other objectives for nanoparticle synthesis application were to design and determine the solubility of silver organometallic complex that could be used to form silver nanoparticles in CO₂ via reduction in the presence of fluororous or non-fluororous stabilizing ligands.

3.1.2 CO₂ Soluble Surfactants for Generating in-Situ EOR Foams

We proposed the use of CO₂ soluble surfactants that can be injected along with CO₂ into the oil reservoir for mobility control and/or permeability alteration. Upon mixing with the reservoir brine, foam would be generated in-situ; especially in watered out zones into which a significant fraction of the CO₂ typically flows with little economic benefit. The fundamental advantages of such a surfactant include (a) a reduction or elimination of the need to inject brine or aqueous surfactant solutions into the reservoir, and (b) the generation of foams along and at the tips of the CO₂ “fingers” where mobility control is needed the most, thereby acting as a “smart fluid” to divert the subsequently injected neat CO₂ to oil-rich zones.

The objective of this study was to form emulsions by mixing of CO₂, water and CO₂-soluble surfactants, and then to characterize the stability of the emulsion by measuring its rate of collapse. CO₂-soluble ionic surfactants with oxygenated hydrocarbon tails composed of acetylated sugar, PPO, or oligo(vinyl acetate) were evaluated along with two nonionic surfactants, iso-stearic carboxylic acid and PPG-PEG-PPG triblock polymer (Mn=3300). Nonionic surfactants are considered to be low-to-moderate foamers relative to ionic surfactants, and were therefore expected to yield less stable emulsions, but nonionic surfactants have less severe problems associated with adsorption or chemical degradation. The stability of the emulsions stabilized with CO₂ soluble ionic surfactants was then contrasted with that the stability of emulsions formed using conventional water soluble ionic surfactants.

3.2 OUR APPROACH

We proposed to explore new types of oxygenated hydrocarbon-based or hydrocarbon-based, novel, inexpensive, biodegradable CO₂ soluble surfactants. Each surfactant will contain two types of segments, one of which will be a novel, highly CO₂-philic, oxygenated hydrocarbon-based or hydrocarbon-based segment. The other would be either a conventional non-ionic or ionic hydrophilic segment, or a nonionic lipophilic segment.

The CO₂ solubility of each surfactant will be evaluated, along with the ability of the surfactant to solubilize water or generate foams in a high pressure variable volume view cell. Auburn University will confirm the solubilization of water into the cores of micelles spectroscopically.

4.0 OXYGENATED HYDROCARBON-BASED IONIC SURFACTANTS

4.1 IONIC SURFACTANTS WITH PERACETYL GLUCONIC TAILS

4.1.1 Materials

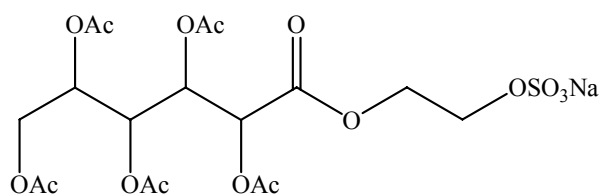
Acetic anhydride, perchloric acid, D-glucose, triethylamine, 1,8-Diazabicyclo[5.4.0]undec-7-ene (DBU), 2-bromoethanol, pyridine sulfur trioxide, sodium bicarbonate, ammonium carbonate were purchased from Aldrich and used as received. All other reagent and solvents were obtained from Aldrich and used without further purification. N₂ (99.995%) and CO₂ (99.99%, Coleman grade) were purchased from Penn Oxygen.

4.1.2. Characterizations

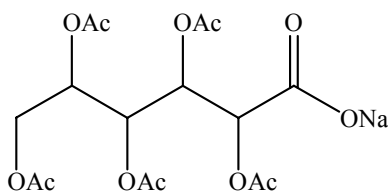
The purities of the ionic surfactants were estimated by ¹H NMR spectra recorded on a Bruker 400 MHz NMR and IR spectra obtained on a Mattson Polaris FTIR. The molecular weights of the ionic surfactants were detected by mass spectra performed on a liquid chromatography/electrospray ionization/quadrupole time-of-flight mass spectrometer.

4.1.3 Synthesis

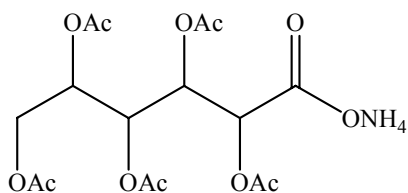
The synthesis of peracetyl gluconic (sugar acetate)-based ionic surfactants with ethyl sodium sulfate, sodium carboxylate and ammonium carboxylate head groups were carried out with the help of Dr. Hamilton's group of Chemistry Department at Yale University.[95] The structures of peracetyl gluconic-based ionic surfactants are shown in Figure 4.1.



Peracetyl Gluconate Ethyl Sodium Sulfate (a)



Peracetyl Gluconate Sodium Carboxylate (b)



Peracetyl Gluconate Ammonium Carboxylate (c)

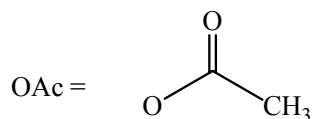


Figure 4.1 Structures of peracetyl gluconic-based ionic surfactants.

The reaction scheme is shown as follows in Figure 4.2, with the synthesis of peracetyl gluconic ethyl sodium sulfate as an example. Peracetyl gluconic carboxylic acid was prepared by acetylation of D-glucose by acetic anhydride, followed by neutralization with sodium bicarbonate.

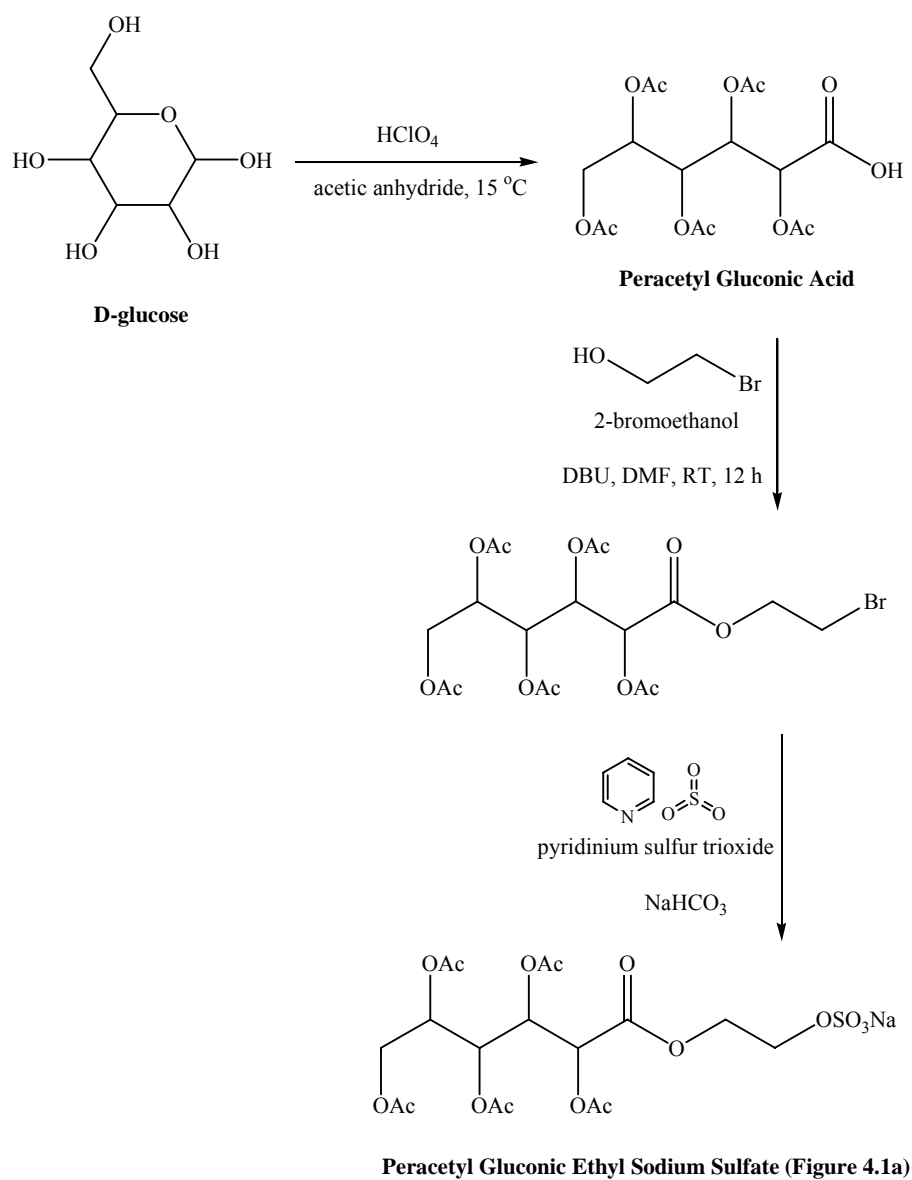


Figure 4.2 Reaction scheme for preparation of peracetyl gluconic ethyl sodium sulfate.

Synthesis of Peracetyl Gluconic Carboxylic Acid

Acetic anhydride (30 mL) was cooled to about 15 °C, 67% HClO₄ (4 g, 39.82 mmol) was then added to the cold acetic anhydride, followed by the addition of D-glucose (5 g, 25.23 mmol). The temperature of the mixture was kept below 40 °C. After brief heating to obtain a homogeneous solution, the mixture was poured on ice and extracted twice with CHCl₃ (2 x 100 mL). The organic layers were pooled and washed with ice-cold water. Water (50 mL) and triethylamine (4 mL) were added to the CHCl₃, followed by overnight stirring to hydrolyze any anhydride. The organic layer was separated and washed with 1 N HCl and dried over anhydrous Na₂SO₄, and CHCl₃ was removed in vacuo to yield 80% 2,3,4,5,6-penta-*O*-acetyl-D-gluconic acid. ¹H NMR δ_H (CDCl₃): 5.618 (t, J = 4.8 Hz, 1H), 5.510 (dt J = 6.4 Hz, 1H), 5.285 (d, J = 3.6 Hz, 1H), 5.055 (m, 1H), 4.301 (dd, J = 12.4 Hz, 4 Hz, 1H), 4.113 (dd, J = 12.4 Hz, 5.6 Hz, 1H), 2.249 (s, 3H), 2.085 (s, 3H), 2.077 (s, 3H), 2.072 (s, 3H), 2.044 (s, 3H).

Synthesis of Peracetyl Gluconic Ethyl Sodium Sulfate (Figure 4.2a)

1,8-Diazabicyclo[5.4.0]undec-7-ene (DBU) (4.8 g, 31.53 mmol) was added to a solution of peracetyl gluconic carboxylic acid (10 g, 24.63 mmol) and 2-bromoethanol (3.94 g, 31.53 mmol) in DMF(10 mL) and stirred at room temperature. After 12 h the mixture was poured into water (100 mL) and extracted with dichloromethane (3 x 50 mL). The organic layers were pooled, washed with water, and dried over anhydrous Na₂SO₄ prior to the removal of solvent. Column chromatographic purification of the crude product over silica gel using 50% ethyl acetate and hexanes as the eluent gave the pure product (9.4 g, yield 85%). The product was dissolved in anhydrous

dichloromethane, pyridine sulfur trioxide (6.3 g, 39.58 mmol) was added, and the mixture was stirred at room temperature for 12 h. The mixture was filtered through a pad of Celite and solvent removed to give the pyridinium salt. The pyridinium salt was dissolved in water (100 mL), and sodium bicarbonate (1.74 g, 20.71 mmol) was added. The resultant mixture was frozen and water was removed using a freeze-dryer to give a white color fluffy solid.

HRMS (ESI) calculated for $C_{18}H_{25}Na_2O_{16}S$ ($[M + Na]^+$) 575.0659, found 575.0630. (Appendix A Figure A.1)

Synthesis of Peracetyl Gluconic Sodium Carboxylate (Figure 4.2b).

Peracetyl gluconic carboxylic acid (5 g, 12.32 mmol) was dissolved in water (50 mL), and sodium bicarbonate (1.04 g, 12.38 mmol) dissolved in water (10 mL) was added. The resultant solution was frozen and water was removed using a freeze-dryer to give white color fluffy solid.

HRMS (ESI): calculated for $C_{16}H_{22}NaO_{12}$ ($[M + H]^+$) 429.1009, found 429.1016. (Appendix A Figure A.2)

Synthesis of Peracetyl Gluconic Ammonium Carboxylate (Figure 4.2c).

Ammonium carbonate (2.0 g, 20.81 mmol) was added to a solution of peracetoxy gluconic carboxylic acid (5 g, 12.32 mmol) dissolved in water (50 mL), and the mixture was stirred. The resultant solution was frozen and water was removed using a freeze-dryer to give a yellow color fluffy solid. HRMS (ESI) calculated for $C_{16}H_{26}NO_{12}$ ($[M + H]^+$) 424.1455, found 424.1422. (Appendix A Figure A.3)

4.1.4 Phase Behavior of Peracetyl Gluconic-Based Ionic Surfactants

4.1.4.1 Experimental Apparatus The CO₂ solubility of surfactants was determined by phase behavior study as function of temperature, pressure and concentration. The apparatus is a high pressure, windowed, variable volume view D. B. Robinson cell with magnetic mixer and temperature control. The schematic apparatus is shown in Figure 4.3 and the variable volume view D.B. Robinson cell with magnetic mixer is illustrated in Figure 4.4. The system is rated to 70 MPa and 200 °C.

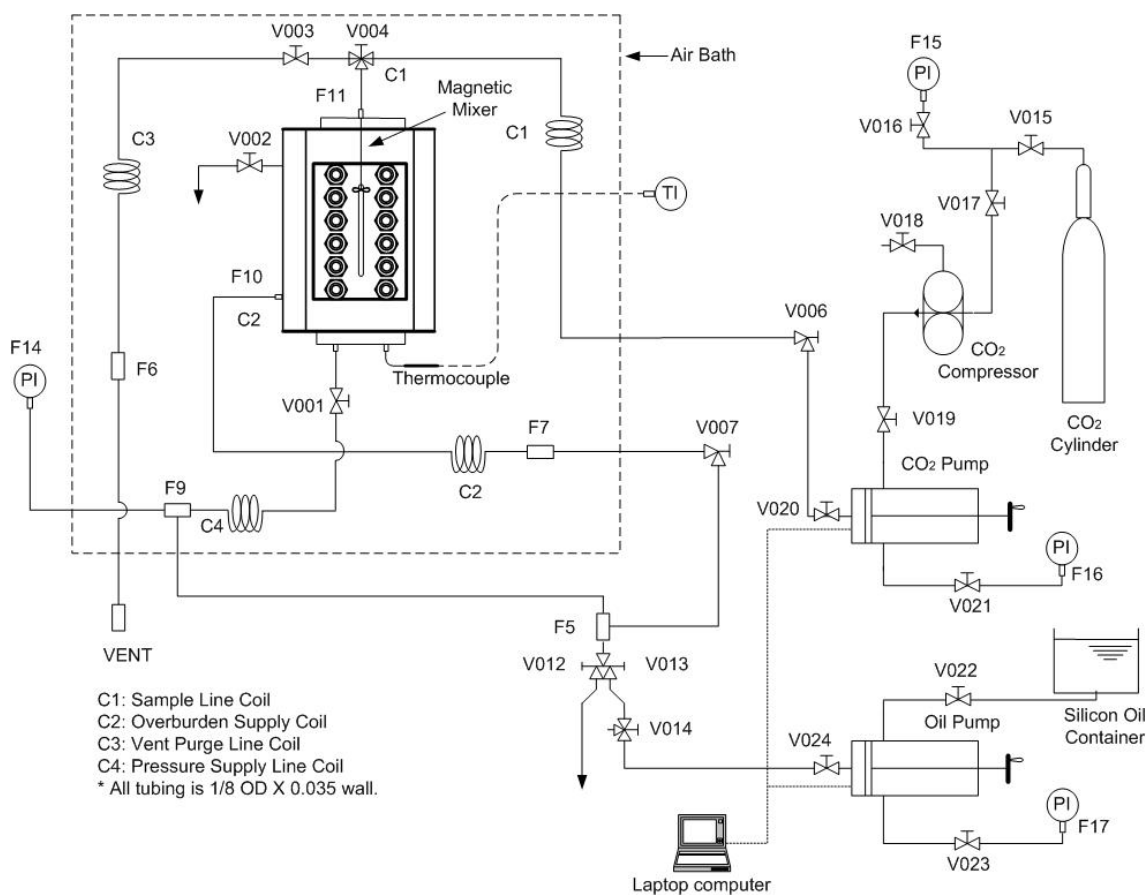


Figure 4.3 Schematic apparatus for solubility/phase behavior measurements.

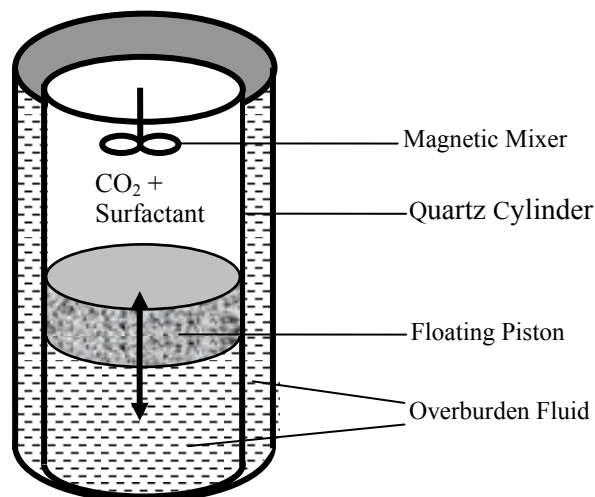


Figure 4.4 Variable volume view D. B. Robinson cell with magnetic mixer

A known amount of surfactant (e.g., 0.0700 ± 0.0001 g) was loaded into the sample volume of a high pressure, windowed, stirred, variable-volume view cell (DB Robinson & Assoc., 3.18 cm i.d., ~ 120 cm³ working volume). In this cell, the sample volume is separated from the overburden fluid by a steel cylinder (floating piston) that retains an O-ring around its perimeter. The O-ring permits the cylinder to move while a seal is retained between the sample volume and the overburden fluid. After purging with carbon dioxide at 0.2 MPa, the sample volume was minimized by displacing the floating piston to the highest possible position within the cell that did not result in the displacement of surfactant out of the sample volume. High pressure liquid carbon dioxide (22 °C, 13.8 MPa) was then introduced to the sample volume as the silicone oil overburden fluid (which was maintained at the same pressure as the CO₂) was withdrawn at the equivalent flow rate using a dual-proportioning positive displacement pump (DB Robinson). This technique facilitated the isothermal, isobaric addition of a known volume

of CO₂ (e.g., 12.50 ± 0.01 mL) into the sample volume. The mass of CO₂ introduced was determined from the displaced volume, temperature, and pressure using an accurate equation of state for carbon dioxide.[96] On the basis of the uncertainties associated with the measurement of temperature, pressure, and volume, and the precision of the equation of state, compositions are estimated to be accurate to within 1% of the specified value (e.g., 0.5 ± 0.005 wt %). The surfactant-CO₂ mixture was compressed to high pressure (e.g., 60 MPa) and mixed thoroughly using a magnetic stirrer (DB Robinson, max. 2500 rpm). If the surfactant did not completely dissolve at these conditions, additional CO₂ was added to the system until a single transparent phase could be attained. Cloud points were determined by standard nonsampling techniques. The high-pressure, single-phase solution of known composition was subjected to a slow, isothermal expansion until the cloud point was attained. Cloud points were reproduced three times to within approximately ± 0.1 MPa for monodisperse surfactants and ± 0.5 MPa for polydisperse surfactants. Temperatures were measured with a type K thermocouple to an accuracy of ± 0.1 °C. Experiments with water were conducted by adding the specified amount of surfactant and double distilled and deionized water to the sample volume, followed by the introduction of CO₂. W is the molar ratio of total amount of loading water to surfactant in the mixture. The W value is “uncorrected” in that this value accounts for the total amount of water in the mixture that may dissolve into the bulk CO₂ and/or be solubilized in the core of reverse micelles. The corrected water/surfactant ratio, W^{corr}, for a transparent single phase mixture can be estimated by assuming that the bulk CO₂ is saturated with water, while the amount of the excess water, which is assumed to reside within the cores of the micelles, is used in the numerator of W^{corr}. [97]

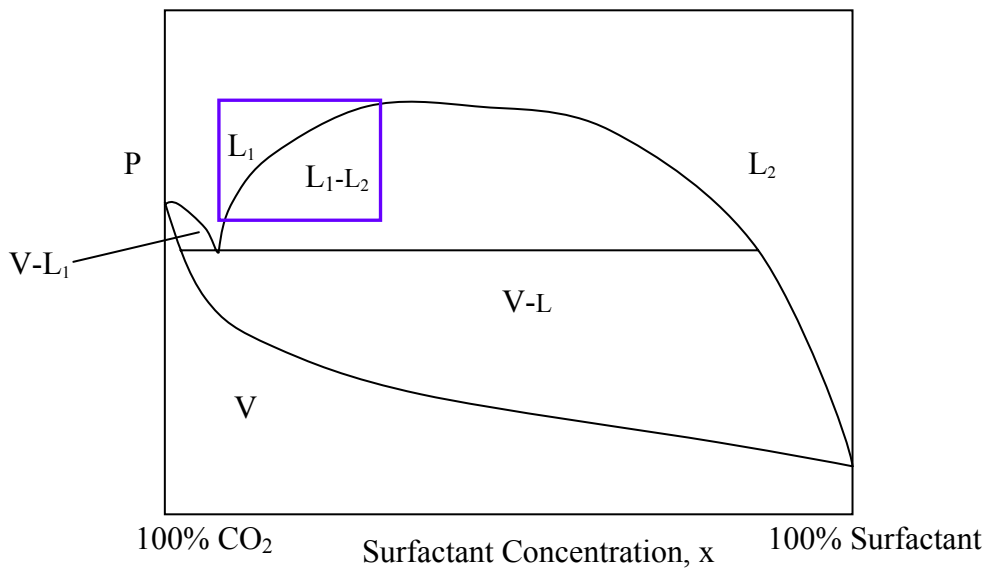
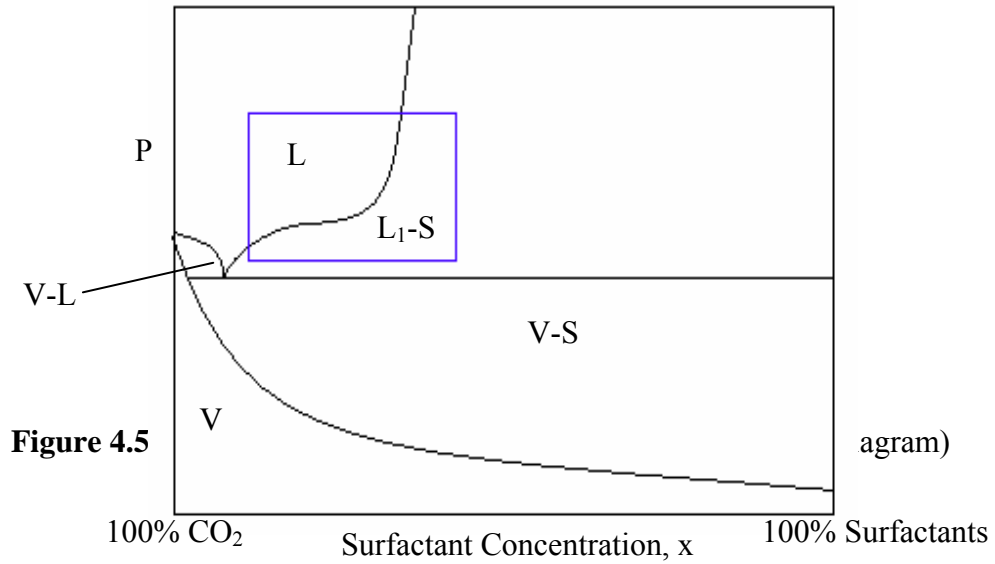


Figure 4.6. Phase diagram for liquid surfactant/CO₂ system (P-x diagram)

The cloud point pressure is the minimum pressure at which the sample is miscible with dense carbon dioxide at that particular temperature and composition. Below this pressure, the system consists of a sample-rich phase and a CO₂-rich phase. Thus we could

obtain a point on the two-phase boundary of a P-x diagram of solid surfactant/CO₂ system and liquid surfactant/CO₂ system, shown in Figure 4.5 and Figure 4.6. A series of these experiments were conducted over a range of overall compositions, enabling the two-phase boundary of the surfactants/CO₂ system to be established.

4.1.4.2 Phase Behavior Results The neat peracetyl gluconic-based surfactants with an ethyl spacer and a sodium sulfate, sodium carboxylate or ammonium carboxylate head group (Figures 4.1 a,b,c) are solids. Peracetyl gluconic ethyl sodium sulfate (PGESS) does not dissolve in CO₂ at 22 °C or 40 °C in the absence of water (W=0), but its solubility increases as water is added, as shown in Figure 4.7. The surfactant is up to 0.6 wt% soluble in CO₂ in the presence of water at a W value of 10 (W is the molar ratio of water to surfactant, uncorrected for dissolved water). At W values of 40 and 50; however, a water phase appeared at the bottom of the cell. Attempts to dissolve 0.7 wt% or more yielded an excess surfactant-rich phase at the bottom of the cell for all values of W. Table 4.1 lists W and W^{crit} for the PGESS surfactant in water and CO₂ mixture at different weight percent and temperature.

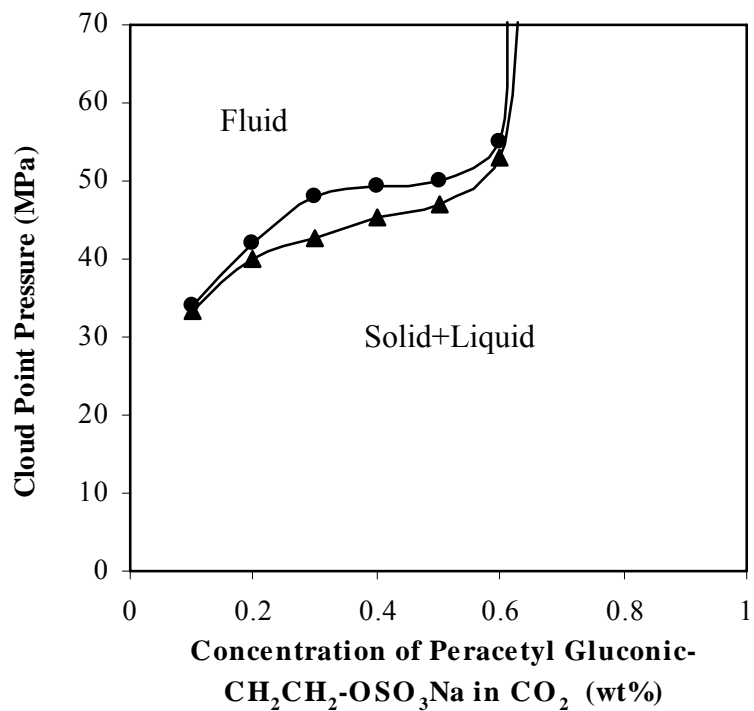


Figure 4.7. Phase behavior of peracetyl gluonic-CH₂CH₂-OSO₃Na/CO₂ mixtures. Insoluble at W = 0; 22 °C, W =10 (●); 40 °C, W=10 (▲). (Appendix A Figure A.4. Surfactant concentration in mM)

Table 4.1. W and W^{corr} for the PGESS surfactant in water and CO_2 mixture at different weight percents and temperature. *When the amount of water is not sufficient to saturate the CO_2 , W^{corr} is reported as 0.

PGESS Concentration, wt%	Temperature, °C	W	W^{corr}*
0.1-0.5	25	10	0
0.6	25	10	0.8
0.1-0.6	40	10	0

Figure 4.8 shows that peracetyl gluconic sodium carboxylate (PGSC) appears to be more CO_2 soluble than PGESS because PGSC can dissolve at 40 °C in the absence of water. The solubility of PGSC decreases slightly with the addition of water. PGSC has a limiting solubility of approximately 0.4 wt% in CO_2 at $W = 10$. Single phase solutions could not be realized at W values of 40, even at surfactant concentrations as low as 0.1 wt%. W^{corr} is 0 at W value of 10 for PGSC surfactant in water and CO_2 mixture at concentration range of 0.1-0.5 wt% is 0 at 40 °C.

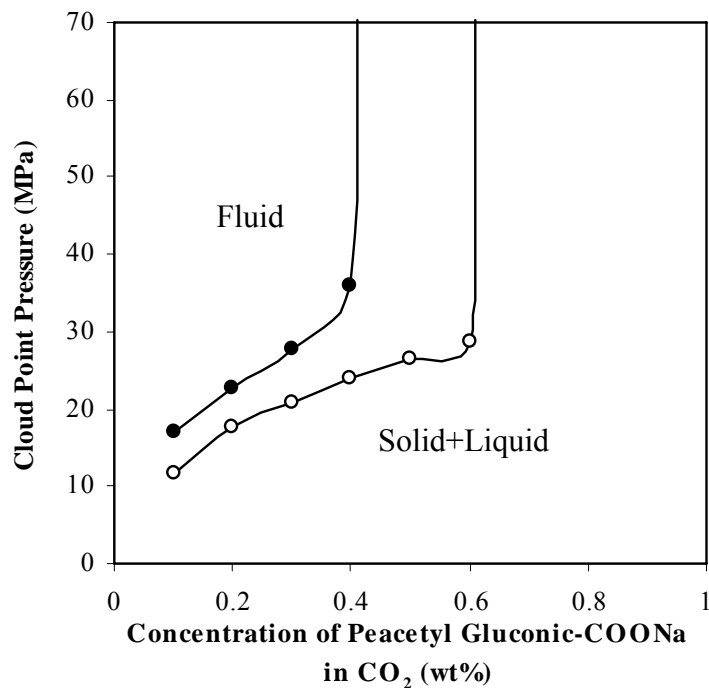


Figure 4.8. Phase behavior of peracetyl gluconic-COONa/CO₂ mixtures at 40 °C. W=0 (○); W=10 (●). (Appendix A Figure A.5. Surfactant concentration in mM).

Figure 4.9 illustrates that peracetyl gluconic ammonium carboxylate (PGAC) can dissolve in CO₂ up to 2 wt% at 40 °C without water. Although this limiting solubility value is significantly greater than those for either PGEES or PGSC, the pressure required to dissolve PGAC at dilute concentrations (up to 0.5 wt%) was greater than that required to dissolve PGSC. The solubility of PGAC decreases with the introduction of water, as does its limiting solubility in CO₂, which is about 0.5 wt% at W value of 10. Single phase solutions could not be realized at W values of 40, even at surfactant concentrations as low as 0.1 wt%. W^{corr} is 0 for W value of 10 over PGSC concentrations up to 0.5 wt% at 40 °C.

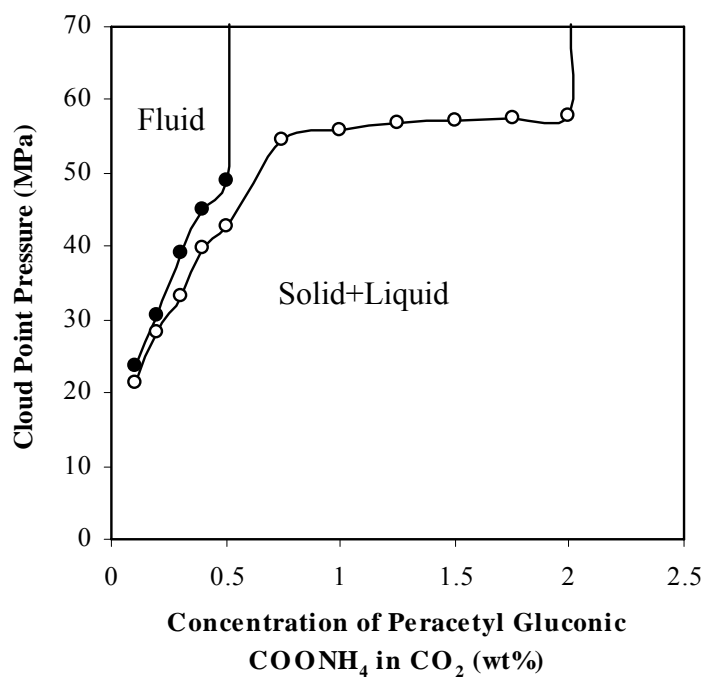


Figure 4.9. Phase behavior of peracetyl gluconic- $\text{COONH}_4/\text{CO}_2$ mixtures at $40\text{ }^\circ\text{C}$. $W = 0$ (○); $W = 10$ (●). (Appendix A Figure A.6. Surfactant concentration in mM).

4.1.5 Dye Solubilization and Spectroscopic Measurements

Dye solubilization and spectroscopic measurements were carried out with the help of Dr. Roberts' group in Chemical Engineering Department at Auburn University.[95]

The ability to form reverse micelles by these CO_2 -soluble surfactants was investigated using the solvatochromic probe methyl orange at system concentration of ca. 4.7×10^{-5} M. Methyl orange is a polar probe that is insoluble in both carbon dioxide and water-saturated carbon dioxide. Furthermore, the location of its absorption maximum is dependent upon the polar environment in which it is dissolved. For instance, it has an

absorption maximum at 416 nm in dry PFPE-NH₄/CO₂ reverse micelles, 421 nm in methanol, 464 nm in water, and 502 nm in CO₂-saturated water.[68, 69] Hence, the solubility of methyl orange in an otherwise ineffective solvent, such as CO₂, indicates the presence of reverse micelles and it also functions as a probe of polarity of the water environment within CO₂ reverse micelles. Consequently, methyl orange has been used successfully to identify the presence of reverse micelles as well as their ability to uptake water in CO₂ reverse micelles.[68, 69, 98-103] It was indicated that the absorption maximum in water-in-CO₂ microemulsions formed by ammonium carboxylate PFPE surfactant approaches that of pure water ($\lambda_{\text{max}} = 460 \text{ nm}$).[66] While a surfactant may show some solubility in CO₂ in the presence of dissolved water, this alone does not guarantee that a polar microenvironment is present. Verification of a polar microenvironment is necessary to confirm that the surfactant does indeed self-assemble in solution to form reverse micelles.

4.1.5.1 Experimental Apparatus A 32 mL stainless steel high-pressure vessel equipped with pressure gauge, resistance temperature detector (RTD), and parallel quartz windows for UV-vis characterization, which has been described previously,[73] was used to perform dye solubilization experiments. A magnetic stir bar was used to facilitate surfactant/CO₂ mixing. For a typical experiment, 100 μL freshly prepared 0.015 M methyl orange (MO) in methanol solution was added into the UV cell, and a gentle stream of N₂ was passed through the cell for ten minutes to fully evaporate the methanol while only maintaining the MO inside of the UV-cell. 0.15 wt% of surfactant was charged into the cell, then specific amount of double distilled and de-ionized water was injected into the cell using a syringe to reach the desired W value. After sealing the

vessel, an ISCO syringe pump was used to add specific quantity of CO₂ to the vessel. Once the vessel was filled with CO₂ to the desired pressure, the system was mixed for at least an hour to reach a single phase before performing spectroscopic analysis. The vessel was placed in a Cary 300E UV-vis spectrophotometer and absorption spectra were recorded to determine the presence of methyl orange solubilized in the surfactant/water/CO₂ mixture. Pressure within the vessel was monitored to approximately ± 0.7 MPa, and temperature was maintained to within ± 0.1 °C.

4.1.5.2 Spectroscopic Results The peracetyl gluconic surfactants were examined at 0.3 wt% in CO₂ at 40 °C and with water loading of $W = 10$. In each case, the CO₂-surfactant solutions were compressed to pressures above the reported cloud point pressure. Specifically, the sodium carboxylate, ammonium carboxylate, and ethyl sodium sulfate forms of the peracetyl gluconic were pressurized to 38, 44.8, and 48.3 MPa, respectively. There was no apparent methyl orange absorption, however, indicating that there was no tendency of the surfactants to form reverse micelles or polar microenvironments. Visual observation showed that, while water was dissolved into the CO₂, dry methyl orange was being left on the surface of the vessel, thus indicating that none of the water in the CO₂-rich phase existed in the form of a bulk water pool within the core of reverse micelles.

4.2 IONIC SURFACTANTS WITH PPG TAILS

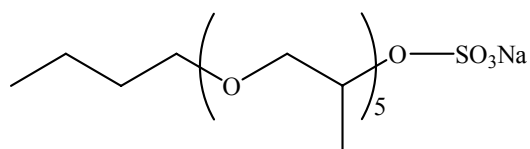
4.2.1 Materials

Poly(propylene glycol) monobutyl ether ($M_n=340, 1000$), pyridinium sulfur trioxide, sodium bicarbonate, fumaryl chloride, sodium hydrogen sulfite were purchased from Aldrich and used as received. All other reagent and solvents were obtained from Aldrich and used without further purification. N_2 (99.995%) and CO_2 (99.99%, Coleman grade) were purchased from Penn Oxygen.

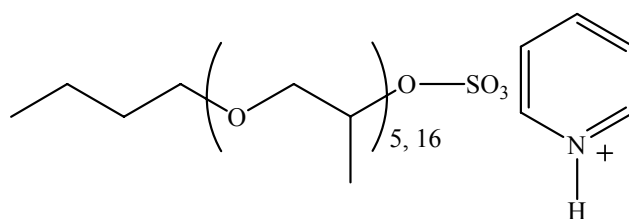
4.2.2 Synthesis

Poly (Propylene Glycol) MonoButyl Ether (PPGMBE) is a secondary alcohol containing propylene oxide repeat units. PPGMBE of different molecular weights ($M_n=340, 1000$) have been identified to be extremely CO_2 soluble at very low pressure. Three kinds of ionic surfactants with sodium sulfate, pyridinium sulfate, and sodium sulfosuccinate head groups were designed and synthesized. The synthesis of PPG-based ionic surfactants with sodium sulfate and pyridinium sulfate head groups were carried out with the help of Dr. Hamilton's group of Chemistry Department at Yale University.[95] AOT (sodium bis-2-ethyl-1-hexyl sulfosuccinate) is a commercially widely used aqueous surfactant, but it doesn't dissolve in CO_2 at all. Sodium bis (3,5,5-trimethyl-1-hexyl) sulfosuccinate (AOT-TMH) with highly methyl branched tail as an AOT analogue was first synthesized by Nave and Eastoe,[60] considering that the pendant methyl groups in the outer blocks have a much lower surface energy (cohesive energy density) than the CH_2 group. Therefore, PPGMBE 340 is combined with the sodium sulfosuccinate head to form a twin tailed AOT analogue as an ionic surfactant. The structures of PPG-based single and twin tailed ionic surfactants are shown in Figure 4.10. The reaction scheme is shown as follows in Figure 4.11, with the synthesis of PPGMBE 340 sodium sulfate as an example. The

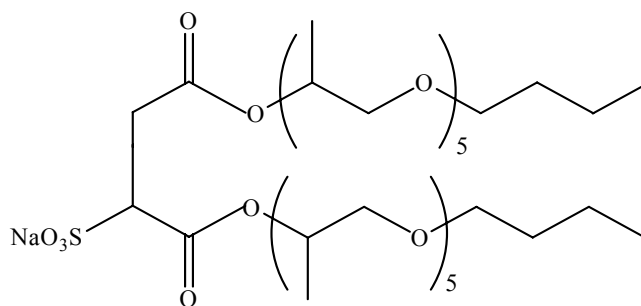
reaction route for the synthesis of sodium bis(PPGMBE 340) sulfosuccinate (AOT Analogue) is shown in Figure 4.12.



PPGMBE 340 Sodium Sulfate (a)



PPGMBE 340, 1000 Pyridinium Sulfate (b, c)



Sodium bis(PPGMBE 340) Sulfosuccinate (d)

Figure 4.10. Structures of peracetyl gluconic-based ionic surfactants.

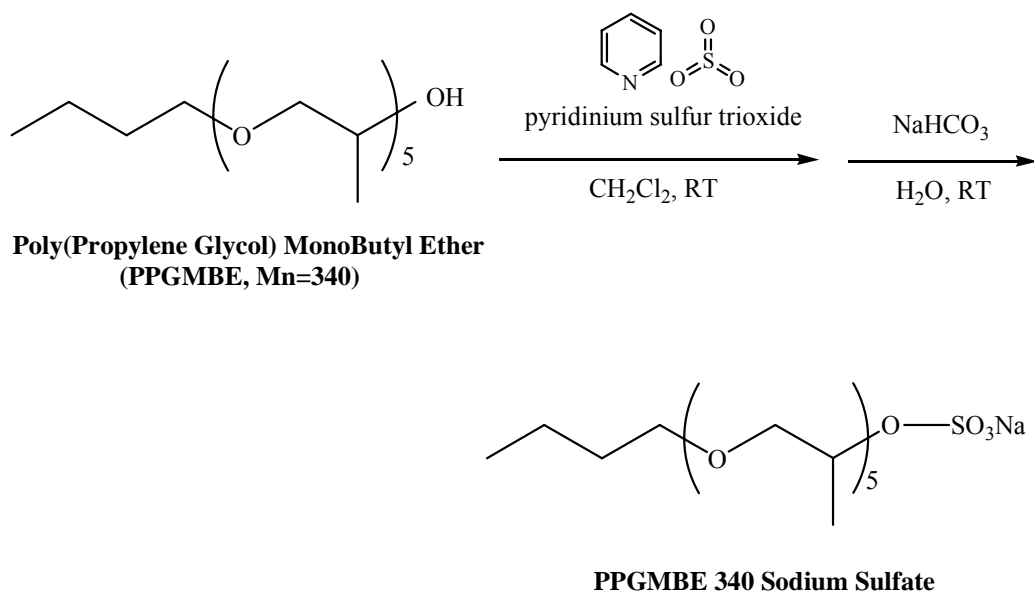


Figure 4.11. Reaction scheme for the synthesis of PPGMBE 340 sodium sulfate.

Synthesis of PPGMBE 340 Sodium Sulfate (Figure 4.10 a)

Poly(propylene glycol) monobutyl ether ($M_n = 340$, 10 g, 29.4 mmol) was dissolved in dichloromethane (150 mL), pyridine sulfur trioxide (10 g, 62.83 mmol) was added, and the mixture was stirred at room temperature for 12 h. The reaction mixture was filtered through a pad of Celite and solvent removed to give the pyridinium salt. The pyridinium salt was dissolved in water (100 mL), and sodium bicarbonate was added until no further effervescence was observed. The resultant mixture was frozen and water was removed using a freeze-dryer to give yellow viscous liquid. Mass spectrum showed that the number-average molecular weight for PPGMBE ($M_n = 340$) sodium sulfate is 445.3. (Appendix A Figure A.7)

Synthesis of PPGMBE 340, 1000 Pyridinium Sulfate (Figure 4.10 b, c)

Poly(propylene glycol) monobutyl ether ($M_n = 340$, 10 g, 29.4 mmol) was dissolved in dichloromethane (150 mL), pyridine sulfur trioxide (10 g, 62.83 mmol) was added, and the mixture was stirred at room temperature for 12 h. The reaction mixture was filtered through a pad of Celite and solvent removed to give the PPGMBE ($M_n = 340$) pyridinium salt. PPGMBE ($M_n = 1000$) pyridinium sulfate was synthesized in the similar way.

Mass spectra showed that the number-average molecular weight for PPGMBE ($M_n = 340$) pyridinium sulfate and PPGMBE ($M_n = 1000$) pyridinium sulfate is 515.2 and 1178.6, respectively.

Synthesis of Na Bis(PPGMBE 340) Sulfosuccinate (AOT Analogue) (Figure 4.10 d)

The esterification of alcohol and fumaryl chloride followed the procedure described by Nave et al.[60] Poly(propylene glycol) monobutyl ether ($M_n = 340$, 10.41 g, 30.62 mmol) and anhydrous THF (60 mL) were charged in a 250 mL three-neck round-bottom flask equipped with a stirring bar and condenser under a steady flow of nitrogen. After cooling to 0 °C, fumaryl chloride (2.81 g, 18.36 mmol) was added dropwise. The reaction mixture was stirred for the next 24 h at room temperature. After rotary evaporation of THF, the mixture was dissolved in 100 mL of diethyl ether and washed with 50 mL of 1 N HCl, 50 mL of saturated NaHCO_3 , and 50 mL of saturated NaCl solutions sequentially. The ether extract was dried over anhydrous Na_2SO_4 and filtered and then ether was removed by rotary evaporation. A pale yellow oil of diester product was obtained with 89% yield (10.37 g). The diester was subject to sulfonation with sodium hydrogen sulfite following the procedure provided by Baczko et al.[104] Sodium hydrogen sulfite (0.89 g, 8.55 mmol) in water (60 mL) was added dropwise to a solution of the diester (5 g, 6.58 mmol) in 2-propanol (80 mL) (both solutions were previously degassed with nitrogen for 20 min). The reaction mixture was then refluxed for the next 24 h. After rotary evaporation of the solvent, the residue was dissolved in chloroform and dried over Na_2SO_4 followed by removal of the solvent and drying of the resulting paste under a vacuum desiccator overnight. A yellow viscous liquid was obtained (4.2 g, yield 74%) The FTIR spectra showed the disappearance of the OH peak at 3471 cm^{-1} and appearance of carbonyl peak at 1723 cm^{-1} . (Appendix A Figure A.8-9) Mass spectrum showed that the number average molecular weight for sodium bis(PPGMBE 340) sulfosuccinate is 913.5. (Appendix A Figure A.10)

4.2.3 Phase Behavior Results

The PPGMBE 340 pyridinium sulfate was insoluble in CO₂. Figure 4.13 illustrates that the PPGMBE 340 sodium sulfate is CO₂-soluble; however, indicating that the sodium counterion is less CO₂ phobic than the pyridinium counterion. The PPGMBE 1000 pyridinium sulfate can dissolve in CO₂, indicating that the longer PPG segment of the tail made the surfactant with the pyridinium sulfate more CO₂ soluble. The addition of water lowers the cloud point pressure, as shown by the PPGMBE 1000 pyridinium sulfate dissolving in CO₂ at 40 °C and concentrations of 0.1-0.6 wt% with at $W = 10$. W^{corr} is 0 for W value of 10 over PPGMBE 1000 pyridinium sulfate concentrations up to 0.5 wt% at 40 °C. In each case, the limiting solubility of this surfactant in CO₂ is approximately 0.5 wt%. Single phase solutions could not be realized at W values of 40, even at surfactant concentrations as low as 0.1 wt%.

The phase behavior of mixtures of CO₂ and a twin tailed sodium bis(PPGMBE 340) sulfosuccinate, Figure 4.10 d, was also determined. This PPG twin tailed AOT analogue surfactant is 2 wt% soluble in CO₂, and its solubility in CO₂ decreases with the addition of water at W value of 10, as shown in Figure 4.13. W^{corr} is 0 for W value of 10 over sodium bis(PPGMBE 340) sulfosuccinate concentrations up to 0.5 wt% at 40 °C. Single phase solutions could not be realized at W values of 40, even at surfactant concentrations as low as 0.1 wt%.

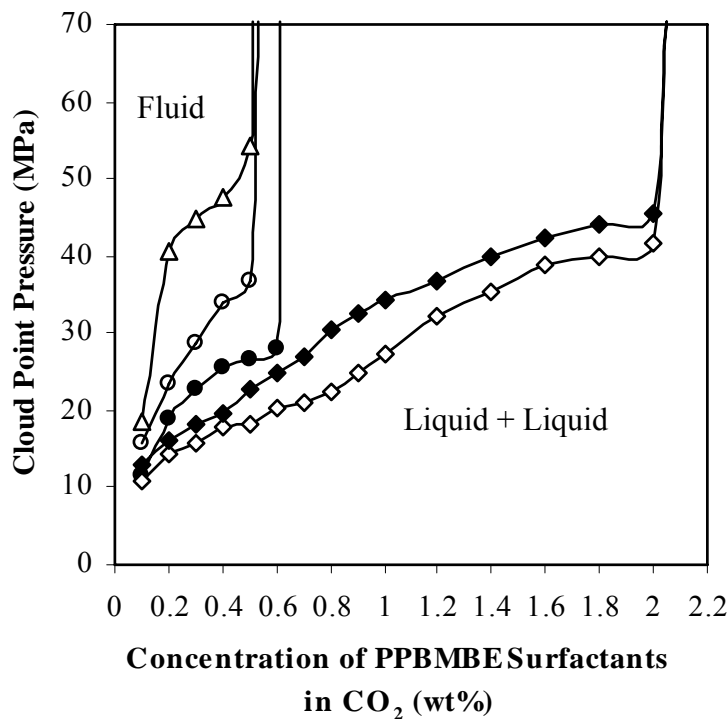


Figure 4.13. Phase behavior of PPGMBE surfactants/ CO_2 mixtures at $40\text{ }^\circ\text{C}$. PPGMBE 340 sodium sulfate, $W=0$ (Δ); PPGMBE 1000 pyridinium sulfate, $W=0$ (\circ); PPGMBE 1000 pyridinium sulfate, $W=10$ (\bullet); Sodium bis(PPBMBE 340) sulfosuccinate, $W=0$ (\diamond); Sodium bis(PPBMBE 340) sulfosuccinate, $W=10$ (\blacklozenge). (Appendix A Figure A.11. Surfactant concentration in mM).

4.2.4 Spectroscopic Results

It was difficult to attain a single phase solution with the PPG-based surfactants, possibly due to the less intense mixing in the UV-vis cell and/or the instability of these surfactants exhibited during the weeks between their synthesis and their evaluation for water uptake. Therefore no evidence of reverse micelle formation was obtained for these surfactants.

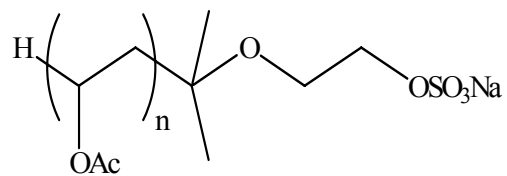
4.3 IONIC SURFACTANTS WITH OLIGO(VINYL ACETATE) TAILS

4.3.1 Materials

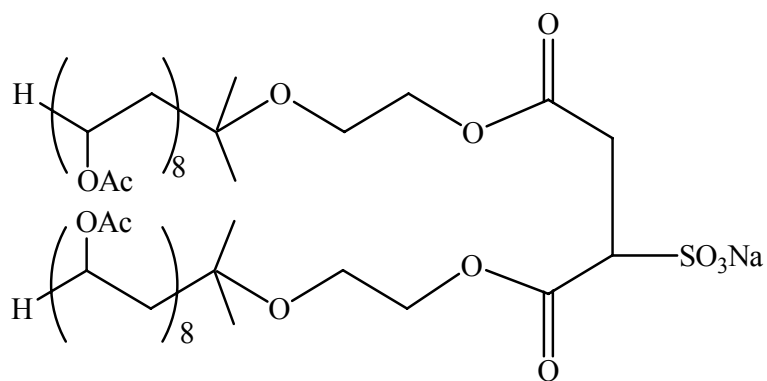
Chlorosulfonic acid, pyridine, sodium hydroxide, sodium carbonate, sodium bicarbonate, fumaryl chloride, sodium hydrogen sulfite were purchased from Aldrich and used as received. The 2,2'-azobisisobutyronitrile (AIBN) was recrystallized in methanol, and vinyl acetate was passed through an inhibitor remover column to remove the inhibitor prior to use. All other reagent and solvents were obtained from Aldrich and used without further purification. N₂ (99.995%) and CO₂ (99.99%, Coleman grade) were purchased from Penn Oxygen.

4.3.2 Synthesis

Oligomerization of vinyl acetate was carried out using AIBN as a free radical initiator with 2-isopropoxyethanol being both the solvent and chain-transfer agent. Hydroxy-functional oligo(vinyl acetate) was then transformed to single tailed oligo(vinyl acetate) sodium sulfate and twin tailed sodium bis(vinyl acetate)₈ sulfosuccinat (AOT analogue) surfactants. The structures of oligo(vinyl acetate)-based ionic surfactants are shown in Figure 4.14. The reaction scheme for the synthesis of single-tailed oligo(vinyl acetate) sodium sulfate is shown as follows in Figure 4.15. The reaction route for the synthesis of twin tailed sodium bis(vinyl acetate)₈ sulfosuccinate (AOT Analogue) is similar to that of sodium bis(PPGMBE 340) sulfosuccinate as shown previously.



Oligo(Vinyl Acetate) (n=6,10, or 17) Sodium Sulfate (a, b, c)



Sodium bis(Vinyl Acetate)8 Sulfosuccinate (d)

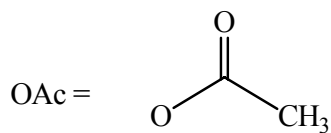


Figure 4.14. Structures of oligo(vinyl acetate)-based ionic surfactants.

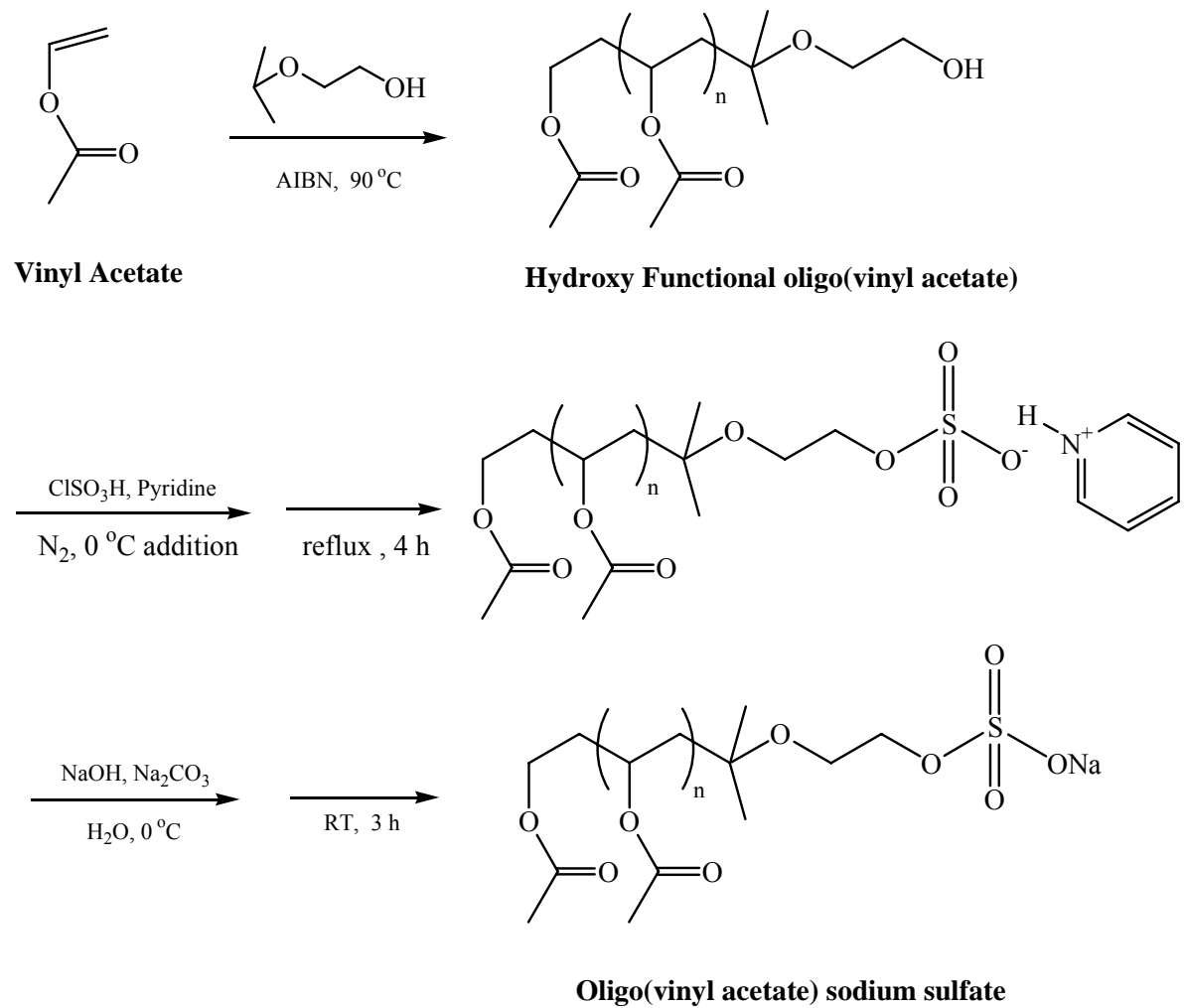


Figure 4.15. Reaction scheme for the synthesis of oligo(Vinyl Acetate) sodium sulfate.

Synthesis of hydroxy-functional oligo(vinyl acetate)

The preparation of hydroxy-functional oligo(vinyl acetate) followed the method of Zimmermann et al.[105] For a typical experiment, a solution of AIBN (0.04 g, 0.24 mmol) in 2-isopropoxyethanol (10 mL) (previously degassed for 15 min) was added to a solution of vinyl acetate (20 g, 232 mmol) in 2-isopropoxyethanol (190 mL) (previously degassed in a 3-neck 500 mL round-bottom flask by bubbling through nitrogen for 30 min). The reaction mixture was refluxed at 90 °C under a N₂ blanket for 24 h. The solvent was removed by rotary evaporation followed by vacuum desiccation at 90 °C overnight. A viscous yellow liquid of hydroxyl-functional oligo(vinyl acetate) with 10 repeat units, designated PVAc10, was recovered (15.8g, yield 79%). ¹H NMR δ_H (CDCl₃): 4.90 (10H, CH), 4.09 (2H, CH₂), 3.59 (2H, CH₂), 3.43 (1H, OH), 2.04 (30H, CH₃), 1.84 (20H, CH₂), 1.20 (6H, CH₃). ¹H NMR spectra showed DP_n=10 and Mn=964 g/mol. Table 4.2 lists the experimental data for the number of repeat units and number average molecular weight of four PVAc-OH samples obtained from the NMR spectra by the polymerization of vinyl acetate in 2-isopropoxyethanol. The concentration of vinyl acetate monomer in 2-isopropoxyethanol was varied to control the molecular weight at constant concentration ratio of AIBN to VAc at 0.1%. Hydroxy-functional oligo(vinyl acetate) with repeat unit of 6, 8, 10, and 17 as determined through NMR spectra were obtained and represented as PVAc6-OH, PVAc8-OH, PVAc10-OH, and PVAc17-OH respectively. The functional hydroxyl end group was verified by FTIR spectra. (Appendix A Figure A.12-19)

Table 4.2. Experimental Data for PVAc-OH Oligomers from ^1H NMR at
 $[\text{AIBN}]/[\text{VAc}]=0.1\%$.

	$[\text{VAc}]^{\text{a}}$ (mol %)	DP_n (^1H NMR)	Mn (^1H NMR, g/mol)
PVAc6-OH	6.3	6	620
PVAc8-OH	8.2	8	792
PVAc10-OH	11.8	10	964
PVAc17-OH	18.6	17	1566

^a Molar Ratio of $[\text{VAc}]/([\text{VAc}]+[2\text{-isopropoxyethanol}])$

Synthesis of oligo(vinyl acetate) sodium sulfate surfactants, Figures 4.14 a,b,c

The oligo(vinyl acetate) sodium sulfate surfactants were prepared according to Murphy and Taggart's procedure.[106] In a typical experiment, chlorosulfonic acid (0.45 mL, 6.76 mmol) was added dropwise to pyridine (10 mL) in a 250 mL round-bottom flask placed in an ice bath. The solution was stirred vigorously during the dropwise addition. A solution of hydroxy-functional oligo(vinyl acetate) PVAc10-OH (5 g, 5.19 mmol) in pyridine (50 mL) was slowly added to the above solution, and cooling and stirring were continued. The contents of the flask were refluxed for about 4 h until a clear yellow solution was formed. The reaction was then quenched and the product converted to the sodium salt by pouring the contents into an ice-cooled sodium hydroxide and sodium carbonate solution (0.27 g NaOH and about 30-40 g Na_2CO_3 in 100 mL deionized water). The reaction mixture was stirred at room temperature for 3 h. The resulting oligo(vinyl acetate) surfactant solution was extracted using n-butanol (2 x 50 mL). The combined organic layers were dried over anhydrous sodium sulfate and filtered. Evaporating the solvents of pyridine and n-butanol by rotary evaporation followed by

vacuum desiccation gave a dark yellow product of PVAc10-SO₃Na (4.86 g, yield 87.9 %, Mn= 1066 g/mol). The NMR spectra of PVAc6, 10, 17-OSO₃Na were illustrated in Appendix A Figure A. 20-22.

Synthesis of sodium bis(vinyl acetate)8 sulfosuccinate, Figure 4.14 d

Twin tailed oligo(vinyl acetate) AOT analogue was synthesized using the PVAc8-OH in a similar way as the PPGMBE (Mn=340) twin tailed AOT analogue that was described previously. A yellow viscous liquid was recovered as product and confirmed by the disappearance of the FTIR peak at approximately 3500 cm⁻¹ (-OH) and the appearance of carbonyl peak at 1741 cm⁻¹. (Appendix A Figure A. 23-24)

4.3.3 Phase Behavior Results

Single tailed oligo(vinyl acetate) sodium sulfate surfactants, Figures 4.14 a,b,c

Viscous liquid oligo(vinyl acetate) sodium sulfate surfactants (Mn=722, 1066, 1668 g/mol) exhibit remarkably high solubility in CO₂, as shown in Figure 4.1. These levels of CO₂ solubility for an ionic surfactant are comparable to those reported for fluorinated surfactants,[11] greater than the other oxygenated hydrocarbon surfactants developed during this work, and greater than those reported for branched hydrocarbon AOT analogs.[62] The PVAc-OSO₃Na surfactants consisting of 6, 10, or 17 repeat units exhibit CO₂ solubility of 4, 7 and 2.5 wt%, respectively, at room temperature and pressure less than 50 MPa. The occurrence of an optimal tail length, 10 repeat units in this case, has been previously observed in the design of surfactants with PFPE tails, and can be attributed to two competing trends. As the number of repeat units in vinyl acetate oligomer decreases, the oligomer itself becomes more CO₂ soluble; however, as the

length of the oligomeric tail decreases the surfactant becomes more hydrophilic (and CO₂ phobic) as the influence of the ionic group becomes more pronounced.[59]

The solubility of oligo(vinyl acetate) surfactant decreases with increasing temperature, i.e., the pressure required to achieve miscibility with CO₂ is higher at 40 °C than it is at 22 °C, as represented in Figure 4.16. The solubility of the oligo(vinyl acetate) surfactant in CO₂ also decreases with the addition of water at W value of 10. The surfactant solubility drops to 0.5 wt% at these conditions. W^{corr} is 0 for W value of 10 over PVAc10-OSO₃Na concentrations up to 0.5 wt% at 40 °C. Single phase solutions could not be realized at W values of 40, even at surfactant concentrations as low as 0.1 wt%.

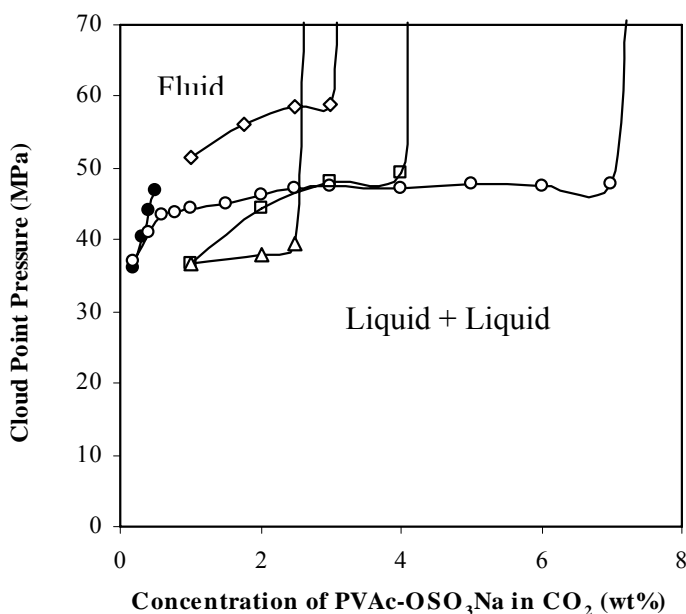


Figure 4.16. Phase behavior of PVAc-OSO₃Na/CO₂ mixtures. PVAc6-OSO₃Na, 22 °C, W=0 (●); PVAc10-OSO₃Na, 22 °C, W=0 (○); PVAc17-OSO₃Na, 22 °C, W=0 (△);

PVAc10-OSO₃Na, 22 °C, W=10 (●); PVAc10-OSO₃Na, 40 °C, W=0 (◇). (Appendix A Figure A.25. Surfactant concentration in mM).

Twin tailed sodium bis(vinyl acetate)8 sulfosuccinate, Figure 4.14 d

The sodium bis(vinyl acetate)8 sulfosuccinate AOT analogue consisting of twin tails of 8 repeat units on each tail (Mn= 1747 g/mol) was a viscous liquid that exhibited CO₂ solubility up to 3 wt% at 22 °C and pressure less than 40 MPa, as shown in Figure 4.17. The solubility decreases with the addition of water at W= 10. This surfactant was the only one (of those illustrated in Figure 4.14) capable of solubilizing water to W values as high as 50, at surfactant concentrations up to 1 wt%. Table 4.3 lists W and W^{corr} for the sodium bis(vinyl acetate)8 sulfosuccinate surfactant in water and CO₂ mixture at different weight percents and 22 °C.

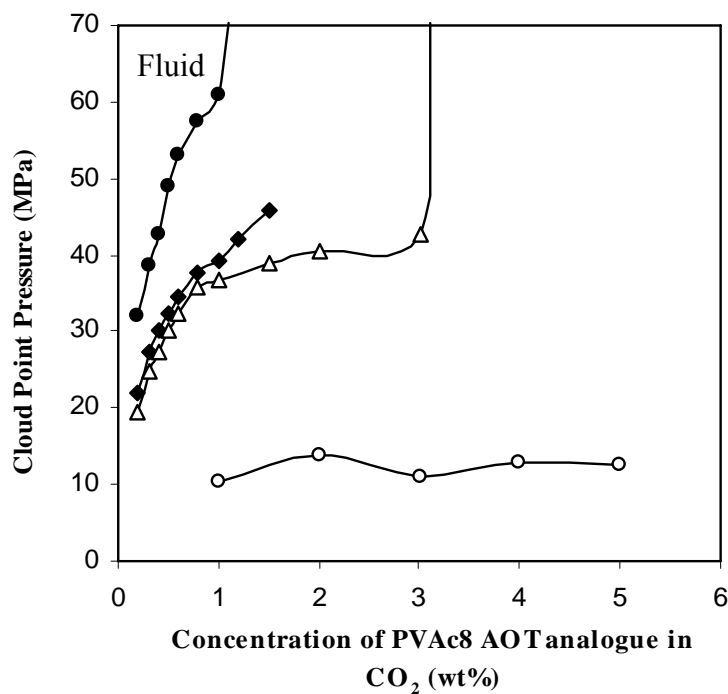


Figure 4.17. Phase behavior of sodium bis(vinyl acetate)₈ sulfosuccinate/CO₂ mixtures at 22 °C. W = 0 (Δ); W = 10 (◆); W = 50 (●). Sodium bis(dodecafluoroheptyl) sulfosuccinate, W=0 (o). [10] (Appendix A Figure A.26. Surfactant concentration in mM).

Table 4.3. W and W^{corr} for sodium bis(vinyl acetate)₈ sulfosuccinate in water and CO₂ mixture at different weight percents and 22 °C. *When the amount of water is not sufficient to saturate the CO₂, W^{corr} is reported as 0.

Sodium bis(vinyl acetate) ₈ sulfosuccinate Concentration, wt%	Temperature, °C	W	W ^{corr} *
0.2-1.5	22	10	0
0.15-0.3	22	50	0
0.4	22	50	10.80
0.5	22	50	17.83
0.6	22	50	22.51
0.8	22	50	28.87
1	22	50	32.69

4.3.4 Spectroscopic Results

The single tailed PVAc₁₀-OSO₃Na was loaded at 0.15 wt% with water loading of W = 10 (W^{corr}=0, 0.025 wt%) and methyl orange at 4.7 x 10⁻⁵ M. The system was pressurized to 38 MPa at 25 °C and stirred for 1 hour. After this mixing period, a methyl orange peak

was observed at 422 nm implied the formation of water-in-CO₂ (w/c) reverse microemulsions. The twin tailed sodium bis(vinyl acetate)8 sulfosuccinate AOT analogue was loaded at 0.15 wt% with water loading of $W = 10, 20, 30, \text{ and } 40$, respectively, (0.015 wt%, 0.03 wt%, 0.045 wt%, and 0.06 wt%, respectively) at $W^{\text{corr}} = 0$, and methyl orange at 4.7×10^{-5} M. After pressurizing to 34.5 MPa at 22 °C, the system was allowed to mix for over an hour to reach a single phase microemulsion. Figure 4.18 shows the UV-vis spectra for the twin tailed sodium bis(vinyl acetate)8 sulfosuccinate w/c reverse microemulsion system. As shown in Figure 4.18, the UV absorption peaks which assigned at about 423 nm indicate the formation of the water-in-CO₂ reverse microemulsions. The intensity of the methyl orange peak increases with the loading water ranging from $W = 10$ to 40, which indicates that the concentration of methyl orange within the microemulsions increases as the amount of loading water increases. However, the absorption maximum wavelength, λ_{max} , doesn't shift to higher wavelengths, which implies the polarity of the microenvironment within the reverse micelles doesn't increase as the increasing of water amount loaded to the system. Methyl orange dissolved in bulk water results in an absorption maximum wavelength at 464 nm. The absorption bands of ~423 nm in these studies indicate that the microenvironment within the reverse micelles of the ionic surfactants with PVAc tails is similar to that of neat methanol (methyl orange absorption at ~421 nm), and slightly more polar than that of the cores of dry PFPE-COONH₄ reverse micelles (~416 nm).[68, 69] Whereas the twin tailed vinyl acetate based surfactants lead to high water loading values up to $W=50$, the methyl orange solubilities and polarities are rather limited. This can be attributed to the relatively low corresponding weight percent of water caused by the low surfactant loading

concentration and the high molecular weight and the $W^{\text{corr}} = 0$ at these conditions, which means the amount of water added to the system would be insufficient to saturate the CO_2 .

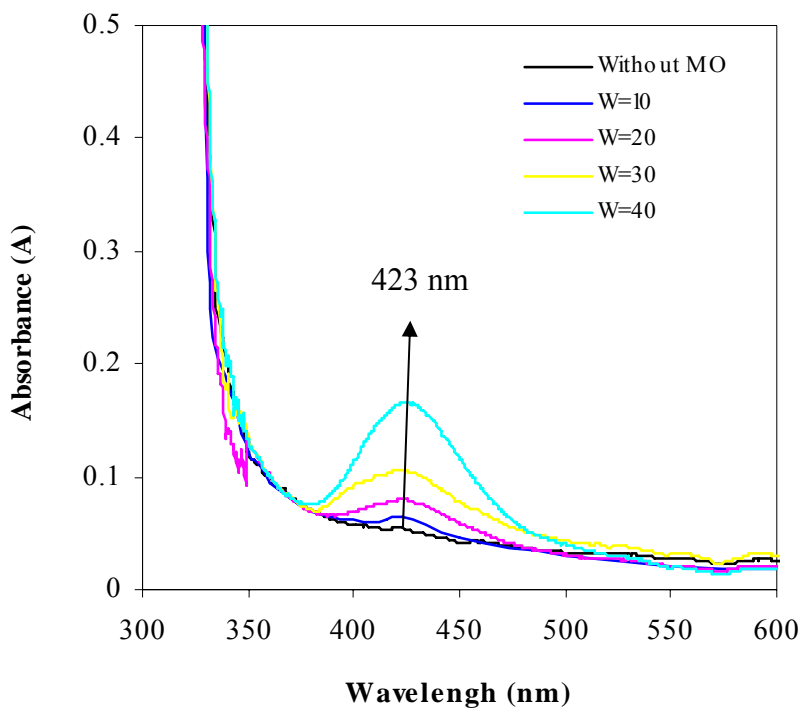


Figure 4.18. UV-vis absorption spectra of methyl orange in 0.15 wt% twin tailed sodium bis(vinyl acetate)8 sulfosuccinate based water-in- CO_2 reverse microemulsions with different loading of water at 34.5 MPa and 25 °C.

4.4 DISCUSSIONS

4.4.1 Modeling Results

Wang and Johnson[95] have optimized the geometries and calculated the binding energies for a single water molecule interacting with an isopropyl acetate (IPA) molecule. Two different binding modes were found for the IPA/H₂O system. As shown in Figure 4.19, for mode (A) the water molecule mainly interacts with the carbonyl oxygen. For mode (B) H₂O binds mainly with the ether oxygen. The interaction energies for the two modes are listed in Table 4.4. The interactions between IPA and water molecules as shown in Table 4.4 are much stronger than the strongest binding energy between IPA and CO₂. [54] The calculations therefore predict that the tails of the acetate functionalized surfactants (Figure 4.1a-c, Figure 4.14 a-d) are hydrophilic.

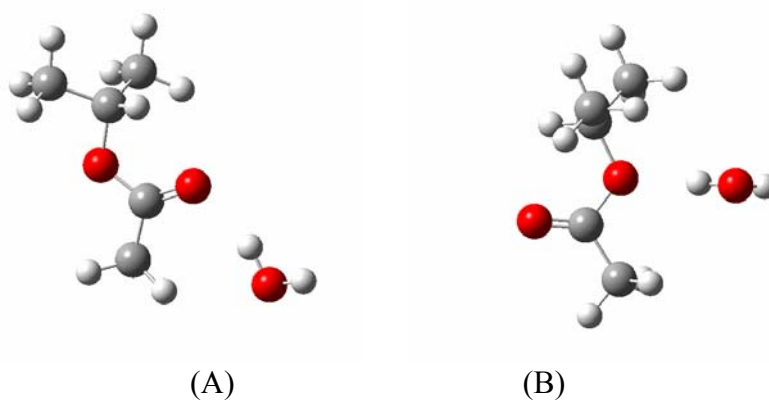


Figure 4.19. Two different binding modes for the isopropyl acetate/H₂O system. (white = H, gray = C, red = O).

Table 4.4 Interaction energies for several different dimers related to the CO₂/H₂O surfactant systems. The energies are computed at the MP2/aug-cc-pVDZ level of theory.

	IPA/H ₂ O		IPA/CO ₂ [*]	H ₂ O/H ₂ O [107]		CO ₂ /CO ₂	
	(A)	(B)				T-shape	Slipped parallel
Interaction energy (kJ/mol)	-27.0	-21.3	-15.9	-19.6	-20.7 ^{**}	-5.1	-5.8

* There are actually three binding modes for the IPA/CO₂ dimer. We chose the mode that has the strongest interaction energy for comparison.[54]

** The value is calculated at the MP2 level of theory and extrapolated to the complete basis set limit.[107]

4.4.2 Water Solubility Values of Three Acetate Functionalized Surfactants

Furthermore, experiments were performed to measure the water solubility of peracetyl gluconic sodium carboxylate (Figure 4.1b), peracetyl gluconic ammonium carboxylate (Figure 4.1c), and oligo(vinyl acetate)10 sodium sulfate (Figure 4.14b). 20 μL of water was initially added to 0.08 g of surfactant (80 wt%), then water was gradually added to the mixture followed by stirring the mixture using a Vortex-Genie® 2 mixer until the surfactant was completely dissolved. The measured solubilities are reported in Table 4.5 and clearly show that both peracetyl surfactants are significantly more water soluble than the vinyl acetate-based surfactant. The head groups on the peracetyl- and vinyl acetate-based surfactants are not identical. However, the sodium sulfate head group of (Figure

4.14b) should make that surfactant more water soluble than the sodium carboxylate head group of (Figure 4.1b) and ammonium carboxylate head group of (Figure 4.1c).

Therefore, we expect that the differences in water solubility are due to the composition of the tail groups is larger than the head groups indicated by the data in Table 4.5.

Table 4.5. Water solubility values of three acetate functionalized surfactants

Surfactant	Water solubility (wt%)
Peracetyl gluconic sodium carboxylic (Figure 4.1b)	64 %
Peracetyl gluconic ammonium carboxylic (Figure 4.1c)	73 %
Oligo(vinyl acetate)10 sodium sulfate (Figure 4.13b)	40 %

4.4.3 Effects of the Addition of Water in Surfactants/CO₂ Systems

The addition of water to CO₂ mixtures containing acetate-based surfactants resulted in an increase in the cloud point pressures. Water molecules will compete with CO₂ molecules for binding to the acetate groups. The acetate tail groups will preferentially bind with water molecules because of the more favorable binding energies (see Table 4.4), thus lowering the CO₂ solubilities of the surfactants. Experiments have shown that the addition of water does indeed increase the cloud point pressures of two of the peracetyl gluconic-based surfactants (Figure 4.1b,c) and also of the PVAc single/twin tailed surfactants (Figure 4.14a-d). These observations are consistent with our theoretical analysis. However, PGESS (Figure 4.1a) exhibits the opposite behavior, which couldn't dissolve in CO₂ in the absence of water, and its solubility increases as water is added.

This may be due to co-solvent effects with water. PGESS is insoluble in CO₂ because of its extremely polar head group. Adding water to the PGESS/CO₂ system acts to shield the sulfate head group from CO₂ and therefore increases the solubility. Therefore, water plays competing roles in the PGESS/CO₂ system. On one hand, it increases solubility by shielding the head group from the nonpolar CO₂ environment. On the other hand, water competes with CO₂ in binding to the CO₂-philic acetate tail.

4.4.4 Formation of the Reverse Micelles

The experiments have shown that only the PVAc-based surfactants can form reverse micelles. None of the peracetyl gluconic-based surfactants exhibit micelle formation, although their tail groups have similar structures to those of PVAc-based surfactants. The formation of micelles requires a tail that is sufficiently hydrophobic to drive water out of the bulk homogeneous phase into confined micelles. Our calculations indicate that the peracetyl tails are very hydrophilic. We therefore speculate that peracetyl tails do not have a large enough hydrophobic driving force to form micelles. In contrast, the methylene groups in the PVAc tails are relatively hydrophobic, which provides enough of an energetic driving force to stabilize the micelles. The difference in water solubilities of peracetyl gluconic-based surfactants and PVAc-based surfactants (Table 4.5) indicates that peracetyl tails are indeed more hydrophilic than PVAc tails. The difference in water solubilities provides a plausible explanation for the observation that PVAc-based surfactants form micelles while the surfactants with peracetyl gluconic tails do not.

5.0 PREPARATION OF SILVER NANOPARTICLES VIA CO₂- SOLUBLE HYDROCARBON-BASED METAL PRECURSOR

The objectives of this study were to determine the solubility of silver acetylacetonate and (if this solubility was low) to design a novel organometallic complex with much greater CO₂-solubility that could be used to form silver nanoparticles in CO₂ via reduction in the presence of fluorous or non-fluorous stabilizing thiols. Silver bis(3,5,5-trimethyl-1-hexyl)sulfosuccinate (Ag-AOT-TMH) was selected as the metal-ligand candidate because of the ease of its synthesis; simply requiring an ion exchange of the CO₂-soluble ionic surfactant AOT-TMH to yield Ag-AOT-TMH. Ion exchange of other ionic surfactants composed of oxygenated hydrocarbon tails was not successful due to the instability of the Ag⁺ counterion during the synthesis.

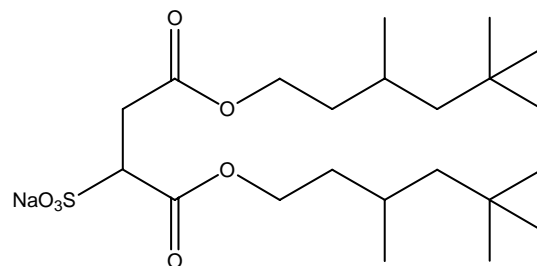
5.1 MATERIALS

Silver acetylacetonate, fumaryl chloride, 3,5,5-trimethyl-1-hexanol, sodium hydrogensulfite, silver nitrate, tert-nonyl mercaptan, 4-tert butylbenzenethiol, and solvents was purchased from Aldrich. The fluorocarbon thiol 1H,1H,2H,2H-

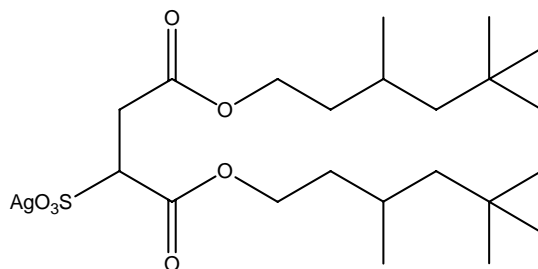
perfluorooctanethiol ($C_6F_{13}C_2H_4SH$) was obtained from Oakwood Product Inc. Poly(mercaptopropyl) methyl siloxane ($M_w=4000-7000$) was obtained from Gelest, Inc. Thiol terminated poly(ethylene oxide) ($M_n=2000$, $M_w=2100$) was obtained from Polymer Science, Inc. H_2 (99.999), N_2 (99.995%) and CO_2 (99.99%) gases were obtained from BOC gases and perfluorobutylmethyl ether (HFE-7100) was obtained from 3M. All chemicals were used as received.

5.2 Synthesis of a CO_2 -Soluble Hydrocarbon-based Silver Precursor

The structures of AOT-TMH and Ag-AOT-TMH are shown in Figure 5.1.



AOT-TMH (a)



Ag-AOT-TMH (b)

Figure 5.1. Structures of sodium bis(3,5,5-trimethyl-1-hexyl) sulfosuccinate (AOT-TMH) and silver precursor, silver bis(3,5,5-trimethyl-1-hexyl) sulfosuccinate (Ag-AOT-TMH).

Sodium bis (3,5,5-trimethyl-1-hexyl) sulfosuccinate (AOT-TMH) with highly methyl branched tail as an AOT analogue was first synthesized by Nave and Eastoe.[60] Ag-AOT-TMH was synthesized via the esterification of fumaryl chloride and 3,5,5-trimethyl-1-hexanol, sulfonation by sodium hydrogensulfite, then ion exchange by AgNO₃, as shown in Figure 5.2.

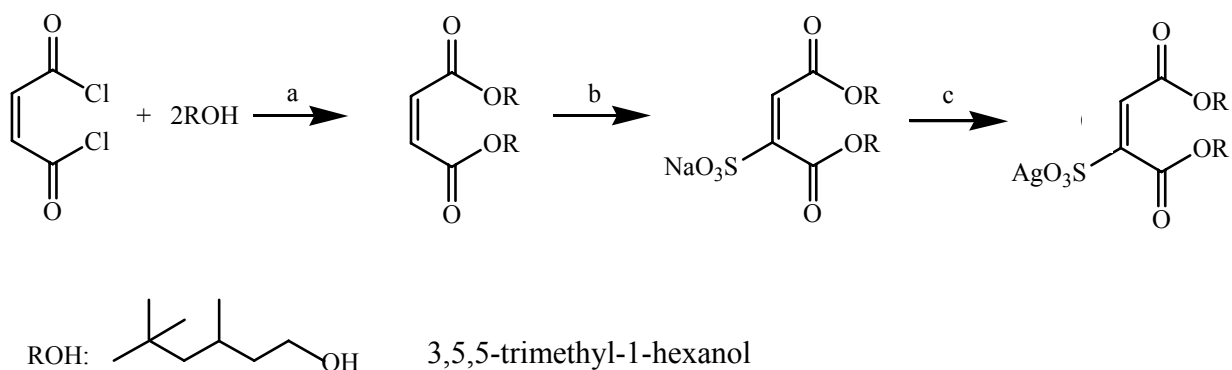


Figure 5.2. Synthesis of Ag-AOT-TMH (a) anhydrous THF, RT, 24 h; (b) NaHSO₃, ⁱPrOH-H₂O, 80 °C, 24 h; (c) AgNO₃, ethanol-H₂O, RT.

The glassware was oven-dried overnight and purge with ultra-high purity nitrogen before use. 3,5,5-trimethyl-1-hexanol (14.4 g, 100 mmol) and anhydrous THF (150 mL) were charged in a 500 mL 3-neck round-bottom flask equipped with a stirring bar and condenser under a steady flow of nitrogen. After cooling to 0 °C, fumaryl chloride (7.65 g, 50 mmol) was added dropwise. The reaction mixture was stirred for the next 24 h at room temperature. After rotary evaporation of THF, the mixture was dissolved in 100 mL diethyl ether, washed with 50 mL 1N HCl, 50 mL saturated NaHCO₃, and 50 mL saturated NaCl solutions sequentially. The ether extract was dried over anhydrous Na₂SO₄ and filtered, then ether was removed by rotary evaporation. 16.56 g pale yellow

oil of diester product was obtained with 90% yield. The obtained diester was subject to sulfonation with sodium hydrogensulfite. A solution of sodium hydrogensulfite (3.45 g, 32.56 mmol) in water (60 mL) (previously degassed for 15 min) was added dropwisely to a solution of the diester (6 g, 16.28 mmol) in isopropanol (80 mL) (previously degassed in a 3-neck round-bottom flask by bubbling through N₂ for 30 min). The reaction mixture was then refluxed for the next 24 h. After rotary evaporation of the solvent, the residue was dissolved in 100 mL ether and the water layer was extracted with ether (2×30 mL). The combined ether extraction was dried over anhydrous Na₂SO₄ and then filtered. White paste was yielded after removing ether. Traces of water were removed by redissolving the paste in chloroform followed by drying over Na₂SO₄. Chloroform was removed by rotary evaporation and the resulting paste was dried under vacuum oven at 40 °C overnight. White solid of AOT-TMH was obtained (5.77 g, yield 75%), which was then transformed to Ag-AOT-TMH via ion exchange. A silver nitrate (5.025 g, 29.58 mmol) aqueous solution (10 mL) was mixed with AOT-TMH (0.8297 g, 1.8 mmol) dissolved in ethanol (5 mL). After mixing for 6 h, ether (6 mL) was added which led to the formation of two separate phases. The lower phase containing NaNO₃ and excess AgNO₃ was removed to leave the upper phase containing the Ag-AOT-TMH. The upper phase was dried on a rotary evaporator, redissolved in isooctane, and centrifuged to separate any residual solids. Finally, isooctane was removed in a vacuum oven at room temperature, and yellow solid of Ag-AOT-TMH was received as product (0.82 g, 84%). The FTIR and ¹H NMR spectra of the intermediate diester and the sodium bis(3,5,5-trimethyl-1-hexyl) sulfosuccinate (AOT-TMH) are shown in Appendix B.1-3. Soil analysis indicates the Ag⁺ exchange for the Na⁺ is around 85% (Appendix B.4).

5.3 PHASE BEHAVIOR STUDY

5.3.1 Experimental Apparatus

The experimental setup of the phase behavior study with silver acetylacetonate, AOT-TMH, and Ag-AOT-TMH is the same as shown in Chapter 4.1.4.1.

5.3.2 Phase Behavior Results

The commercially available silver acetylacetonate was tested for CO₂ solubility at 40 °C. At concentrations as low as 0.01 wt% and pressures as high as 70 MPa, there was no evidence of dissolution, swelling or melting point reduction of the silver acetylacetonate particles.

The solubility of AOT-TMH and Ag-AOT-TMH in CO₂ were then evaluated. Figure 5.3 presents a pressure-composition diagram for this mixture at 40 °C. Although the AOT-TMH was initially insoluble when CO₂ was introduced, the solid surfactant melted in CO₂ immediately at room temperature and 13.8 MPa and then formed a single transparent solution after 1 h stirring at 1500 rpm. Figure 5.3 illustrates that the cloud point pressure increases with AOT-TMH concentration, reaching a limiting value of about 1 wt% at 50 MPa. Ag-AOT-TMH also melted in CO₂ immediately and reached a limiting solubility of 1.2 wt% at 52 MPa.

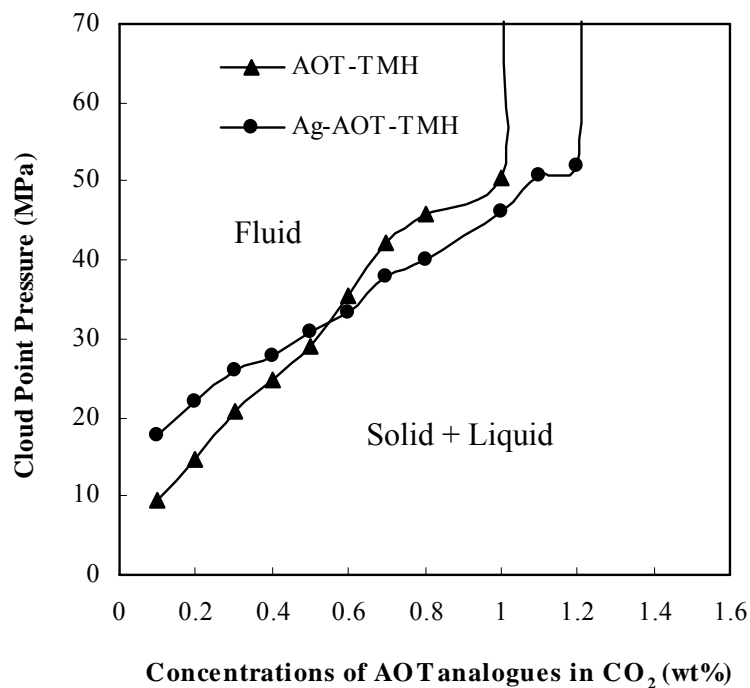


Figure 5.3. Phase behavior of AOT-TMH and Ag-AOT-TMH at 40 °C. (Appendix B Figure B.4. Surfactant concentration in mM).

5.4 SILVER NANOPARTICLE FORMATION

Silver nanoparticle formation experiment was carried out at Dr. Roberts' group in Chemical Engineering Department at Auburn University.[108]

5.4.1 Experimental Apparatus

Nanoparticles were synthesized in a 32 mL stainless steel high-pressure vessel equipped with pressure gauge, resistance temperature detector (RTD), and parallel quartz windows

for UV-vis characterization. A magnetic stir bar was used to facilitate mixing. The vessel was initially filled with 0.06 wt% Ag-AOT-TMH, 0.5 wt% fluorinated thiol. After sealing the vessel, an ISCO syringe pump was used to add specific quantity of CO₂ to the vessel to reach the desired pressure of 28.6 MPa. The temperature of the vessel was raised to 40 °C by using a heating tape which was wrapped around the vessel and connected to the temperature controller. The system was mixed for one hour to reach a single phase. Reducing agent was then injected by forcing in 200 μL of a 0.8 M NaBH₄/ethanol solution with additional carbon dioxide.

5.4.2 Nanoparticle Formation Results

The CO₂ solution turned into dark red color in less than 2 minutes after the introduction of the reducing agent, but unfortunately, due to the highly optical absorbance of the silver nanoparticles, the collection of accurate UV-vis data was not possible. The particles were stable in solution for 24 h as the solution maintained its visible red color. The vessel was subsequently depressurized, and the particles were redispersed in HFE-7100 and placed onto a transmission electron microscopy (TEM) grid for analysis.

Figure 5.4 shows the TEM image of silver nanoparticles. A statistical analysis of the TEM image yields an average size of 3.5 nm in diameter, a standard deviation of 0.8 nm, and the size distribution is shown in Figure 5.5. Energy dispersive spectroscopy (EDS) was also performed on the particles and identified that the particles consist of silver with the fluorinated thiol ligand present as indicated by the absorbance of silver, fluorine, and sulfur in Figure 5.6. The large copper peak is due to the copper support of the TEM

sample grid. This analysis reveals the effectiveness of the fluorocarbon thiol molecule as a stabilizing ligand on the silver nanoparticles.

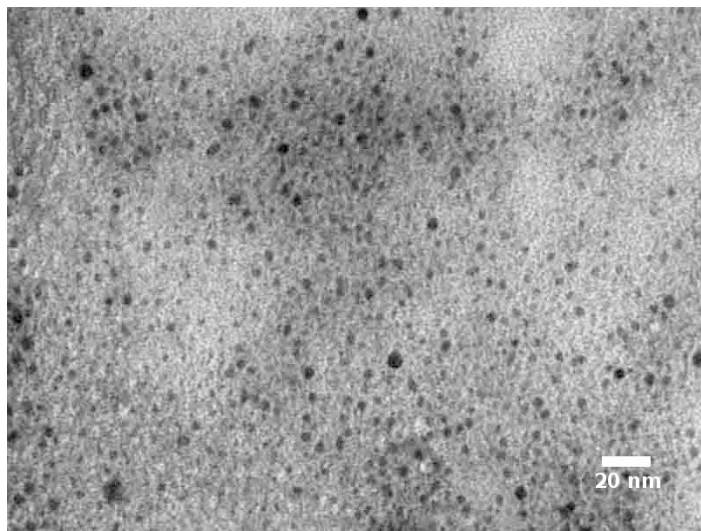


Figure 5.4. TEM Image of silver nanoparticles formed by reducing CO_2 solution containing Ag-AOT-TMH and fluorinated thiol stabilizing ligands using NaBH_4 as reducing agent.[108]

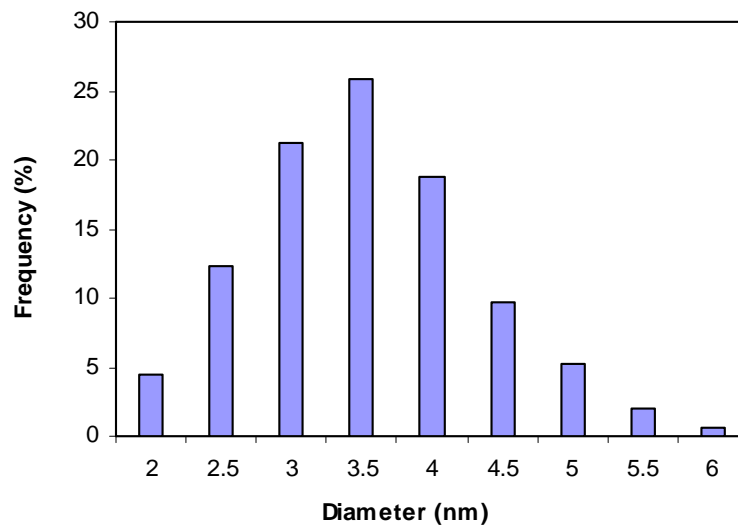


Figure 5.5. Size distribution of silver nanoparticles synthesized in CO₂. P = 28.6 MPa, t = 40 °C, [Ag-AOT-TMH] = 0.06 wt%, [Fluorinated Thiol] = 0.5 wt%.[108]

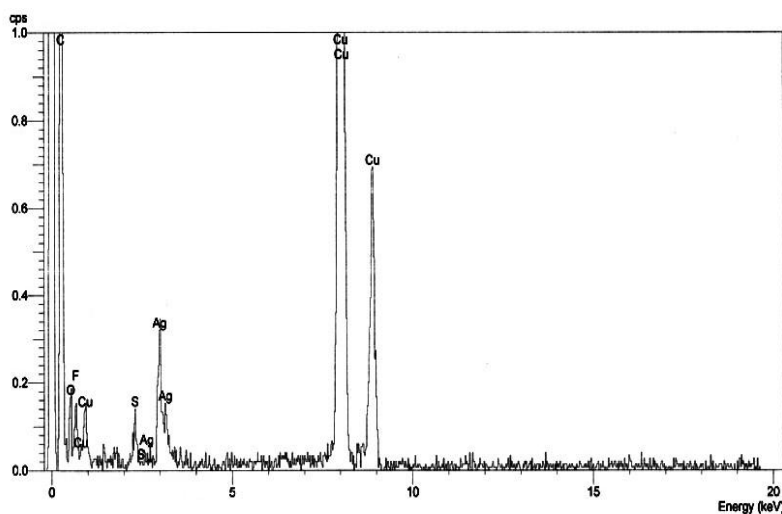
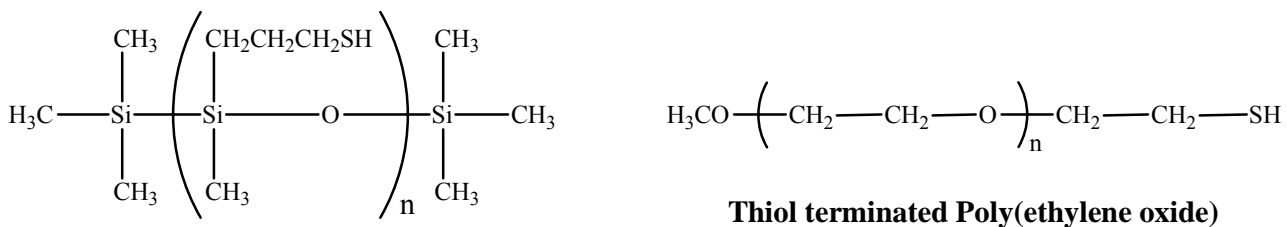


Figure 5.6. EDS measurement of the silver nanoparticles. The spectrum shows the presence of silver along with fluorine and sulfur indicating the presence of the fluorinated thiol stabilizing agent.[108]

5.5 NON-FLUOROUS THIOLS RESULTS

Non-fluorous thiols, including silicone-based, PEG-based, and hydrocarbon-based thiols, were also investigated for CO₂ solubility study and their abilities to stabilize nanoparticles in CO₂. Figure 5.7 shows the structures of silicone-based and PEG-based thiols investigated in this study. Poly(mercaptopropyl) methyl siloxane and thiol terminated poly(ethylene oxide) are insoluble in CO₂ at room temperature at concentrations as low as 1 wt%. Hydrocarbon-based thiols containing tert-butyl group, 4-tert-butylbenzenethiol and tert-nonyl mercaptan, are very miscible with CO₂ at moderate pressure values, as shown in Figure 5.8 and Figure 5.9. Tert-nonyl mercaptan is more branched than the 4-tert-butylbenzenethiol, and therefore is more miscible with CO₂. However, these hydrocarbon-based thiols were unable to disperse and stabilize the silver nanoparticles.



Poly(mercaptopropyl) methyl siloxane

Figure 5.7. Structures of silicone-based and PEG-based thiols investigated in this study.

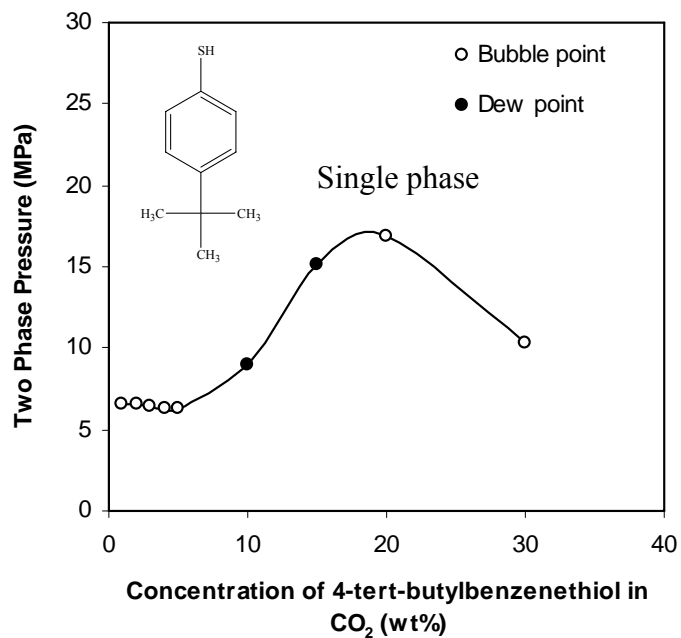


Figure 5.8. Phase behavior of 4-tert-butylbenzenethiol at 22 °C.

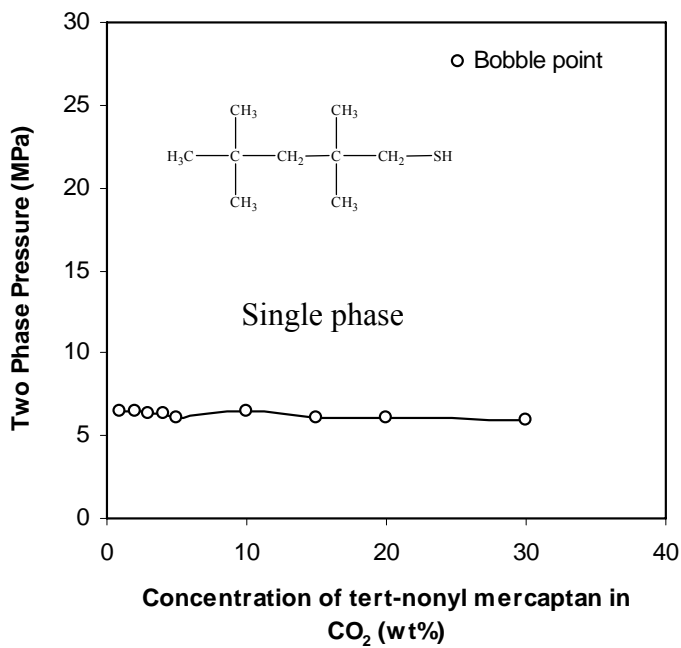


Figure 5.9. Phase behavior of tert-nonyl mercaptan at 22 °C.

5.6 CONCLUSIONS

A previously reported CO₂ soluble hydrocarbon complex, silver acetylacetonate, is less than 0.01 wt% CO₂ soluble at 40 °C and 70 MPa, whereas the Ag-AOT-TMH synthesized during this investigation can dissolve in CO₂ up to 1.2 wt% at 40 °C and 52 MPa. Silver nanoparticles (1–6 nanometers in diameter) were synthesized at 40 °C and 28.6 MPa from Ag-AOT-TMH in CO₂ using NaBH₄ as a reducing agent. A CO₂-soluble fluorinated thiol was used to sterically stabilize the silver nanoparticles, as evidenced by TEM and EDS analysis. Attempts to produce the silver nanoparticles in a completely non-fluorous system were unsuccessful because stabilization could not be attained with silicone-, PEG-, or hydrocarbon-based thiols.

6.0 STABLE DISPERSION OF SILVER NANOPARTICLES IN CARBON DIOXIDE WITH HYDROCARBON-BASED LIGANDS

6.1 STABLE DISPERSION OF NANOPARTICLES IN CARBON DIOXIDE WITH LIGANDS

In order to disperse particles in a given solvent, it is common to use ligands extending from the surface of the nanoparticles that can interact with the solvent molecules. Favorable interactions between the solvent molecules and the ligand tails provide enough repulsive force between particles to overcome the attractive Van der Waals forces that occur between particles in solution. Unfortunately, CO₂ is a poor solvent for most commonly available ligands and surfactants. As a result, fluorinated surfactants have been required to stabilize nanoparticles in CO₂ or to form microemulsions for the synthesis of nanoparticles within CO₂. Early studies showed the ability of these fluorinated compounds to support water in CO₂ microemulsions[68, 69] based on better surfactant tail – solvent interactions. These water in CO₂ microemulsion systems have since been used to form a variety of nanoparticles in CO₂[109-115]. The need for surfactants, and a separate water phase, during synthesis of nanoparticles in CO₂ was

eliminated by Shah et al.[81, 82] and McLeod et al.[75] They synthesized and subsequently precipitated nanoparticles in single CO₂ phase. The approach in these studies was to reduce CO₂-soluble metallic precursors in a single CO₂ phase and to prevent agglomeration by capping the particles with CO₂-soluble fluorinated ligands that provide for steric stabilization of the particles. Unfortunately, these processes continue to require the use of fluorinated ligands to disperse the nanoparticles. These CO₂ soluble fluorinated compounds suffer from the disadvantages of being both expensive and environmentally unfriendly[116, 117].

Several research groups[10, 61, 116, 118-126] have sought to find non-fluorinated compounds that would be soluble in CO₂ in the hopes of creating non-fluorinated polymers as well as surfactants where the latter could be used to form microemulsions in CO₂. Research has shown that branched, methylated, and stubby surfactants can be used to form micelles in supercritical CO₂, because of higher tail solvation and smaller tail-tail interactions[44, 45, 61, 127]. Although some success has been reported in forming fluorine-free microemulsions using hydrocarbon surfactants[46, 128] and in making macroemulsions using silica nanoparticles[129], ionic hydrocarbon surfactants[130, 131], or trisiloxane surfactants[127] in CO₂, no reports to date have demonstrated the synthesis or dispersion of nanoparticles within these non-fluorinated surfactant systems in CO₂. To make full use of the advantages of supercritical CO₂, a stable dispersion of fluorine-free nanoparticles in a single CO₂ phase would be ideal. While metallic nanoparticles have been stably dispersed in pure liquid and supercritical CO₂[132, 133], fluorinated ligands were required. The objective of this study is to illustrate the ability to stably disperse ligand coated metal nanoparticles in neat CO₂ without the need for fluorinated

constituents. To accomplish this, iso-stearic acid, received from Nissan Chemicals, as structure shown in Figure 6.1, was chosen as a ligand for dispersion of silver nanoparticles in CO₂ solvent.

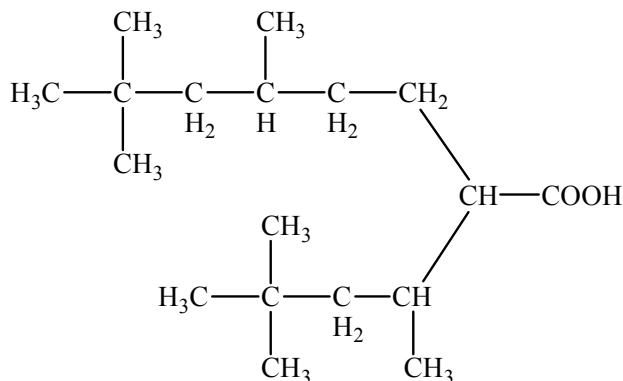


Figure 6.1. Structure of iso-stearic acid, Mn = 284 g/mol.

6.2 EXPERIMENTAL APPARATUS

The experimental setup of the phase behavior study with iso-stearic is the same as shown in Chapter 4.1.4.1.

6.3 PHASE BEHAVIOR RESULTS

Figure 6.2 presents a pressure-composition diagram for the iso-stearic acid-CO₂ mixture demonstrating that iso-stearic acid is highly CO₂-soluble. Iso-stearic acid, a short, stubby compound with branched, methylated tails, is completely miscible with CO₂ at pressures above 13 MPa at 22 °C, as shown in Figure 6.2. No data was collected for the small VL1 two phase region at the CO₂-rich end of the diagram. The high CO₂ solubility may be attributable to the highly methylated branched tails, in which the surface energy of the pendant methyl groups is much lower than that of the CH₂ groups of linear tails[30].

These interactions between the ligand tails and CO₂ are also what make iso-stearic acid a useful ligand to sterically stabilize metallic nanoparticles in CO₂. Iso-stearic acid coated silver nanoparticles have been stably dispersed in carbon dioxide with hexane cosolvent. Neat carbon dioxide has successfully dispersed iso-stearic acid coated silver nanoparticles that had been deposited on either quartz or polystyrene surfaces. These results are the first reports of sterically stabilized nanoparticles in carbon dioxide without the use of any fluorinated compounds.[134]

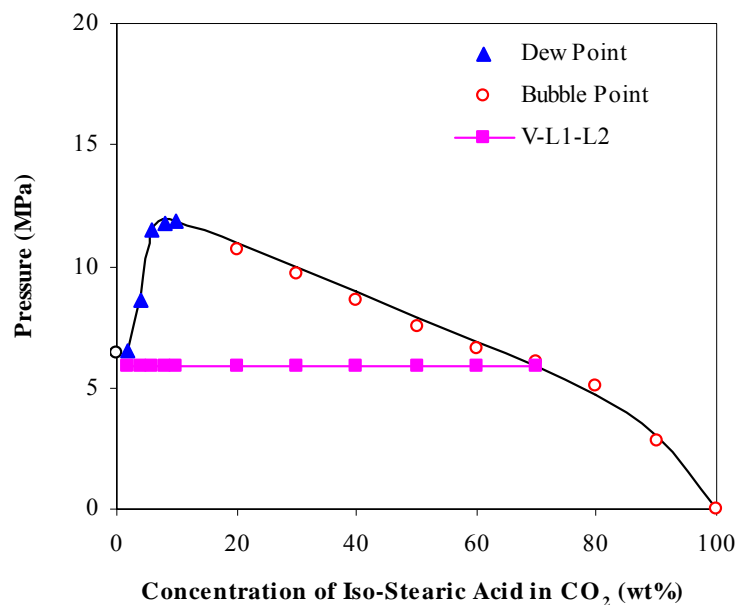


Figure 6.2. Phase behavior of iso-stearic acid/CO₂ mixture at 22 °C. No data was collected for the small VL1 two phase region at the CO₂-rich end of the diagram.

7.0 STABILITY OF CO₂-WATER EMULSIONS STABILIZED WITH CO₂-SOLUBLE SURFACTANTS

7.1 INTRODUCTION

Carbon dioxide is an attractive fluid for enhanced oil recovery (EOR) processes because it is a good solvent for light crude oils and it is available in large quantities from natural reservoirs at high purity and pressure. Currently, about 1.5 billion standard cubic feet (SCF) per day of CO₂ are injected into domestic reservoirs, resulting in the recovery of nearly 200,000 barrels of oil per day. An inherent disadvantage to this CO₂ flooding process is the low viscosity of CO₂ (0.03-0.1 cp) relative to that of the oil being displaced (0.1-50 cp), causing mobility control problems. The high mobility of CO₂ (permeability/viscosity) in the sandstone or limestone causes CO₂ “fingering” its way towards the production well, bypassing much of the oil in the reservoir and reducing the areal sweep efficiency. Moreover, the low viscosity of CO₂ also contributes to the low vertical sweep efficiency, especially in stratified reservoirs that include two or more layers into which the CO₂ may enter. For example, the formation may contain a highly permeable, water-rich zone caused by decades of prior water flooding, while the other less permeable layer is oil-rich because the water preferred to enter the high permeability

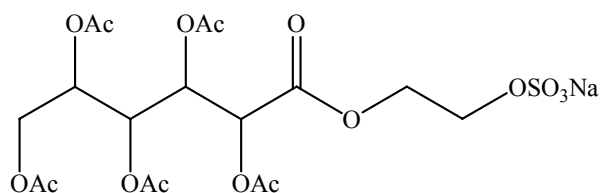
zone. The high mobility of CO₂ induces it to preferentially enter the highly permeable water-rich zone, leaving oil residing in the less permeable zone.

The mobility of a CO₂ foam or emulsion (e.g. 80-95 vol% dense CO₂, 1% surfactant, and 9% brine) in porous media is much lower than that of CO₂ alone. Therefore, CO₂ foams have been investigated as a means of reducing fingering by making moderate decreases in mobility, or for diverting CO₂ to low permeability oil-rich zones by initially forming a very low mobility foam in the water-rich zone. CO₂ foams have been studied by both academic groups [42, 88-90, 135-137] and by industrial researchers [91, 92, 138-141]. In all previously reported applications, an aqueous surfactant solution has been injected into the porous media, followed by CO₂ injection in a process referred to as surfactant-alternating-gas (SAG). The in-situ generation of foams results in high phase volume CO₂ foams in which bubbles of the supercritical CO₂ (or droplets of liquid CO₂) are separated by thin aqueous films. Shorter cycles are recommended in the SAG process to obtain a more uniform foam quality. Bernard and coworkers [138] have presented mobility control results indicating that the CO₂ mobility can be reduced by almost 50% using a commercially available surfactant, Alipal CD-128 (ammonium sulfate ester), as the foaming agent. Researchers at Shell Development Company [141, 142] demonstrated a relationship between surfactant compositions and surfactant adsorption, foam stability, and mobility control using a series surfactants of alcohol ethoxy glyceryl sulfonates (AEGS) and alpha olefin sulfonates (AOS). The stability of CO₂ foams formed by water soluble surfactants depends on many factors such as the texture of the foams (bubble size, shape, and distribution), salinity, pH, surfactant concentration, pressure and temperature.[89, 135, 136] The method of foam generation is

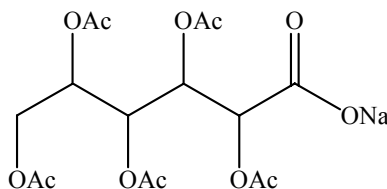
also a major factor that determines the texture and quality of the foam that will ultimately establish the concentration required to prolong stability.[143] The anionic surfactants used for the SAG process include Chaser CD 1045,[135, 136, 143] Rhodapex CD-128,[143] Witcolate 1276,[88, 89] and Enordet X2001,[88] which have been investigated for foam stability and mobility control in both the laboratory and field at concentrations ranging from 0.01-0.1 wt%. Problems associated with CO₂ foam flooding or the SAG process include corrosion, surfactant adsorption, and control of foam mobility within the reservoir for extended periods of time. In this work, we propose the dissolution of an ionic surfactant in dense CO₂, rather than the injection of a water-soluble surfactant into the brine slug followed by the injection of a CO₂ slug. The single-phase solution of surfactant in CO₂ would be injected into the reservoir and form CO₂ foams in-situ as it mixes with the brine retained within the formation. These low mobility foams could form in water-out high permeability zones, thereby diverting the subsequently injected neat CO₂ to oil-rich zones. If the mobility decrease induced by the foam could be moderated, then the surfactant-CO₂ solution could also be used for mobility control purposes. The potential advantages of this process include the elimination of aqueous surfactant slug injection and the generation of foams along and at the tips of the CO₂ “fingers” where mobility control is most needed.

The objective of this study was to form emulsions by mixing of CO₂, water, and CO₂-soluble surfactants, and to characterize the stability of the emulsion by measuring its rate of collapse. CO₂-soluble ionic surfactants with CO₂-philic hydrocarbon or oxygenated hydrocarbon tails and conventional ionic head groups that have been presented in Chapter 4, and 5 were investigated for the foam stability study. CO₂-soluble

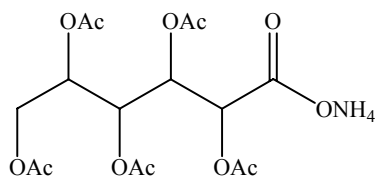
ionic surfactants with oxygenated hydrocarbon or hydrocarbon tails composed of acetylated sugar, PPO, oligo(vinyl acetate), and 3,5,5-trimethyl-1-hexyl were evaluated along with two nonionic surfactants. The structures of these ionic and nonionic surfactants are shown in Figure 7.1 and Figure 7.2, respectively. The ionic surfactants with oxygenated hydrocarbon or hydrocarbon tails were synthesized as described in Chapter 3 and 4, while the nonionic surfactants of iso-stearic carboxylic acid and PPG-PEG-PPG triblock polymer ($M_n=3300$) were obtained from Nissan Chemical and Aldrich, respectively. Several prior investigators[30, 56] have noted the CO_2 solubility of oligomeric block copolymers of PPG and PEG. Nonionic surfactants are considered to be low-to-moderate foamers relative to ionic surfactants and were therefore expected to yield less stable emulsions. However, nonionic surfactants have less severe problems associated with adsorption or chemical degradation. The stability of the emulsions stabilized with CO_2 soluble ionic surfactants was then contrasted with the stability of emulsions formed using conventional water soluble ionic surfactants.



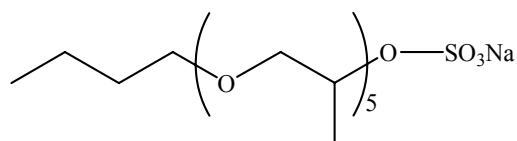
Peracetoxy Gluconate Ethyl Sodium Sulfate (a)



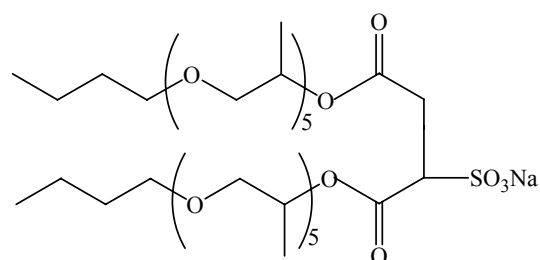
Peracetoxy Gluconate Sodium Carboxylate (b)



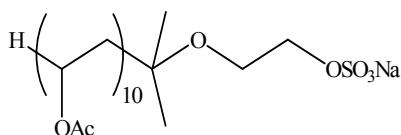
Peracetoxy Gluconate Amonium Carboxylate (c)



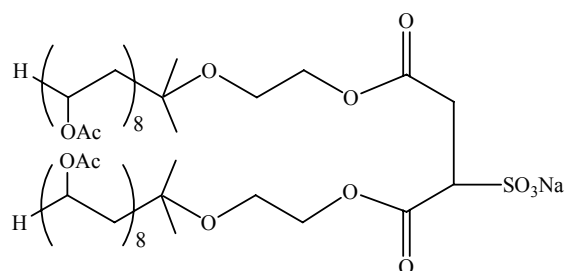
PPGMBE 340 Sodium Sulfate (d)



**Sodium bis(PPGMBE 340) Sulfosuccinate
(PPGMBE 340 AOT Analogue) (e)**



Oligo(Vinyl Acetate)10 Sodium Sulfate (f)



**Sodium bis(Vinyl Acetate)8 Sulfosuccinate
(OVAc8 AOT Analogue) (g)**

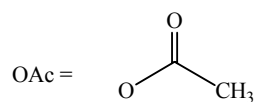
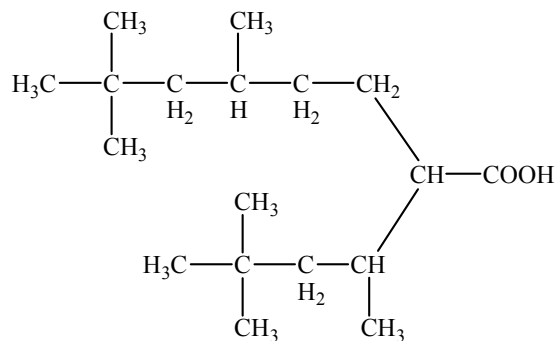
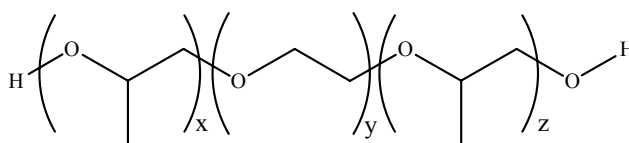


Figure 7.1. Structures of ionic surfactants with oxygenated hydrocarbon CO₂-philic tails.



Iso-Stearic Acid (a)



PPG-PEG-PPG (Mn=3300) (b)

Figure 7.2. Structures of nonionic surfactants.

7.2 EXPERIMENTS

Foam stability experiments were conducted in a high pressure, windowed, stirred, variable-volume view cell (DB Robinson & Assoc., 3.18 cm ID, $\sim 120 \text{ cm}^3$ working volume), as described previously for phase behavior study.[95] The sample volume of this apparatus is a cylinder of variable height and fixed diameter. A specified amount of surfactant (e.g., $0.004 \pm 0.0001 \text{ g}$) and double distilled and de-ionized water (e.g., $45.9 \pm 0.1 \text{ mL}$) were added to the sample volume of the view cell and followed by the introduction of equal volume of CO_2 (e.g., $45.90 \pm 0.1 \text{ mL}$) at 2000 psi. The amount of surfactant corresponded to 0.01 wt% based on the mass of CO_2 . In this cell, the sample

volume is separated from the overburden fluid by a steel cylinder (floating piston) that retains an O-ring around its perimeter. The O-ring permits the cylinder to move easily while retaining a seal between the sample volume and the overburden fluid. The sample volume was minimized by displacing the floating piston to the highest possible position within the cell that did not result in the displacement of surfactant-water mixture out of the sample volume. High pressure liquid carbon dioxide (22 °C, 13.8 MPa) was then introduced to the sample volume as the silicone oil overburden fluid (which was maintained at the same pressure as the CO₂) was withdrawn at the equivalent flow rate using a dual-proportioning positive displacement pump (DB Robinson). This technique facilitated the isothermal, isobaric addition of a known volume of CO₂ into the sample volume. The mass of CO₂ introduced was determined from the displaced volume, temperature, and pressure using an accurate equation of state for carbon dioxide.[96] Pressure within the vessel was monitored to approximately ± 0.5 MPa, and temperature was measured with a type K thermocouple to an accuracy of ± 0.1 °C. The system was then compressed to 34.5 MPa. The surfactants are both CO₂ soluble and water soluble at these conditions, and no attempts were made to quantify the partitioning of the surfactant between the phases.

The cell was inverted, allowing the mixer to be at the bottom of the sample volume. The position of the original interface between water and liquid CO₂ prior to mixing (and emulsion generation) was then measured using a ruler that was adjacent to the window. The mixture was then mixed thoroughly for 10 minutes at 2000 rpm using a slotted propeller-type impeller magnetic stirrer on the bottom of the sample volume (DB Robinson, max. 2500 rpm). After the mixing ceased, a white, creamy, opaque emulsion

formed immediately within the entire sample volume. Subsequently, clear CO₂-rich upper phase and aqueous lower phase appeared. The emulsion stability and volume were evaluated by periodically measuring the position of the top (CO₂-emulsion) and bottom (water-emulsion) interfaces of the white emulsion. The volume of the foam was measured as the percentage of the original CO₂ and aqueous phases that were occupied by the emulsion.

$$\text{Foam volume} = \frac{H(t)}{H(0)} \times 100\% \quad (1)$$

where t is time, $H(t)$ is the height of the CO₂ or H₂O emulsion layers with time, and $H(0)$ is the initial height of the CO₂ or H₂O layer. In all cases, the foam volume was initially 100% of both the CO₂ and water layers, but the foam decayed thereafter. The final volume corresponded to either 0, which corresponded to the complete collapse of the foam, or a finite % value that was indicative of a stable middle phase emulsion. Stable foams were characterized by slow collapse and the occurrence of a stable middle phase emulsion.

7.3 RESULTS AND DISCUSSIONS

Peracetyl Gluconic-based Ionic Surfactants, Figures 7.1a,b,c

Foam stabilities of peracetyl gluconic-based ionic surfactants with an ethyl spacer and a sodium sulfate, sodium carboxylate or ammonium carboxylate head group (Figures 7.1a,b,c) are shown in Figure 7.3. The emulsion generated by peracetyl gluconic ammonium carboxylate is much more stable than those generated by the other two

peracetyl gluconic-based ionic surfactants, taking about 250 minutes to collapse to a stable middle phase emulsion that occupied about 22% of the original CO₂ volume. The emulsion formed by the peraceyl gluconic ethyl sodium sulfate required about 200 minutes to collapse to a middle phase emulsion that occupied about 15% of the CO₂ volume. The emulsion formed by the peracetyl gluconic sodium carboxylate collapsed in about 120 minutes to a volume that was 5% of the CO₂ volume. In all cases, the emulsion percentage in the aqueous phase collapsed quickly from 100% to 0%.

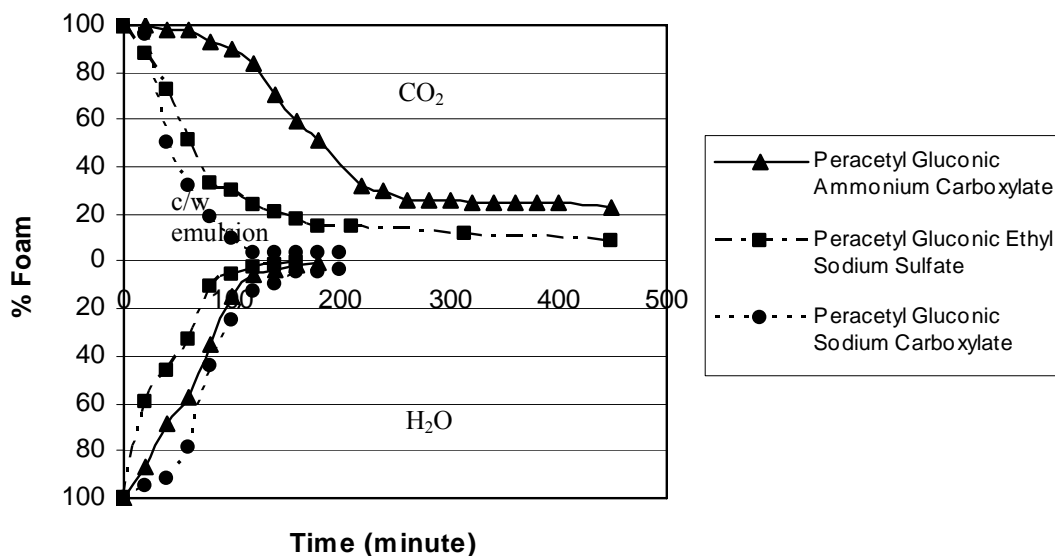


Figure 7.3. Foam stability of peracetyl gluconic-based ionic surfactants at concentration of 0.01 wt% in CO₂, 22 °C and 34.5 MPa.

Poly(Propylene Glycol) MonoButyl Ether(PPGMBE)-based Ionic Surfactants, Figures 7.1d,e

Emulsions formed by twin tailed AOT analogue of sodium bis(PPGMBE 340) sulfosuccinate are slightly more stable than those formed by the single-tailed PPGMBE

340 sodium sulfate, as shown in Figure 7.4 in that the emulsions collapsed at comparable rates, requiring about 160 minutes to reach steady state values of 15% and 5% of the original CO₂ volume, respectively. The portion of the emulsion that originally formed in the aqueous phase collapsed at a comparable rate, and a portion of the final emulsion volume, about 5% of the water volume, resided below the original CO₂-water boundary.

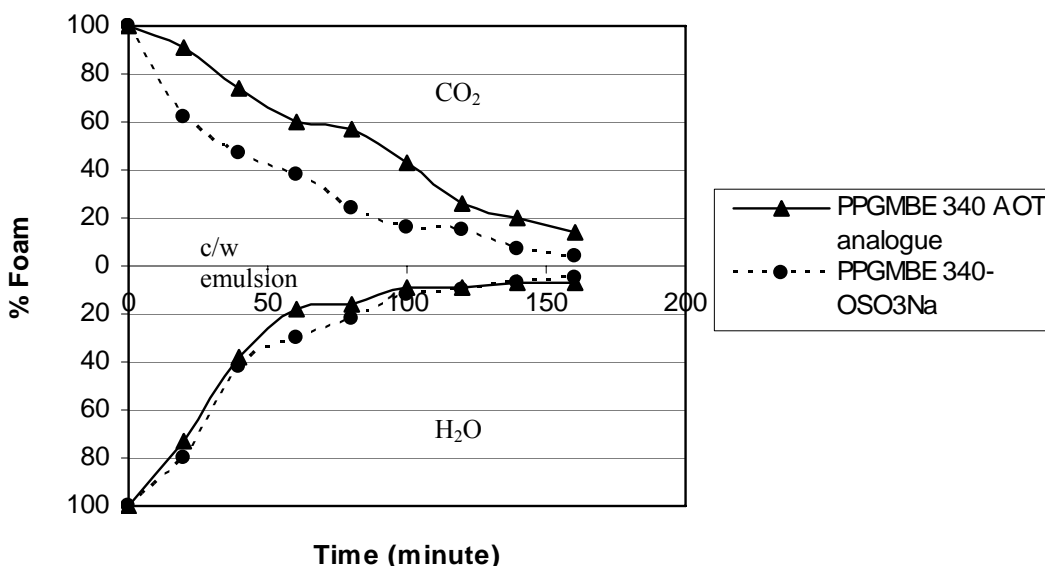


Figure 7.4. Foam stability of PPGMBE-based ionic surfactants at concentration of 0.01 wt% in CO₂, 22 °C and 34.5 MPa.

Oligo(Vinyl Acetate)-based Ionic Surfactants, Figures 7.1f,g

Single-tailed oligo(vinyl acetate)₁₀ sodium sulfate (OVAc₁₀-OSO₃Na) formed emulsions that were only slightly more stable than the twin-tailed AOT analogue of sodium bis(vinyl acetate)₈ sulfosuccinate (OVAc₈ AOT analogue). As shown in Figure 7.5, it took roughly 400 minutes for the emulsion formed by 0.01 wt% OVAc₁₀-OSO₃Na to collapse to about 10% of the original CO₂ volume, while emulsions formed by OVAc₈

AOT analogue took about 300 minutes to collapse to a comparable volume. The portion of the emulsion in the aqueous layer decayed first and collapsed to 0.

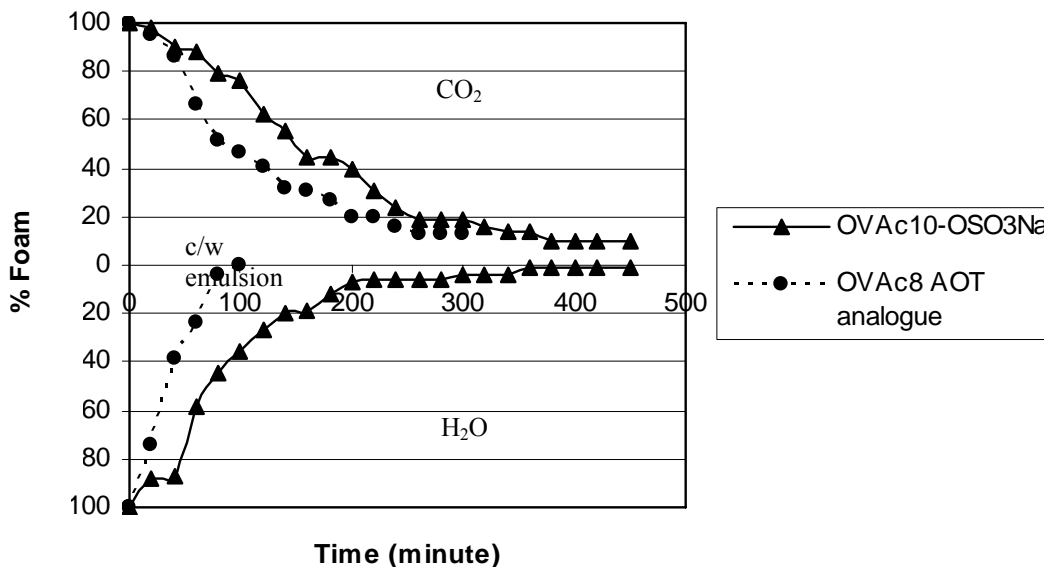


Figure 7.5. Foam stability of oligo(vinyl acetate)-based ionic surfactants at concentration of 0.01 wt% in CO₂, 22 °C and 34.5 MPa.

Comparison of Oligo(Vinyl Acetate)10 Sodium Sulfate and Commercial Chaser CD 1045

The oligo(vinyl acetate)10 sodium sulfate demonstrated the best foam stability in both CO₂ and H₂O layers, which was chosen for comparison with the commercial water soluble ionic surfactant of Chase CD 1045. The foam stability comparison was presented in Figure 7.6. The stability of CO₂ emulsions formed by both surfactants at 0.01 wt% are comparable. It took roughly 400 minutes for the CO₂ emulsions to collapse to about 10% of the original CO₂ volume. The portion of the emulsion in the aqueous layer formed by

Chaser CD 1045 decayed faster and collapsed to 0 at about 200 minutes, while that of oligo(vinyl acetate)10 sodium sulfate lasted 400 minutes to collapse to 0.

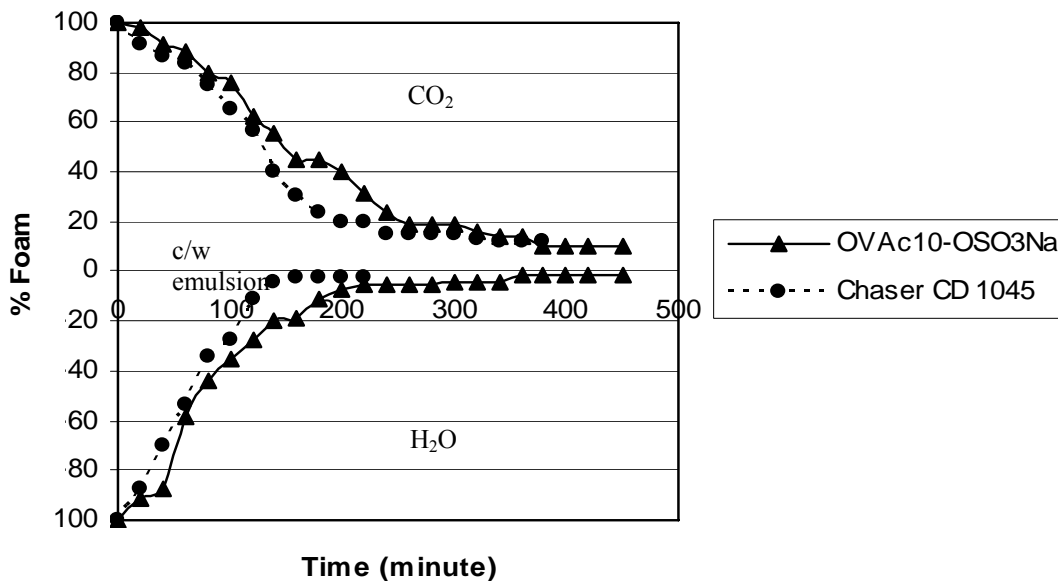


Figure 7.6. Foam stability of OVAc10-OSO₃Na and Chaser CD 1045 at concentration of 0.01 wt% in CO₂, 22 °C and 34.5 MPa.

Nonionic surfactants, Figures 7.2a,b

The emulsions generated by the nonionic surfactants decayed at a much faster rate than the ionic surfactants, as shown in Figure 7.7. The emulsion formed by the iso-stearic acid collapsed completely in less than an hour. The emulsion formed by the PPG-PEG-PPG reached its steady-state value of about 10% of the aqueous phase volume in just over an hour.

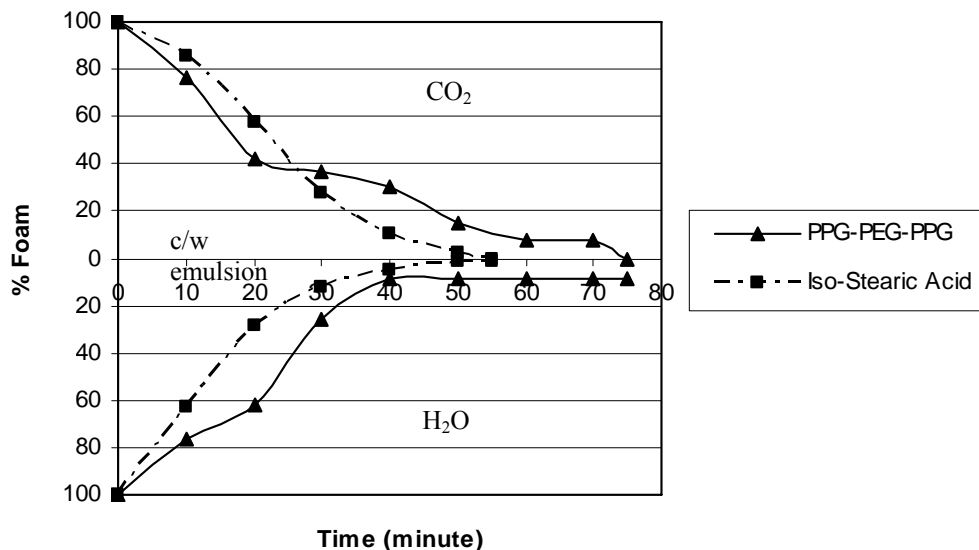


Figure 7.7. Foam stability of iso-stearic acid and PPG-PEG-PPG nonionic surfactants at concentration of 0.01 wt% in CO₂, 22 °C and 34.5 MPa.

7.4 CONCLUSIONS

At constant conditions of 0.01 wt% surfactant in CO₂, 22 °C and 34.5 MPa, it is apparent that the emulsions formed by the ionic surfactants displayed a significantly greater stability than those formed by the nonionic compounds. Of the ionic surfactants, the peracetyl gluconic ammonium carboxylate demonstrated the best CO₂ foam stability, with around 20% of the CO₂ foams lasting for over 450 min. The oligo(vinyl acetate)10 sodium sulfate demonstrated the best foam stability in both CO₂ and H₂O layers, with around 10% and 1% of foams respectively remaining stable for over 450 min. Further tests on the salinity of the H₂O present, pressure, temperature, and varied surfactant

concentrations would be evaluated further for the most potential candidate of oligo(vinyl acetate)10 sodium sulfate to be used in EOR processes.

8.0 NONIONIC SURFACTANTS

8.1 EFFECT OF ALKYL CHAIN LENGTH

Some commercially available nonionic surfactants were also investigated for CO₂ solubility. First, the effect of alkyl chain length to surfactants solubility in CO₂ was investigated. Poly (propylene) butyl ether and poly(propylene) stearyl ether (Chemron) have almost the same PPO repeat units while different alkyl chains length; see their structures in Figure 8.1. PBE-14 is extremely CO₂ soluble up to 80wt%. PSE-15 is much less CO₂ soluble, only up to 15wt% could be dissolved in CO₂ at much higher pressure (Figure 8.2). That means short alkyl chain is much more CO₂-philic than longer alkyl chain.

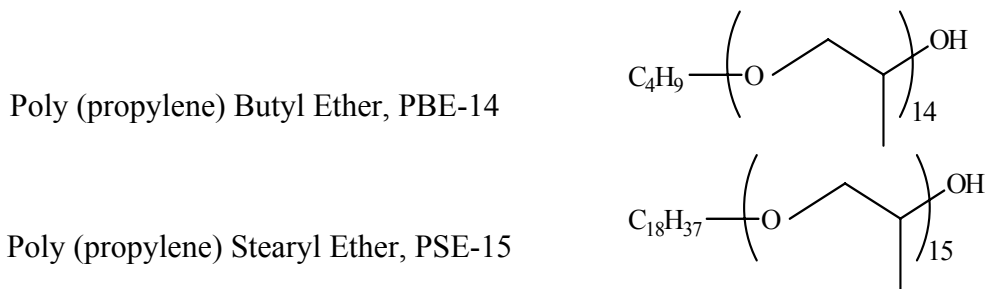


Figure 8.1. Structures of PBE-14 and PSE-15.

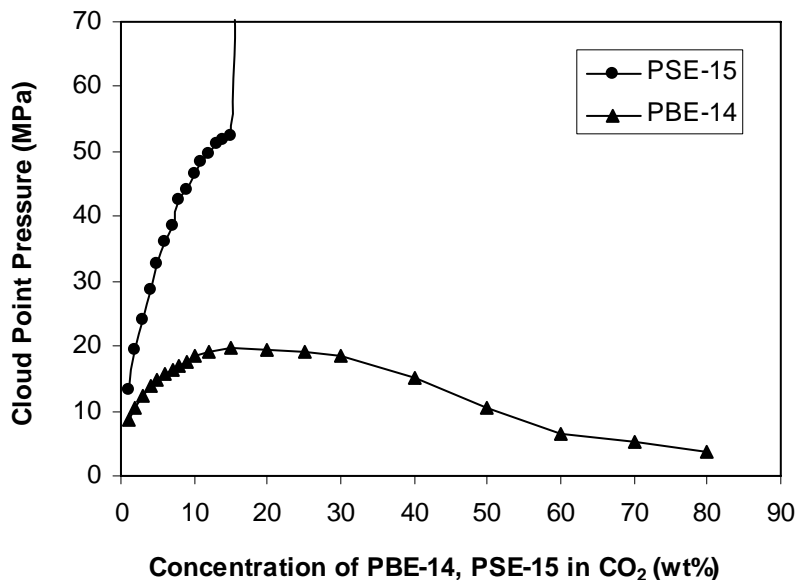


Figure 8.2. Phase behavior of PBE-14, PSE-15/CO₂ mixtures at 22 °C.

8.2 EFFECT OF ETHYLENE OXIDE AND PROPYLENE OXIDE

The function of PEO and PPO to CO₂ solubility was also studied. The solubility of commercial nonionic surfactants containing ethylene oxide and propylene oxide including Vanwet9N9, LS-54 (Cognis), TD-23 and TD-29 (Chemron) were compared at room temperature. Water in TD-23 and TD-29 was removed by vacuum distillation before the phase behavior study. Figure 8.3 shows their structures. Phase behavior results in Figure 8.4 illustrate that Vanwet9N9 is the least soluble because it contains only PEO repeat units, while the LS-54, TD-23 and TD-29 are much more CO₂ soluble due to the CO₂ philic PPO units. Further, TD-29 is more soluble than LS-54 and TD-23 because its relatively higher composition of PPO.

9.0 CONCLUSIONS

- (1) Oxygenated hydrocarbon based ionic surfactants composed of acetylated sugars, poly(propylene oxide) tails are 0.1-2 wt% soluble in CO₂.
- (2) Oxygenated hydrocarbon based ionic surfactants composed of oligo(vinyl acetate) tails are highly CO₂ soluble.
 - i. Single-tailed OVAc-OSO₃Na are 2-7 wt% soluble in CO₂
 - ii. Twin-tailed OVAc8 AOT analogue is 3 wt% soluble in CO₂
 - iii. Both single and twin-tailed OVAc ionic surfactants can form water-in-CO₂ microemulsions at W values as high as 40.
 - iv. OVAc ionic surfactants represent the first reports of highly CO₂ soluble ionic surfactants with tails composed solely of C, H and O that can form water-in-CO₂ microemulsions.
- (3) Ag-AOT-TMH, a hydrocarbon-based metal precursor, is 1.2 wt% soluble in CO₂. It was reduced to silver nanoparticles in CO₂.
- (4) Iso-stearic acid, a highly branched nonionic surfactant, is completely miscible with CO₂ and it is the first report of metallic nanoparticles dispersed in pure CO₂ without the use of fluorinated ligands.
- (5) The oligo(vinyl acetate)₁₀ sodium sulfate demonstrated the best foam stability in both CO₂ and H₂O layers, with around 10% and 1% of foams respectively remaining stable for over 450 min.

(6) Short alkyl chain is much more CO₂-philic than long alkyl chain and poly (propylene oxide) (PPO) is much more CO₂-philic than poly (ethylene oxide) (PEO).

10.0 FUTURE WORK

Our future work will continue to design oxygenated hydrocarbon-based or hydrocarbon-based CO₂ soluble surfactants for nanoparticle formation, foam generation, interfacial tension reduction and other chemical engineering applications. The interactions between the tail and the CO₂ must be strong enough to impart CO₂-philicity to the surfactant that contains a CO₂-phobic segment. Further, the CO₂ soluble surfactant must be able to form water-in-CO₂ microemulsions, stabilize nanoparticles, generate foams, increase viscosity or reduce interfacial tension.

APPENDIX A

SPECTRA AND PHASE BEHAVIOR OF SURFACTANTS IN

CHAPTER 4

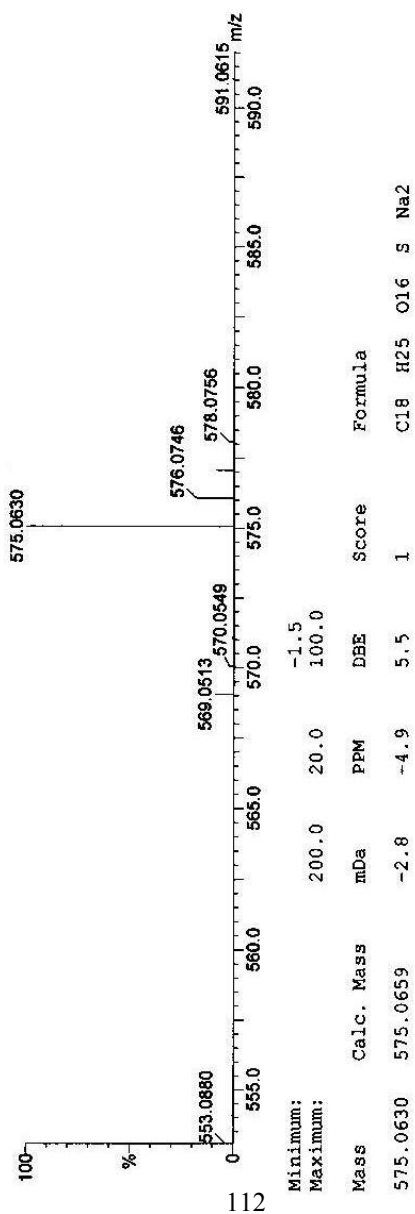


Figure A.1. Mass spectrum of peracetyl gluconic ethyl sodium sulfate

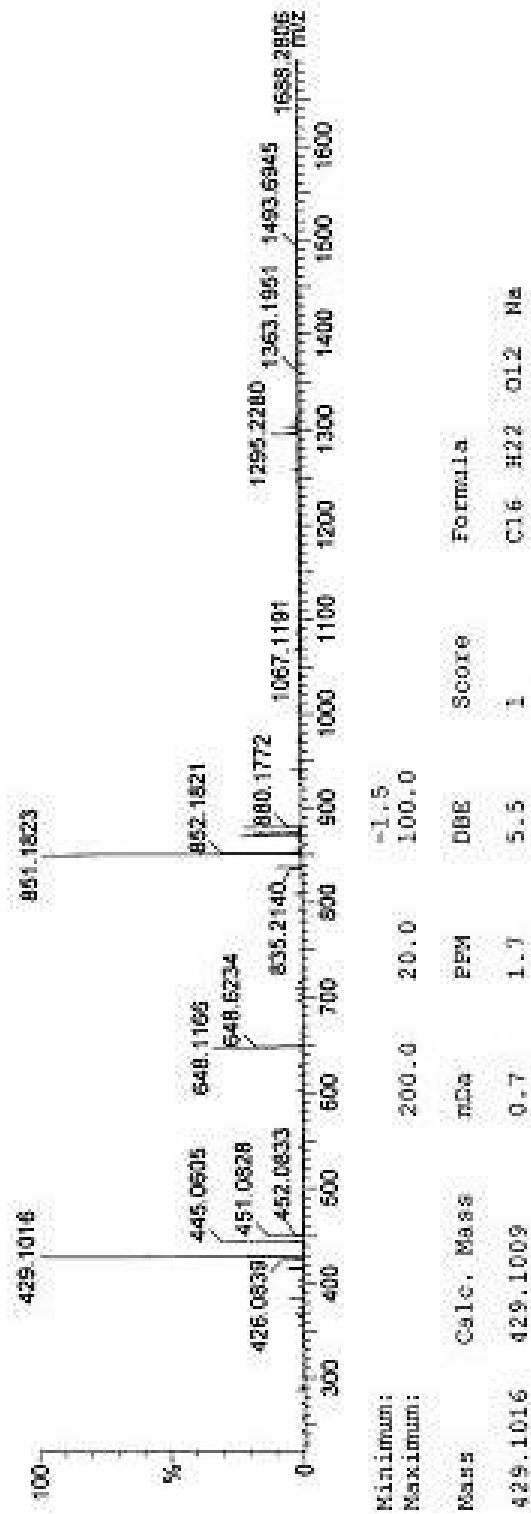


Figure A.2. Mass spectrum of peracetyl gluconic sodium carboxylate

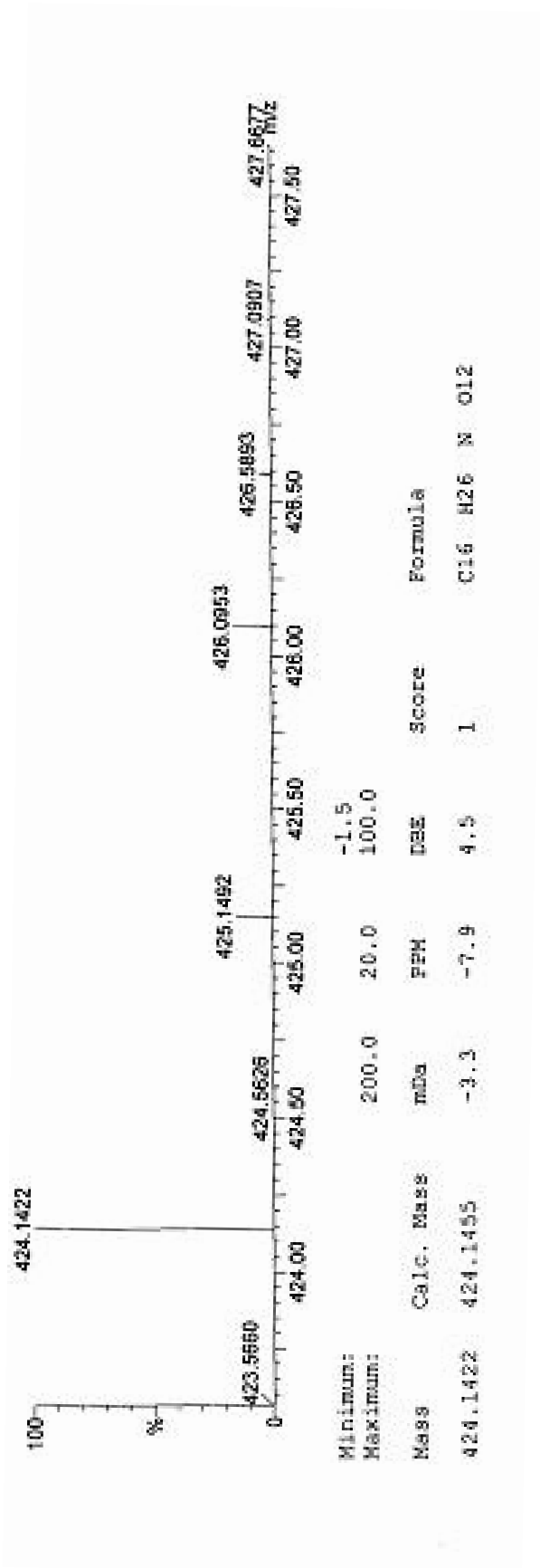


Figure A.3. Mass spectrum of peracetyl gluconic ammonium carboxylate

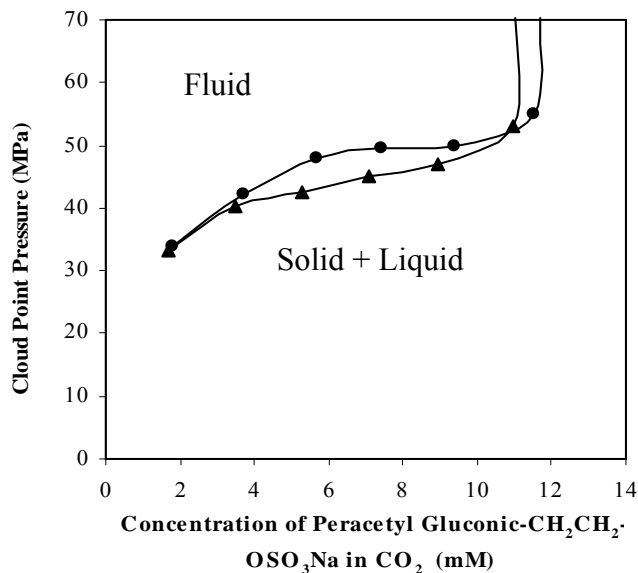


Figure A.4. Phase behavior of peracetyl gluconic-CH₂CH₂-OSO₃Na/CO₂ mixtures. Insoluble at W = 0; 25 °C, W =10 (●); 40 °C, W=10 (▲). (Surfactant concentration in mM).

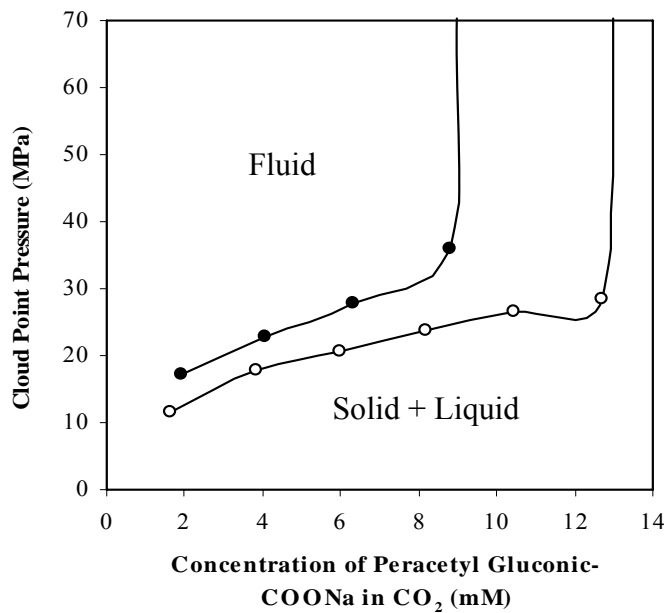


Figure A.5. Phase behavior of peracetyl gluconic-COONa/CO₂ mixtures at 40 °C. W=0 (o); W=10 (●). (Surfactant concentration in mM).

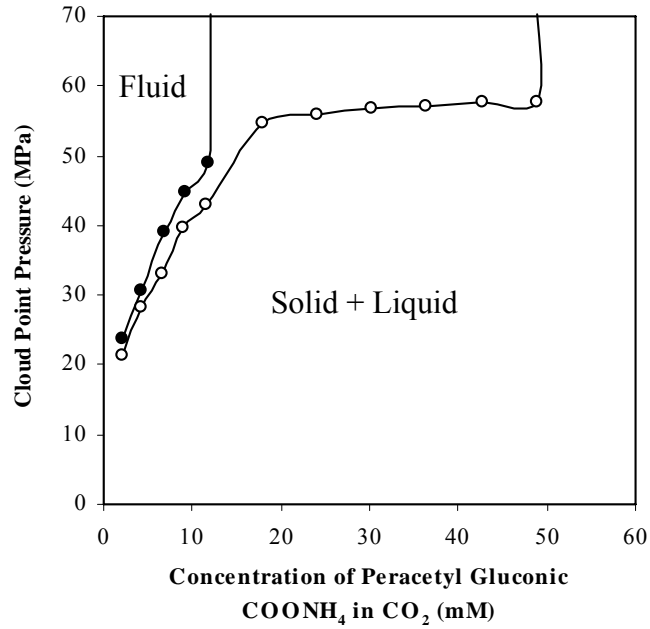


Figure A.6. Phase behavior of peracetyl gluconic-COONH₄/CO₂ mixtures at 40 °C. W =0 (o); W =10 (●). Surfactant concentration in mM. (Surfactant concentration in mM).

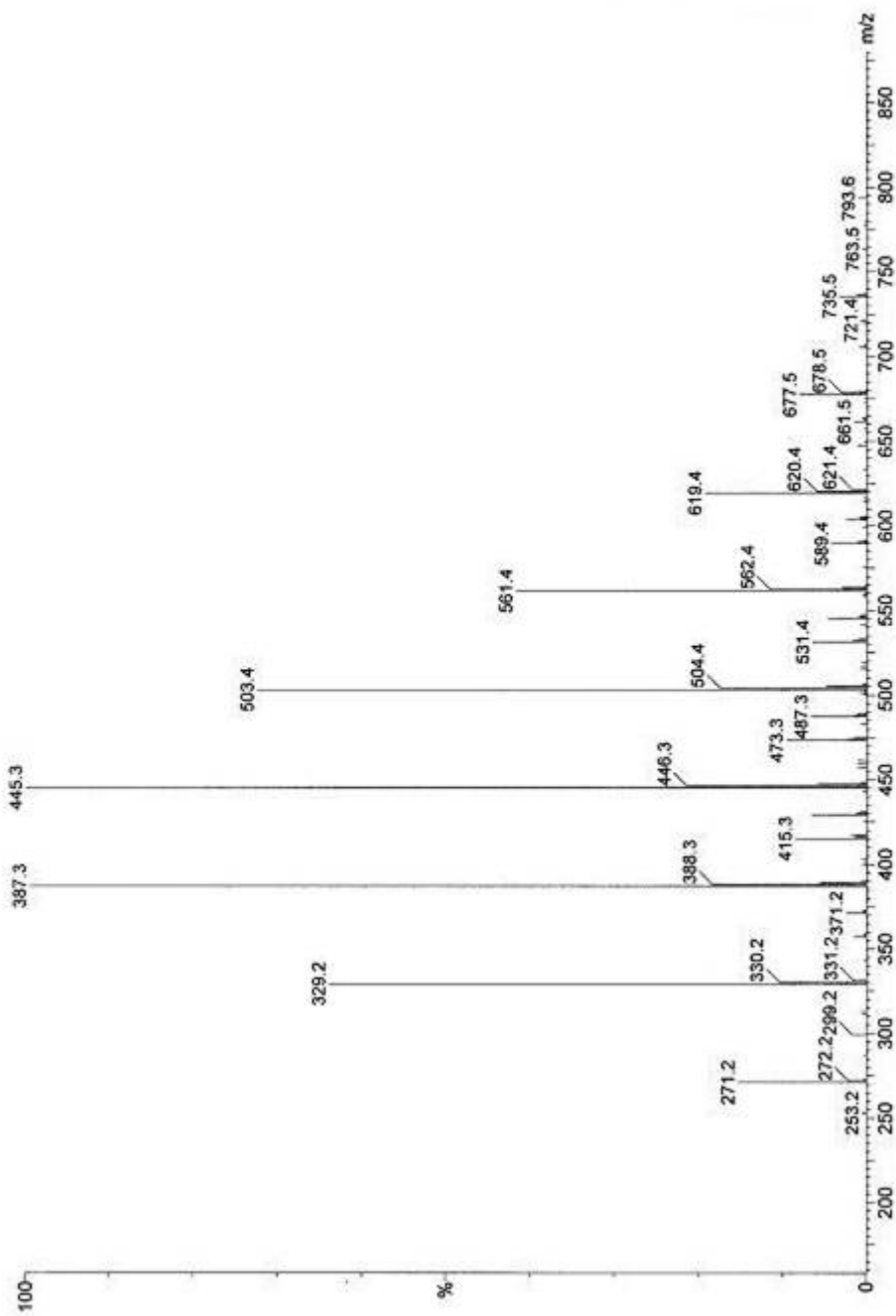


Figure A.7. Mass spectrum of PPGMBE 340 sodium sulfate

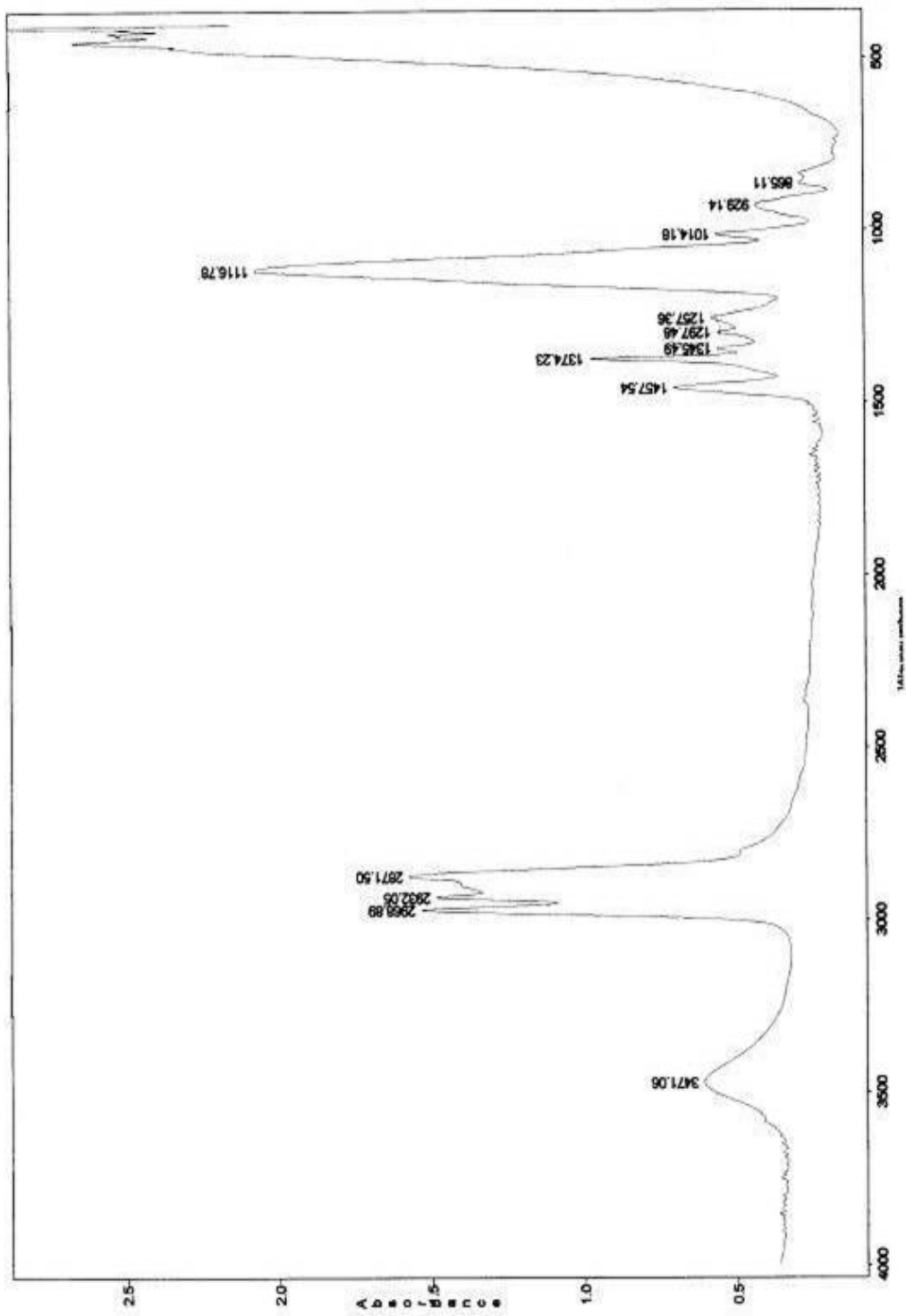


Figure A.8. FTIR spectrum of PPGMBE 340

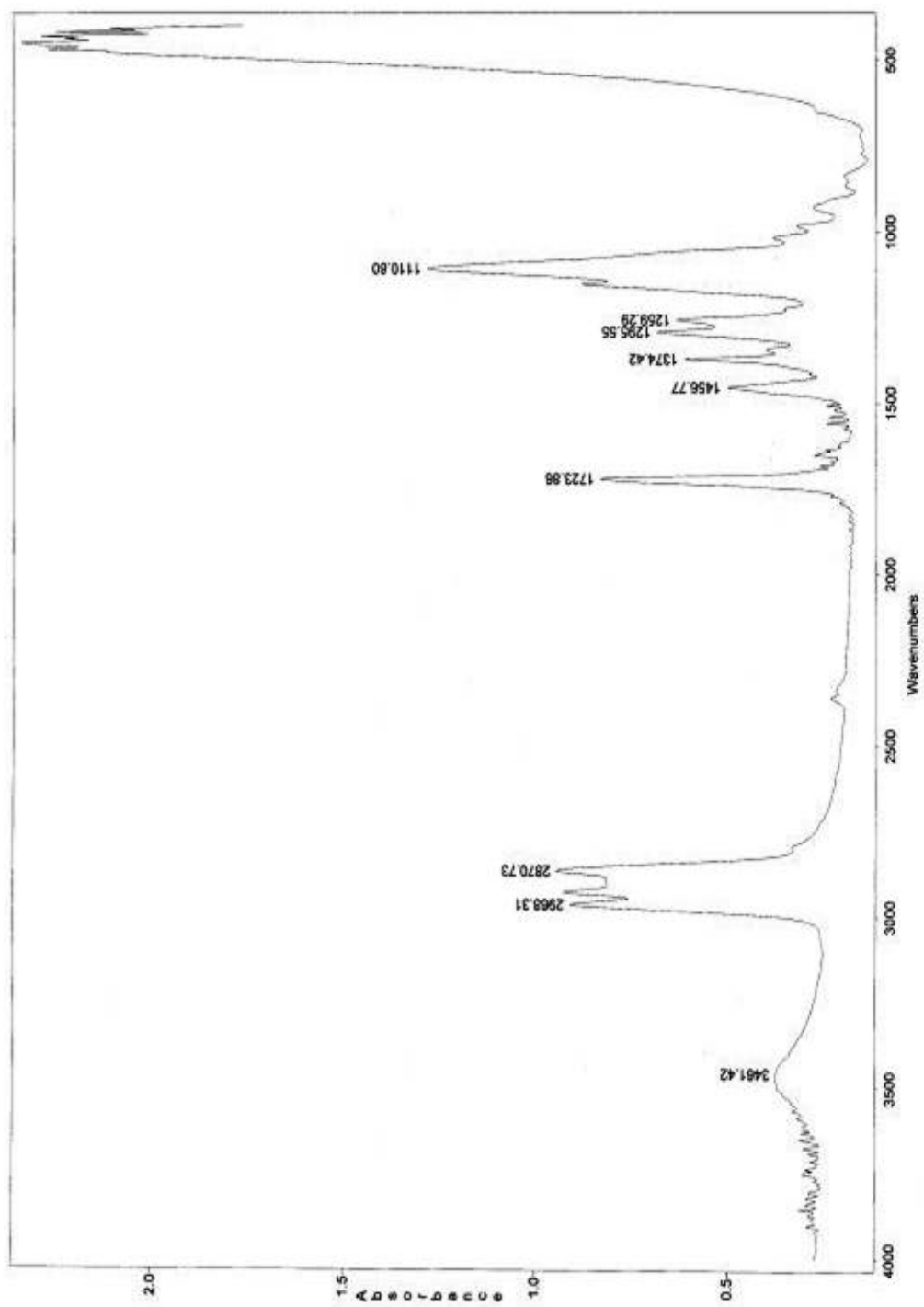


Figure A.9. FTIR spectrum of PPGMBE 340 diester

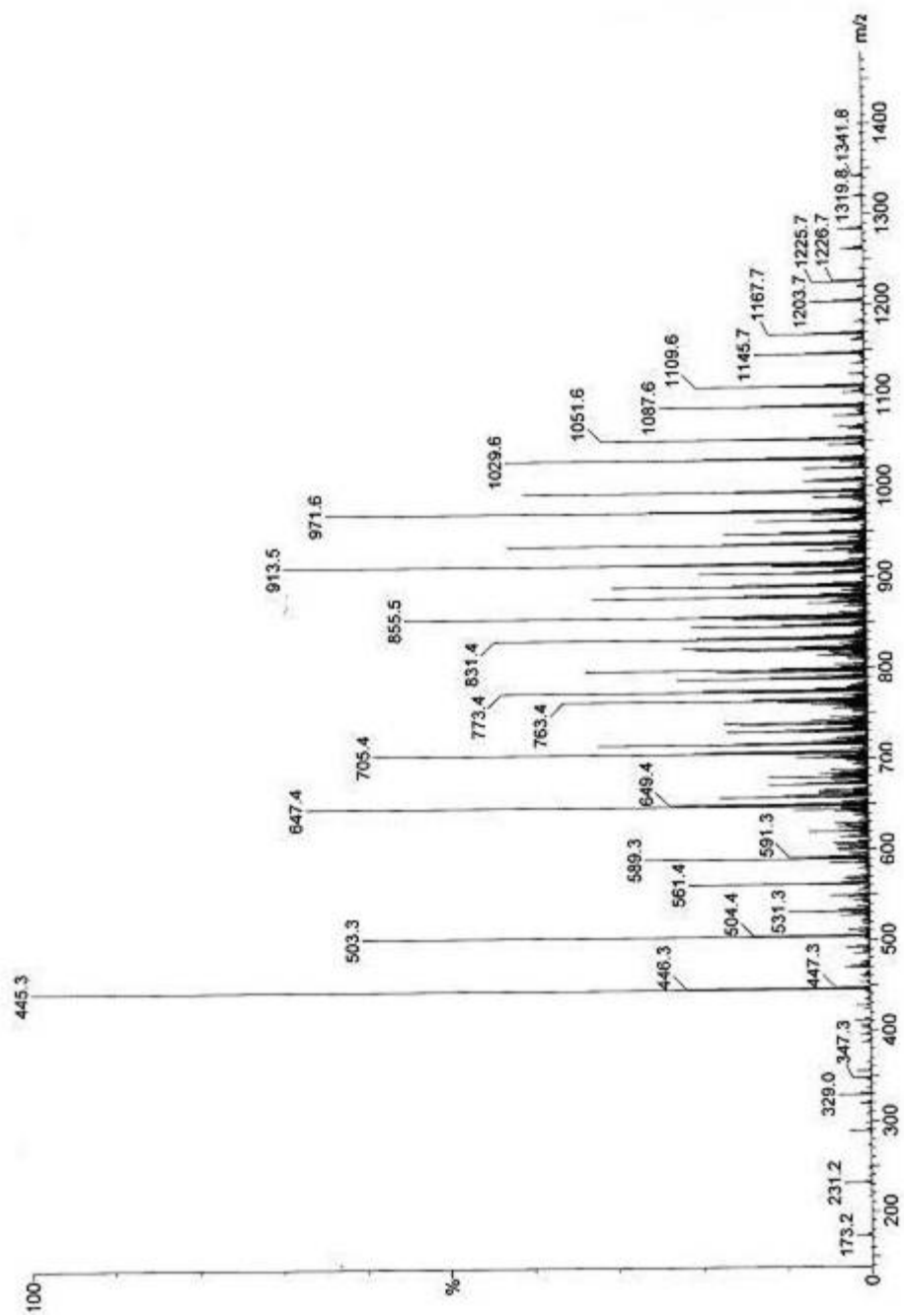


Figure A.10. Mass spectra of sodium bis(PPGMBE 340) sulfosuccinate

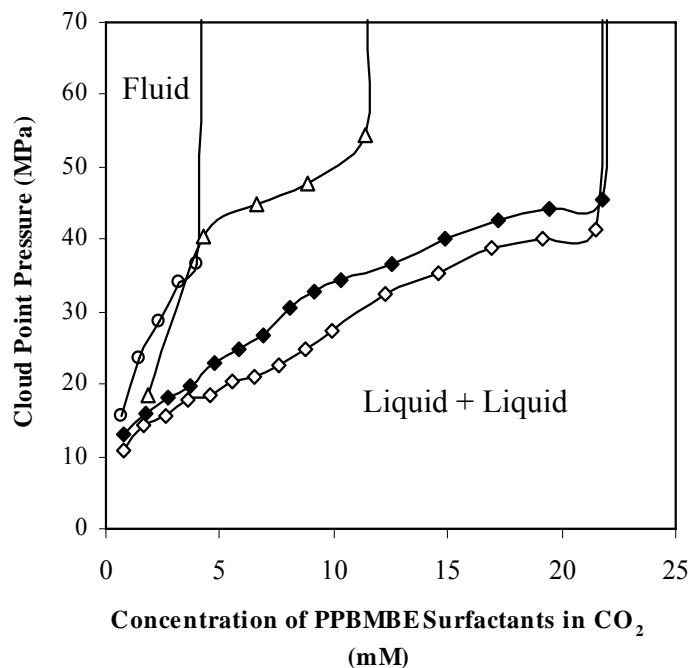


Figure A.11. Phase behavior of PPGMBE surfactants/CO₂ mixtures at 40 °C. PPGMBE 340 sodium sulfate, W=0 (Δ); PPGMBE 1000 pyridinium sulfate, W=0 (o); PPGMBE 1000 pyridinium sulfate, W=10 (\bullet); Sodium bis(PPBMBE 340) sulfosuccinate, W=0 (\diamond); Sodium bis(PPBMBE 340) sulfosuccinate, W=10 (\blacklozenge). (Surfactant concentration in mM).

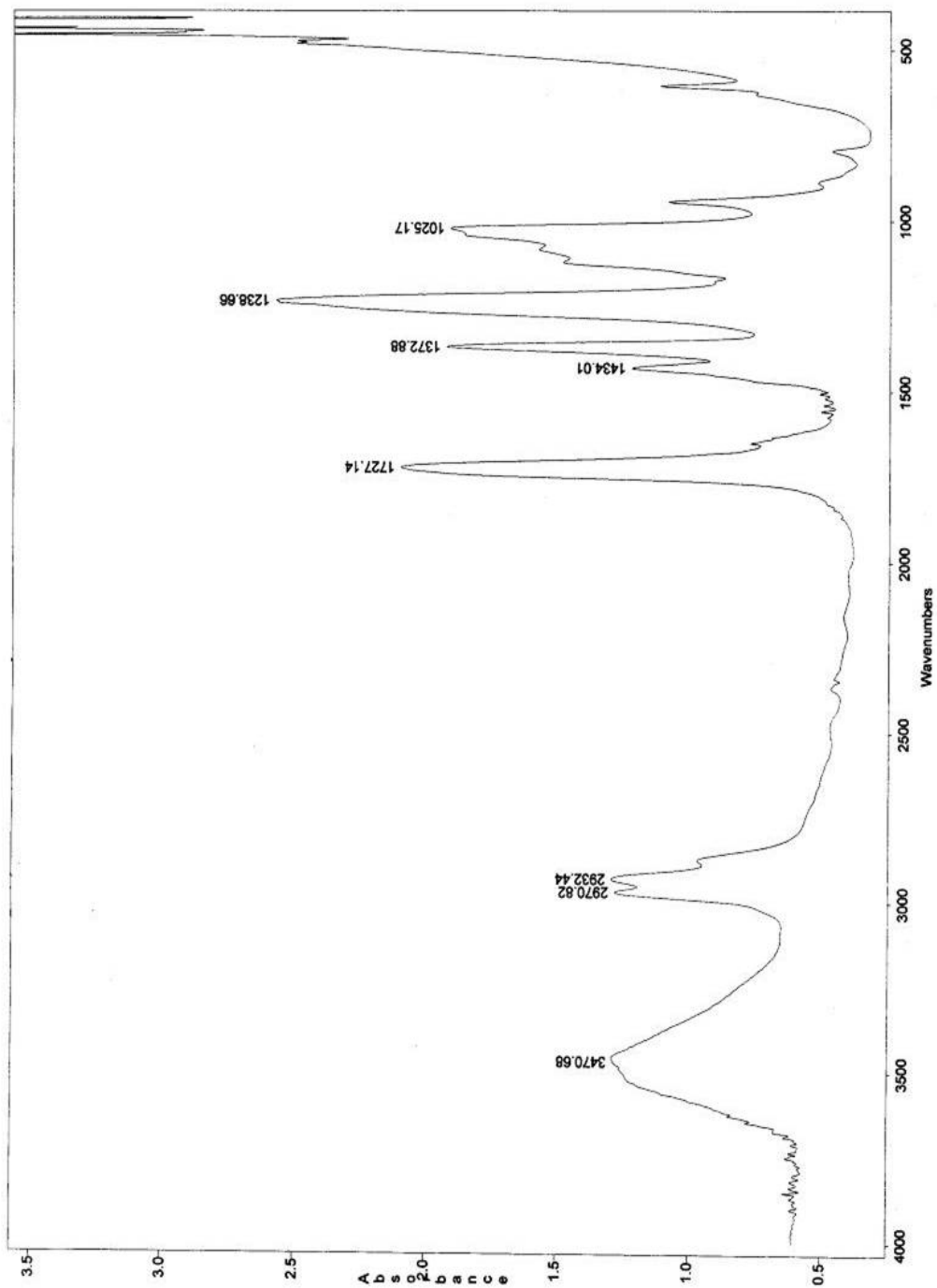


Figure A.12. FTIR spectrum of OVAc6-OH

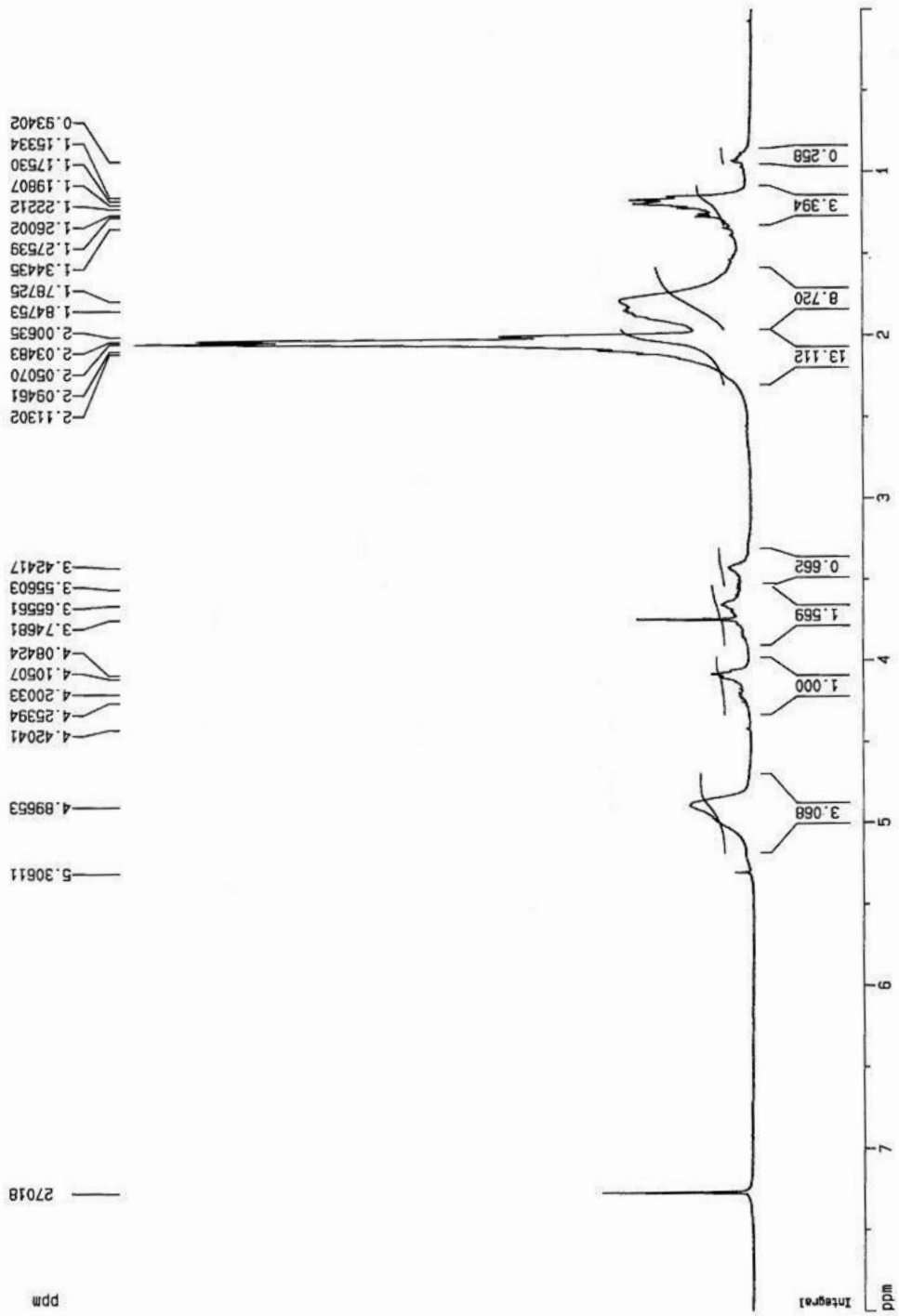


Figure A.13. ¹H-NMR spectrum of OVAc6-OH

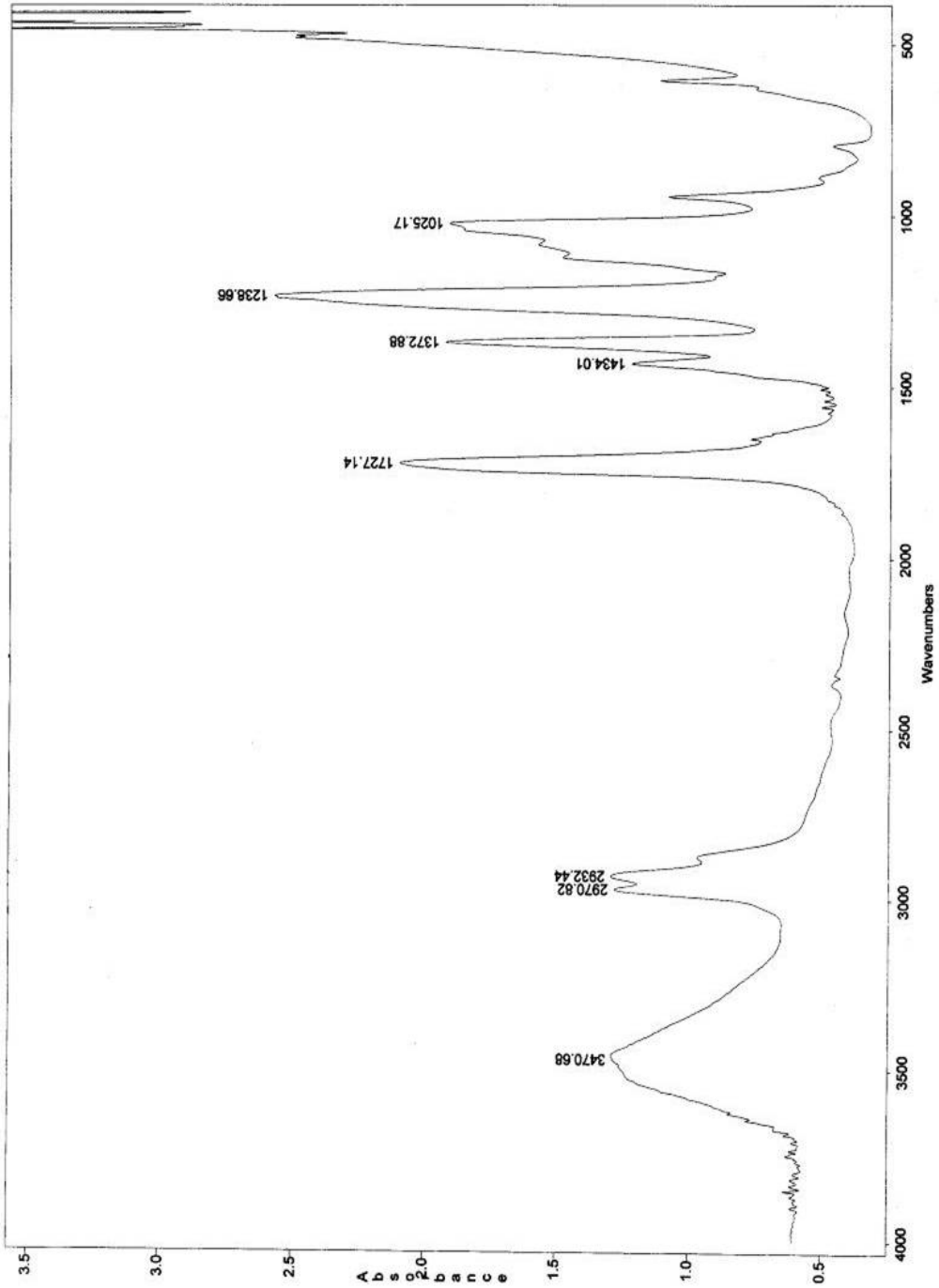


Figure A.14. FTIR spectrum of OVAc8-OH

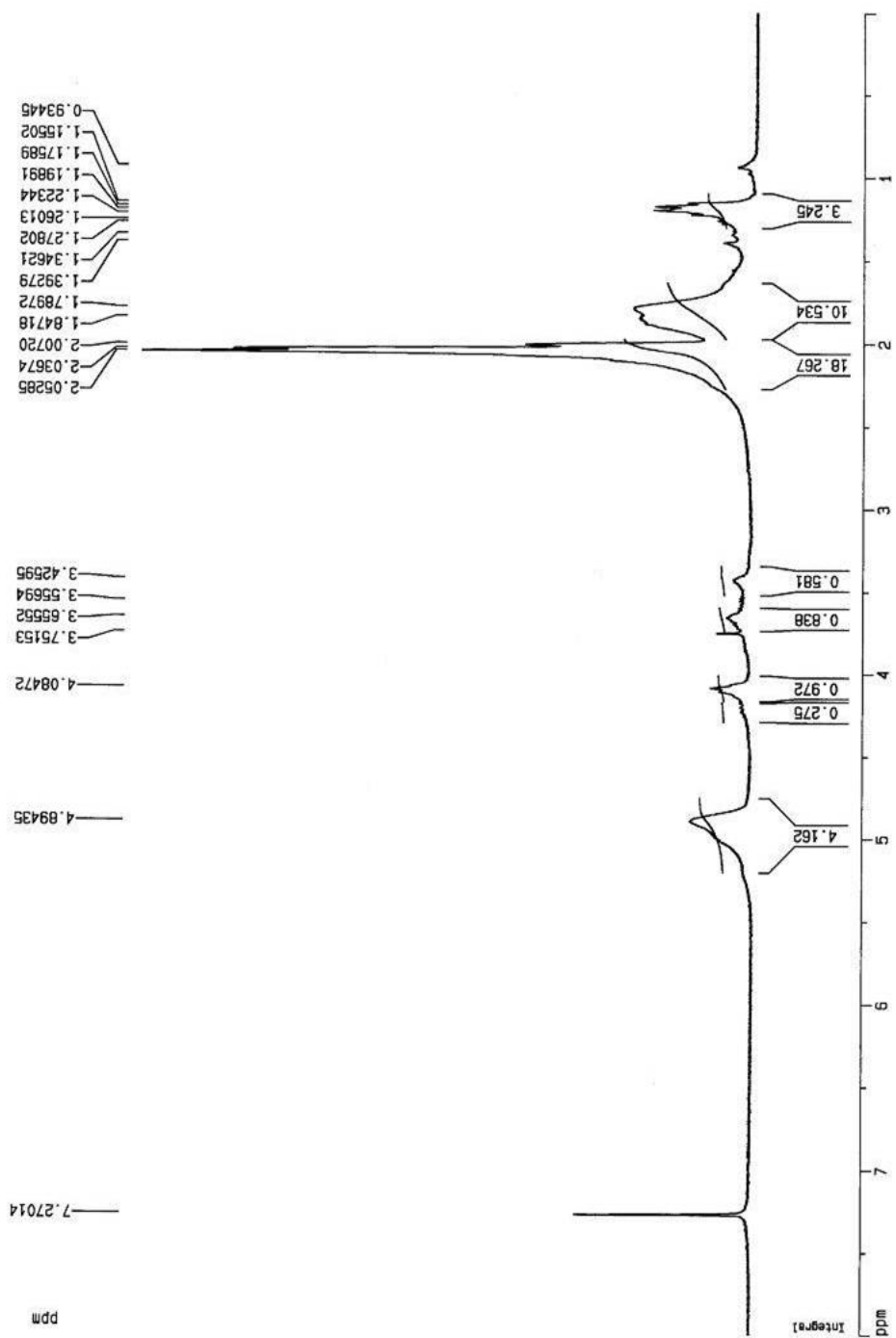


Figure A.15. ¹H-NMR spectrum of OVAc8-OH

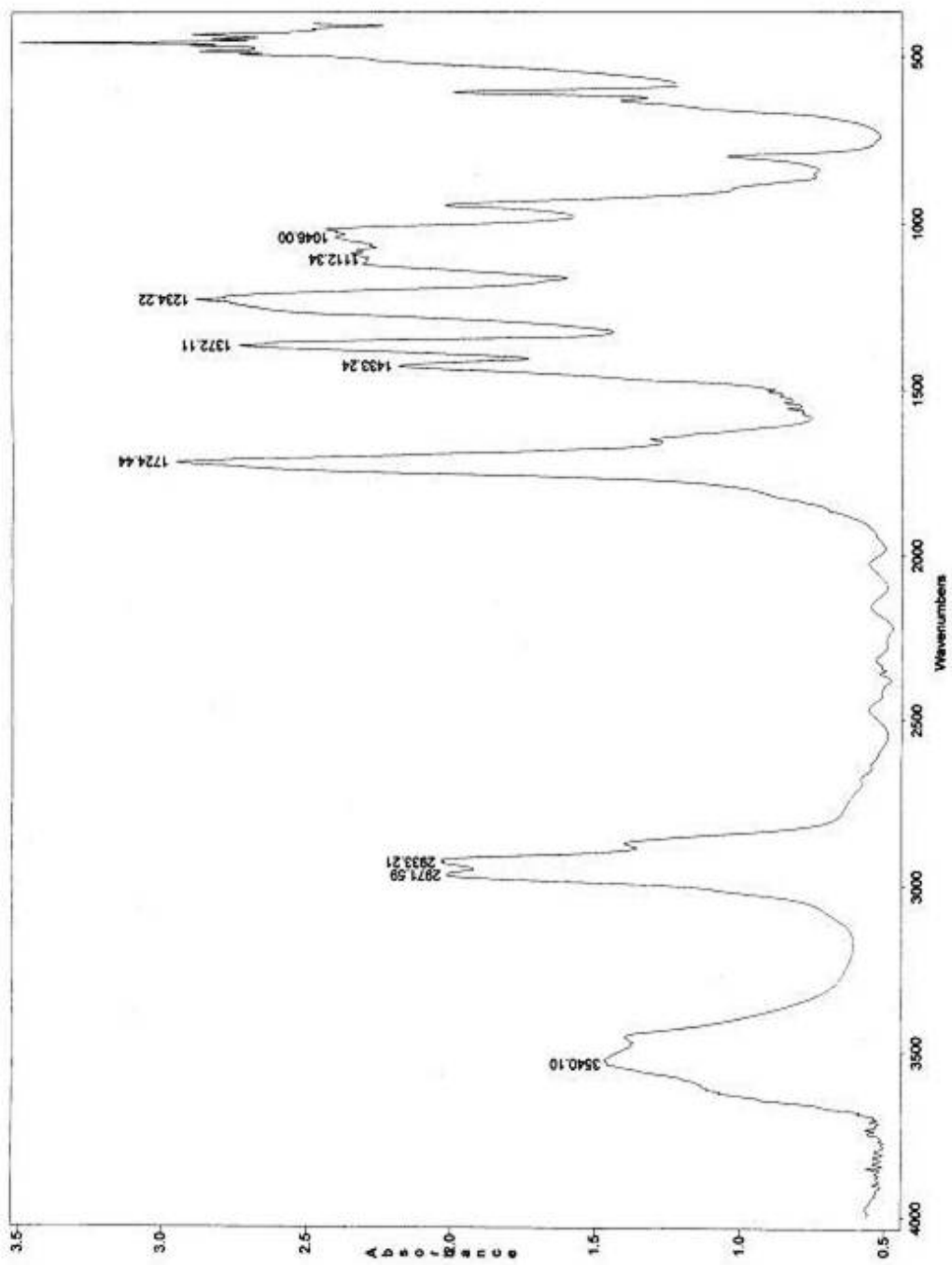


Figure A.16. FTIR spectrum of OVAc10-OH

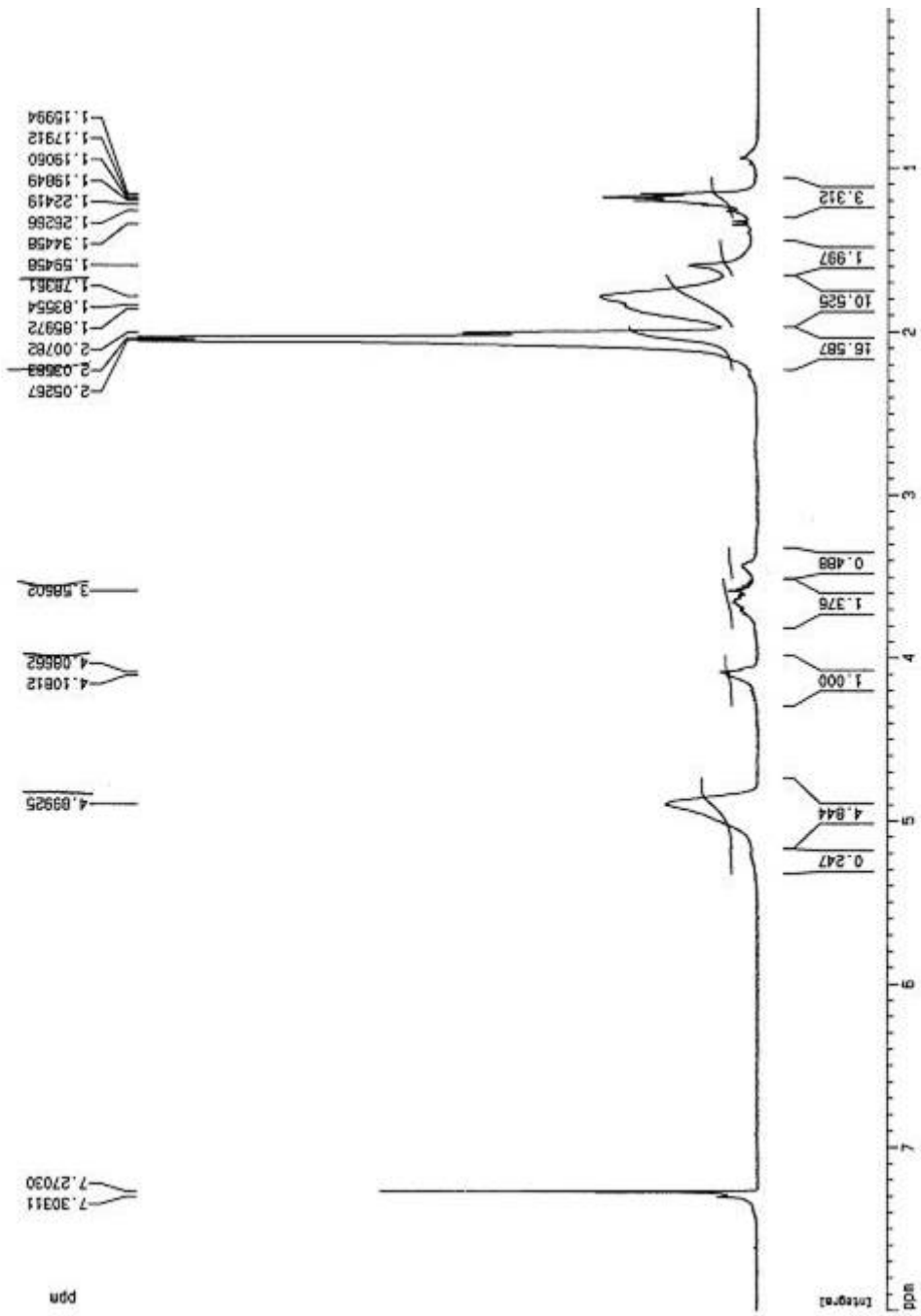


Figure A.17. ¹H-NMR spectrum of OVAcl0-OH

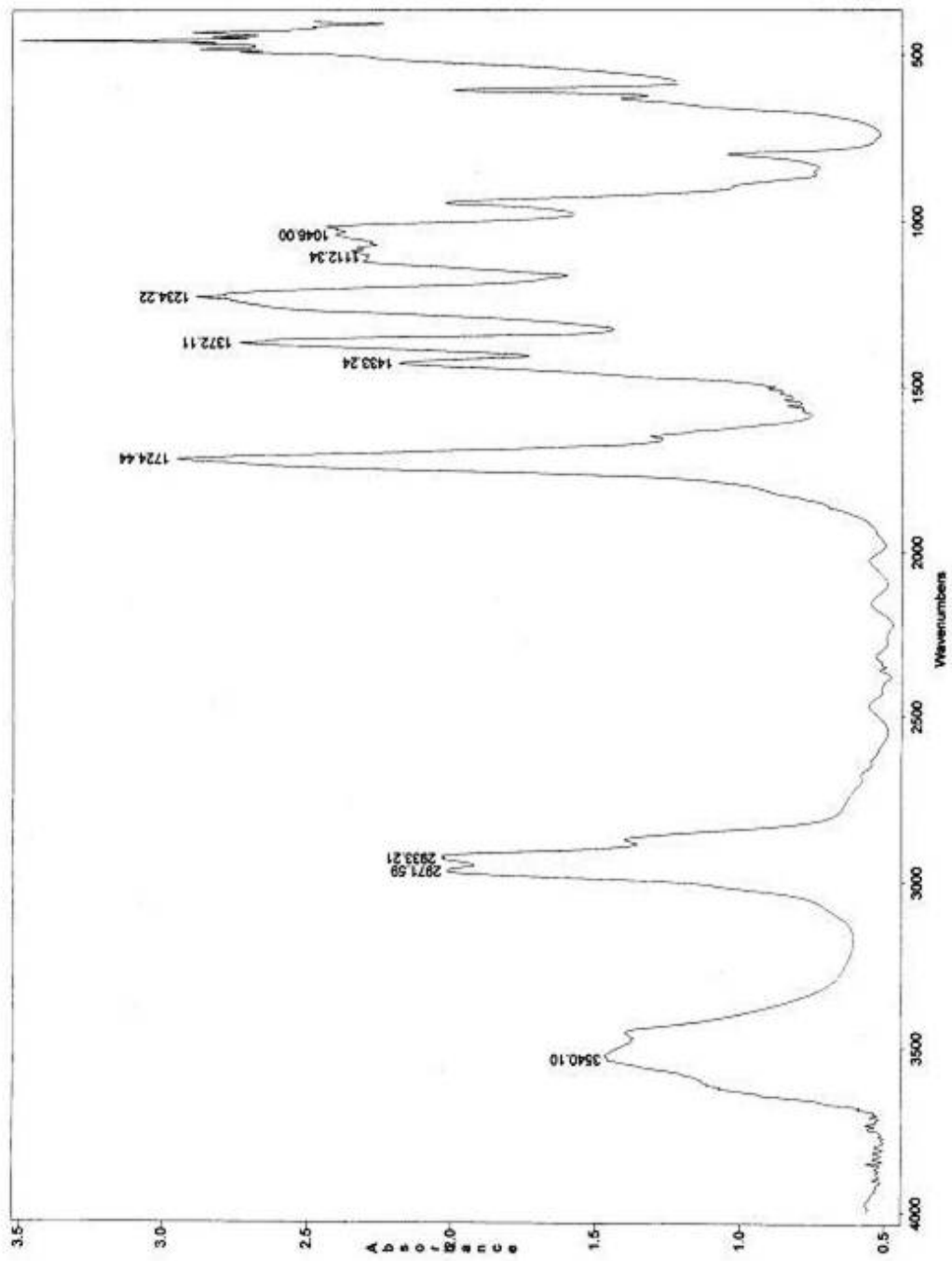


Figure A.18. FTIR spectrum of OVAc17-OH

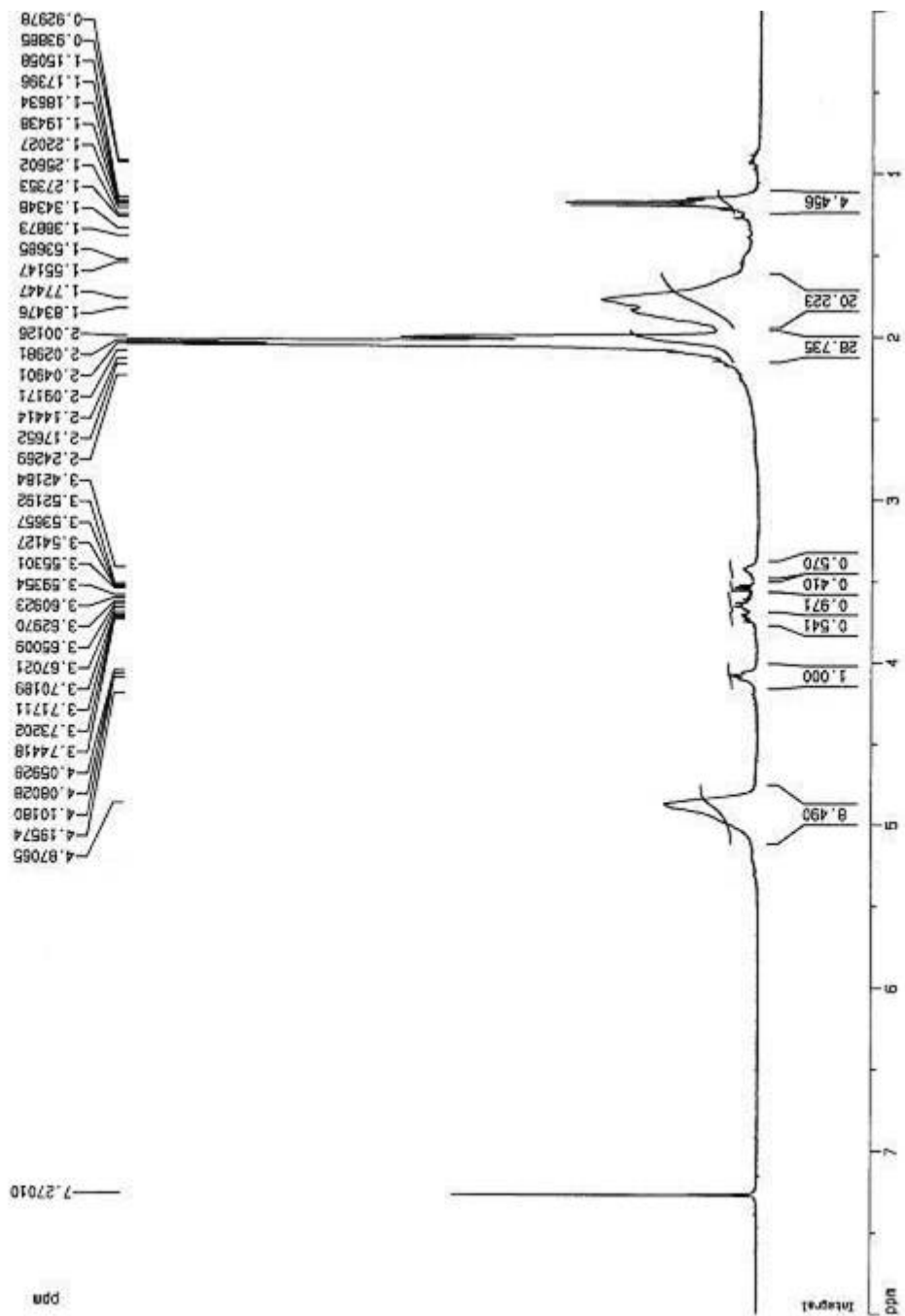


Figure A.19. ¹H-NMR spectrum of OVAcl7-OH

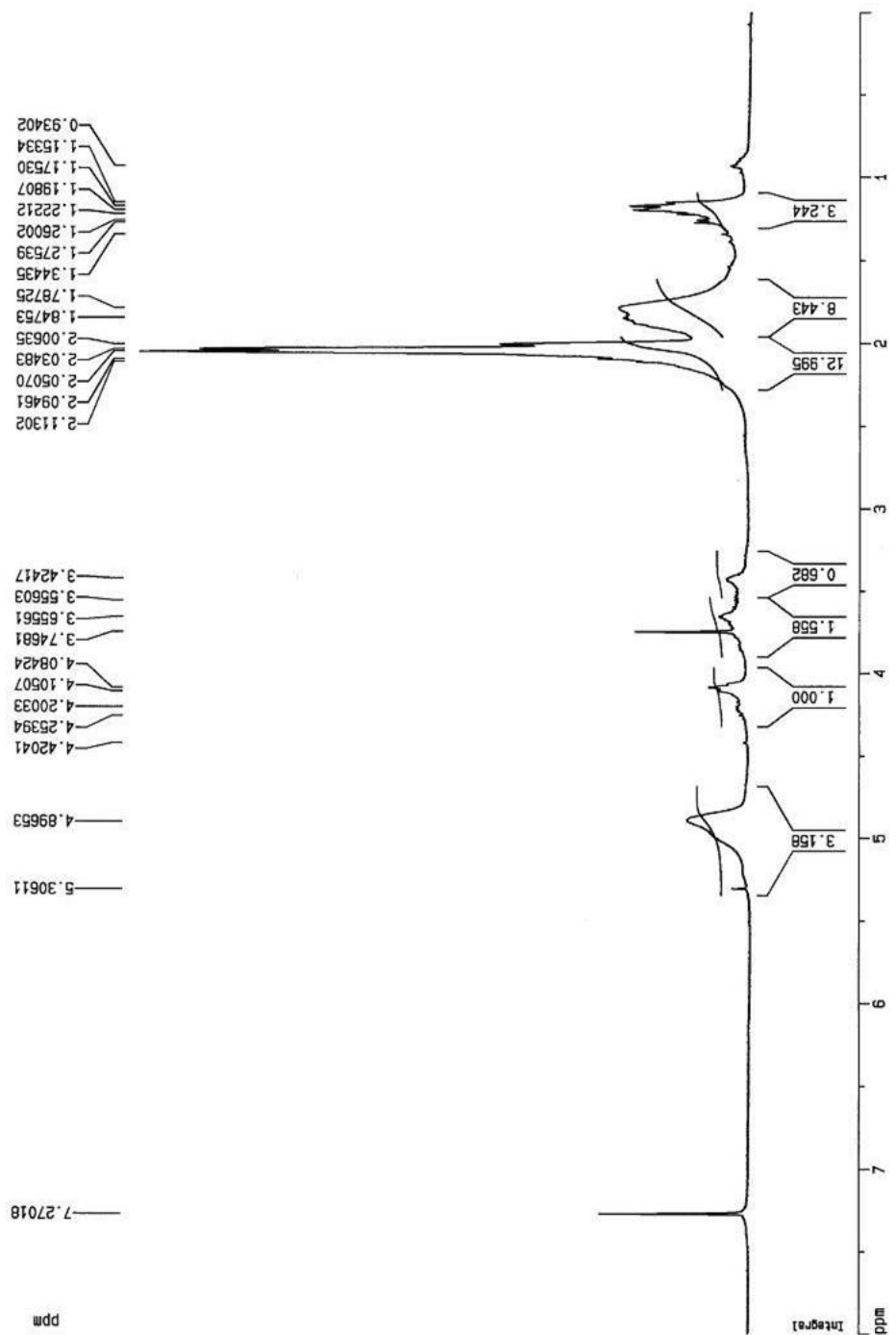


Figure A.20. $^1\text{H-NMR}$ spectrum of $\text{OVAc}_6\text{-OSO}_3\text{Na}$

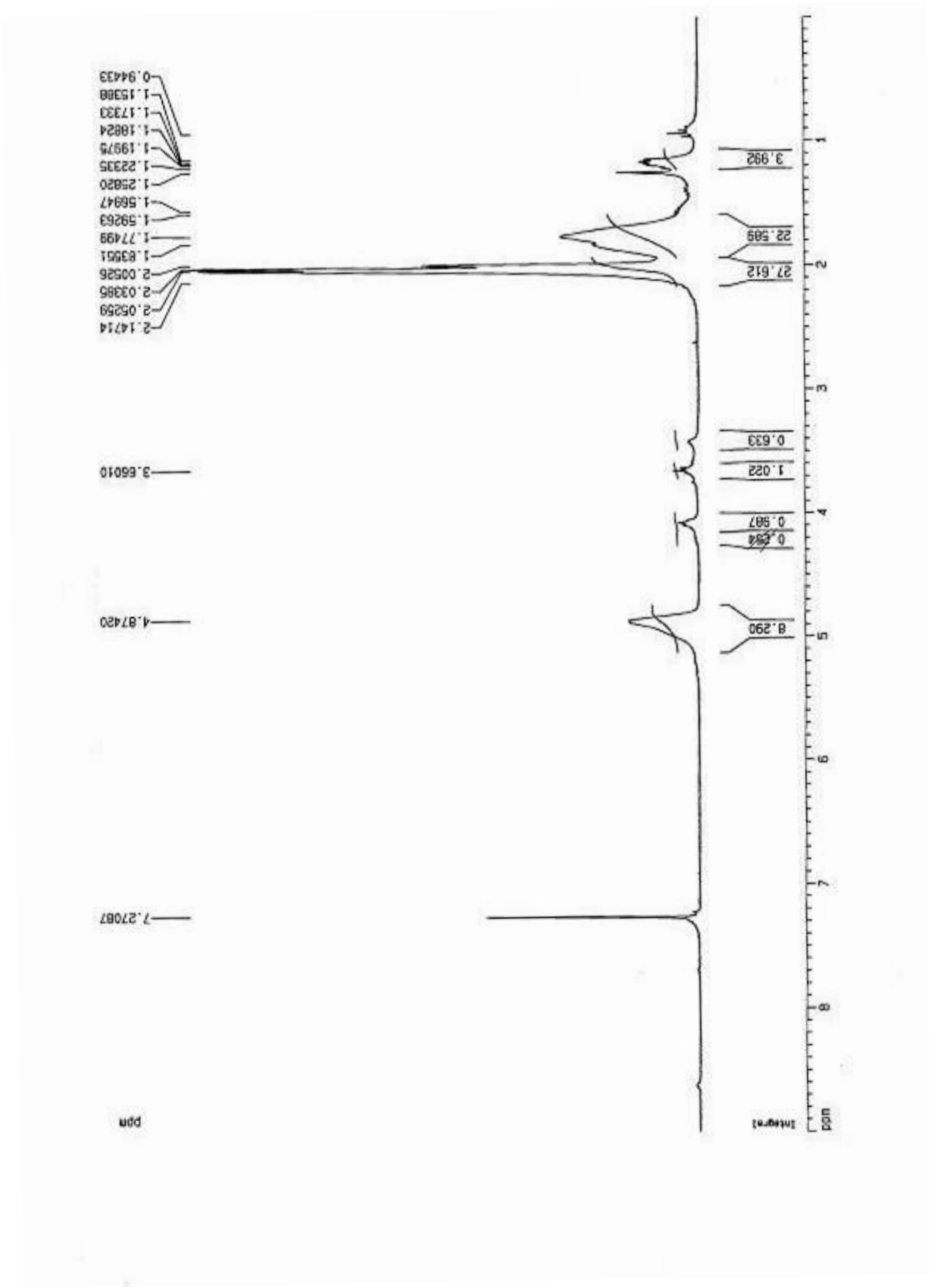


Figure A.22. $^1\text{H-NMR}$ spectrum of OVAc17-OSO₃Na

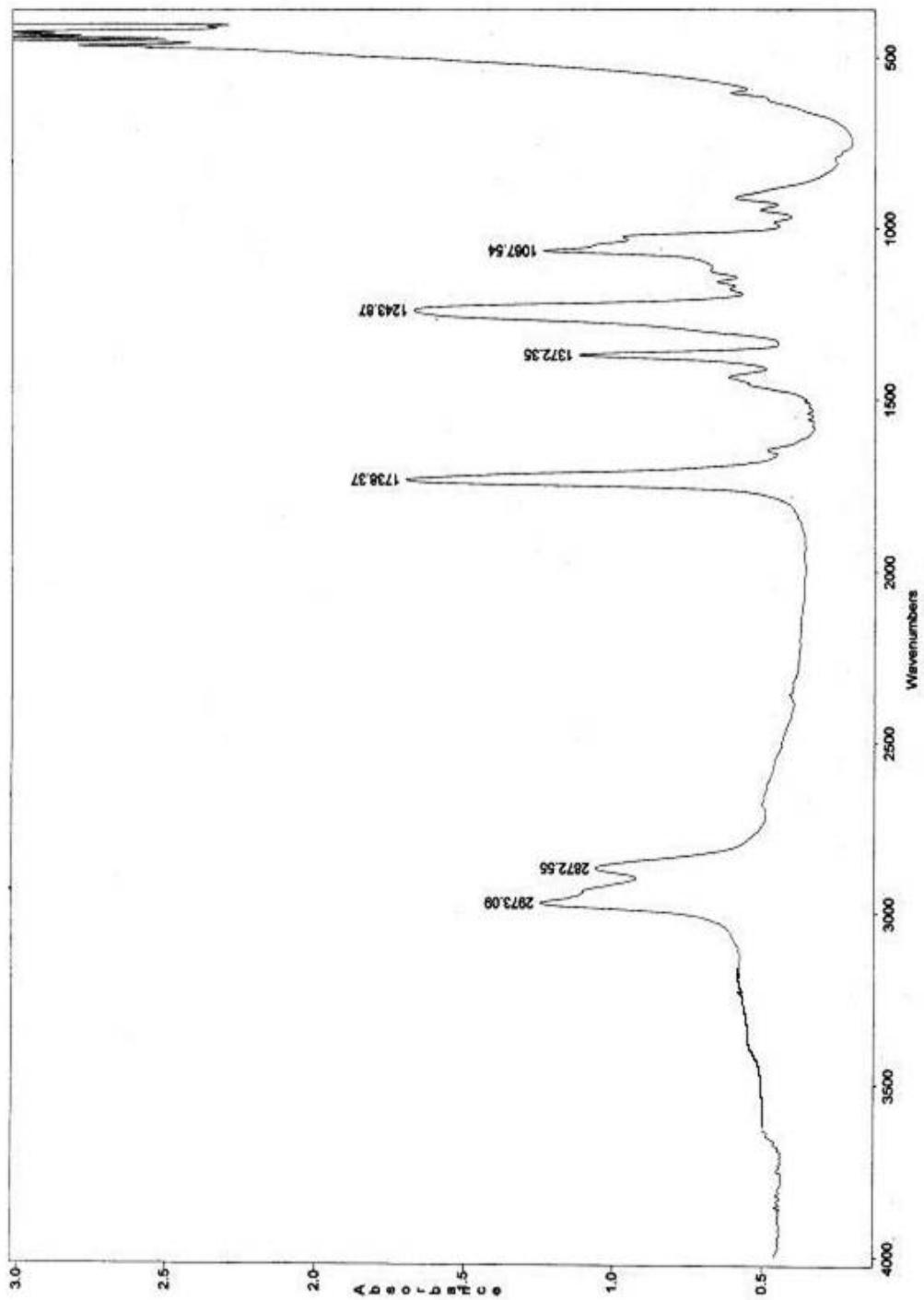


Figure A.23. FTIR spectrum of OVAc8 diester

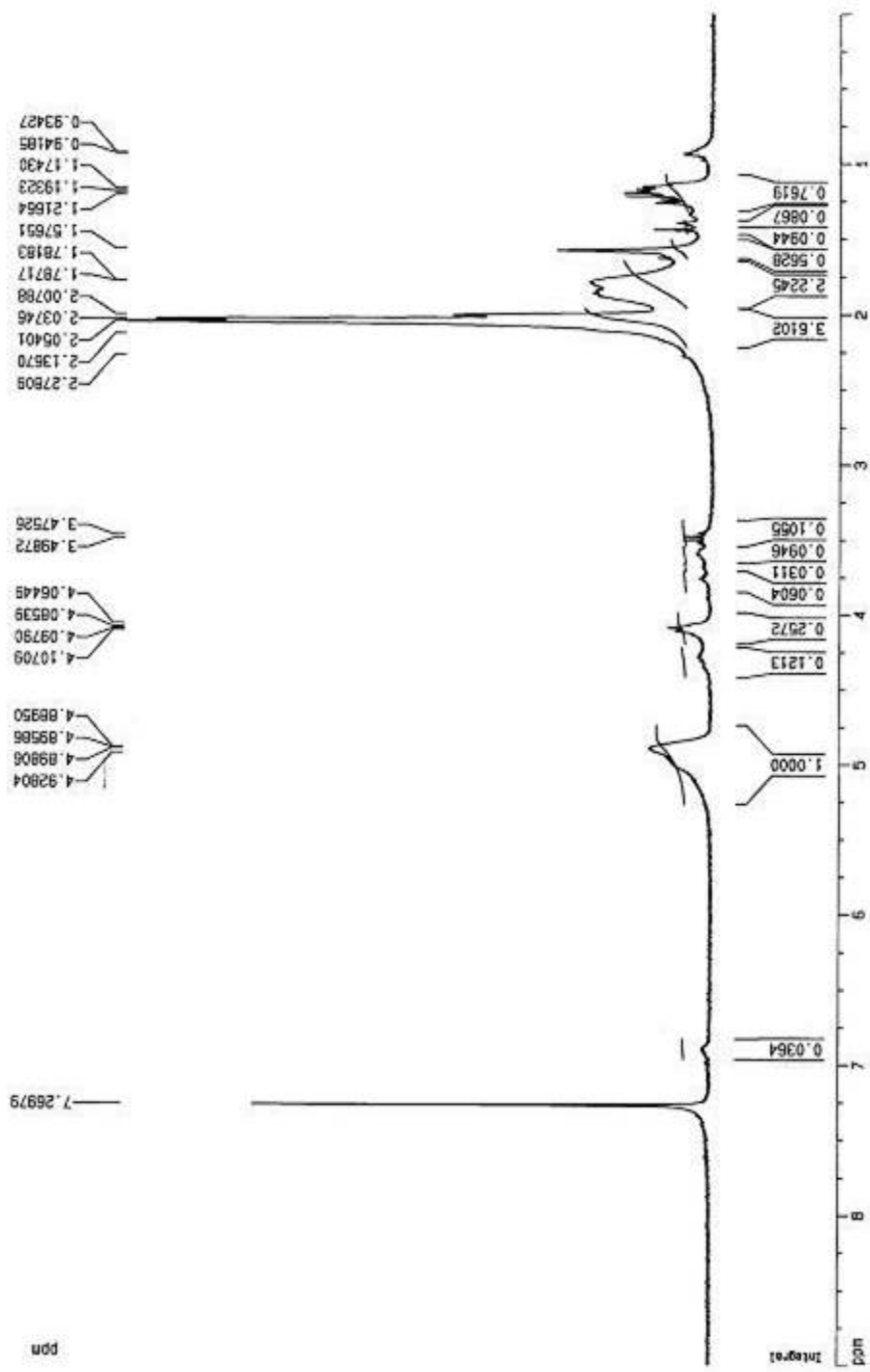


Figure A.24. ¹H-NMR spectrum of OVAc8 diester

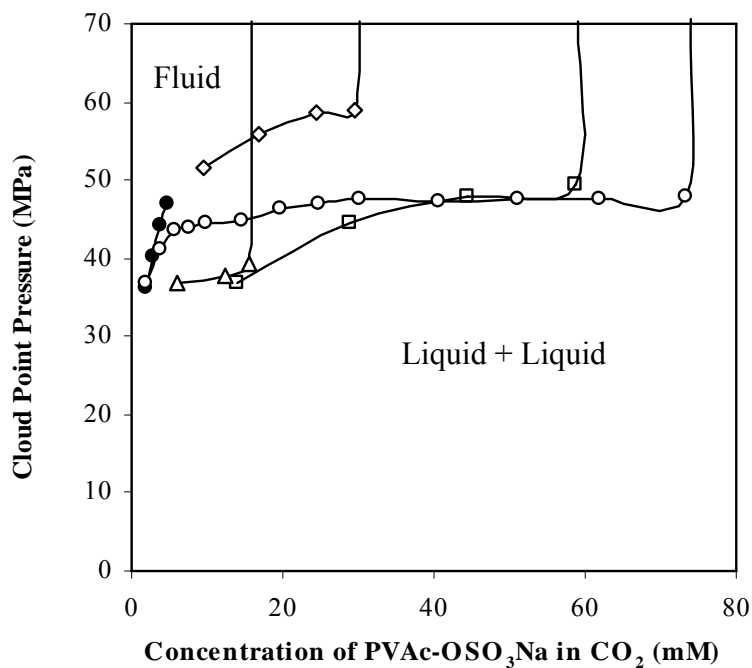


Figure A.25. Phase behavior of PVAc-OSO₃Na/CO₂ mixtures. PVAc6-OSO₃Na, 25 °C, W=0 (□); PVAc10-OSO₃Na, 25 °C, W=0 (○); PVAc17-OSO₃Na, 25 °C, W=0 (Δ); PVAc10-OSO₃Na, 25 °C, W=10 (●); PVAc10-OSO₃Na, 40 °C, W=0 (◇). (Surfactant concentration in mM).

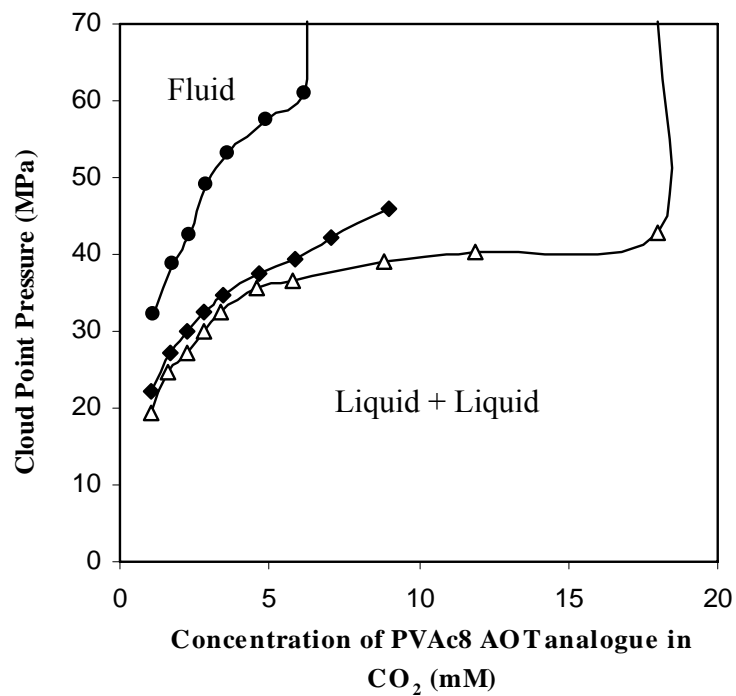


Figure A.26. Phase behavior of sodium bis(vinyl acetate)₈ sulfosuccinate/CO₂ mixtures at 25 °C. W = 0 (Δ); W = 10 (◆); W = 50 (●). (Surfactant concentration in mM).

APPENDIX B

SPECTRA AND PHASE BEHAVIOR OF SURFACTANTS IN

CHAPTER 5

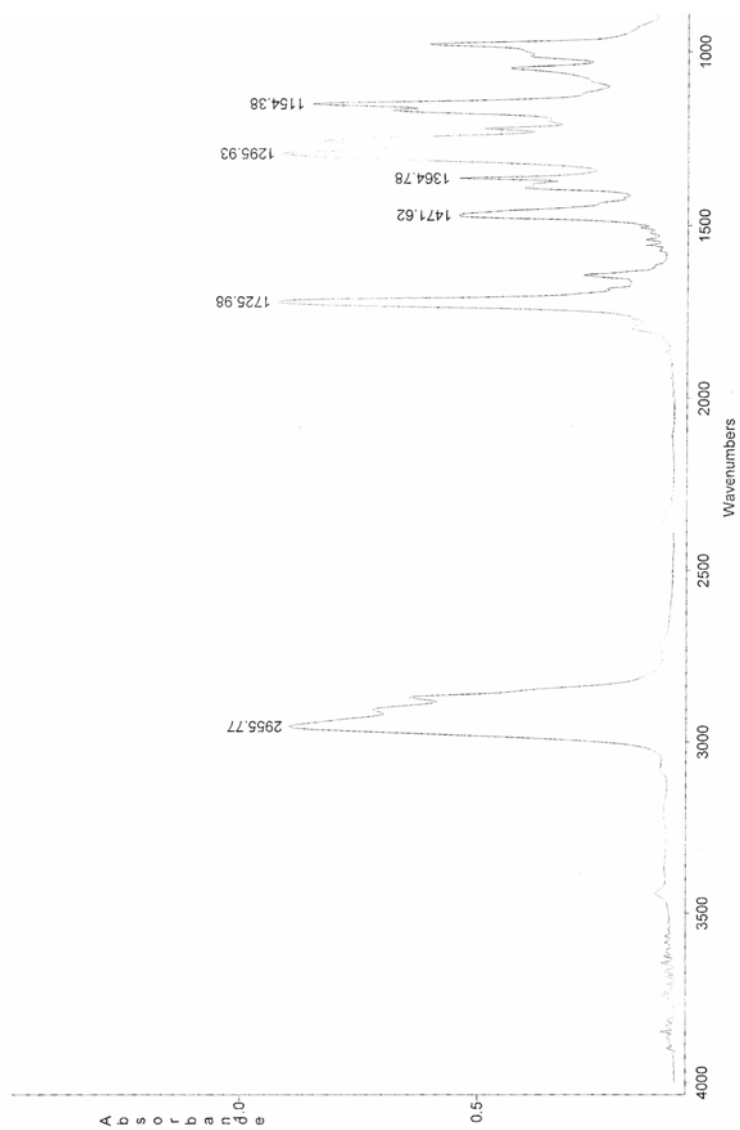


Figure B.1. FTIR spectrum of diester of AOT-TMH

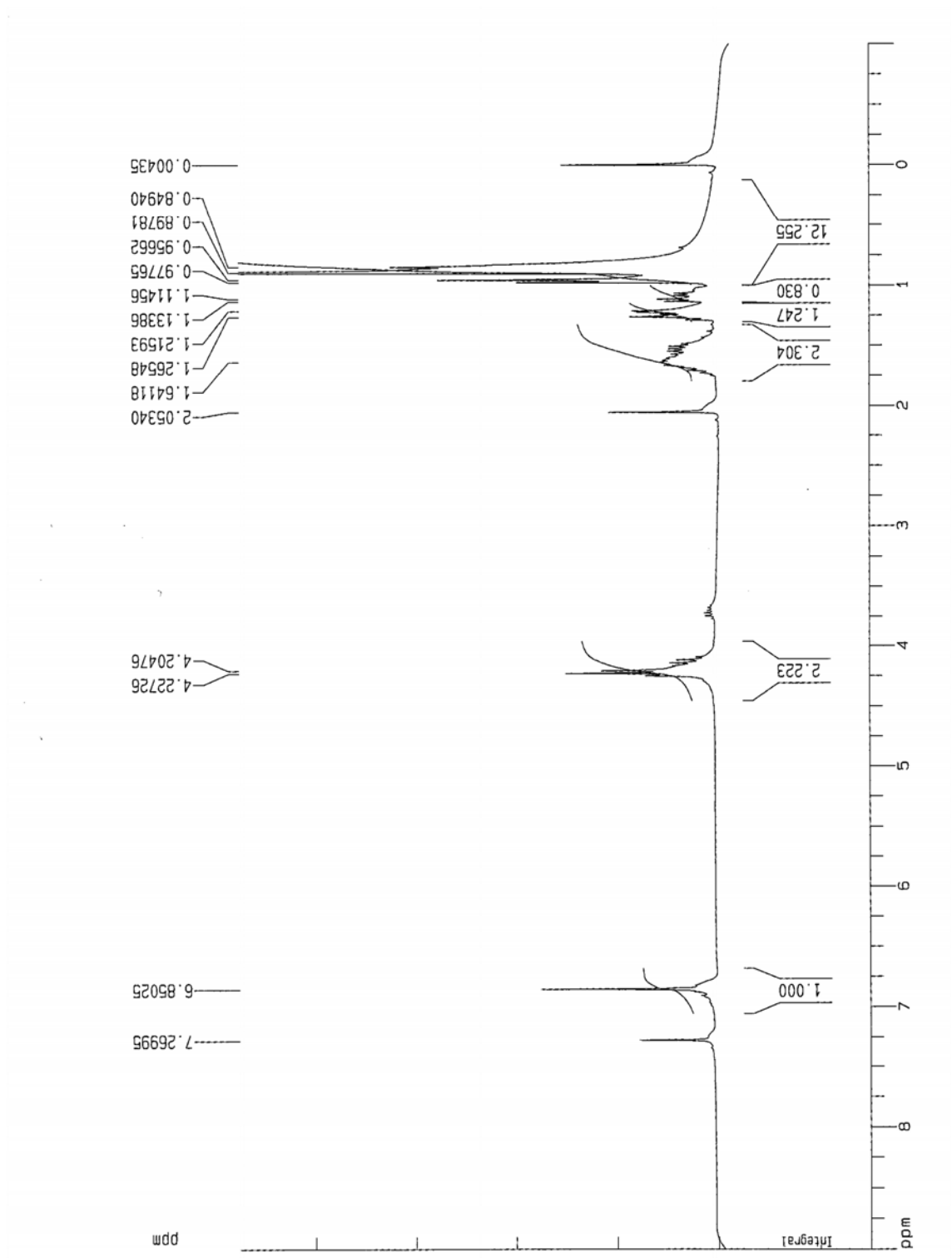


Figure B.2. ¹H-NMR spectrum of diester of AOT-TMH

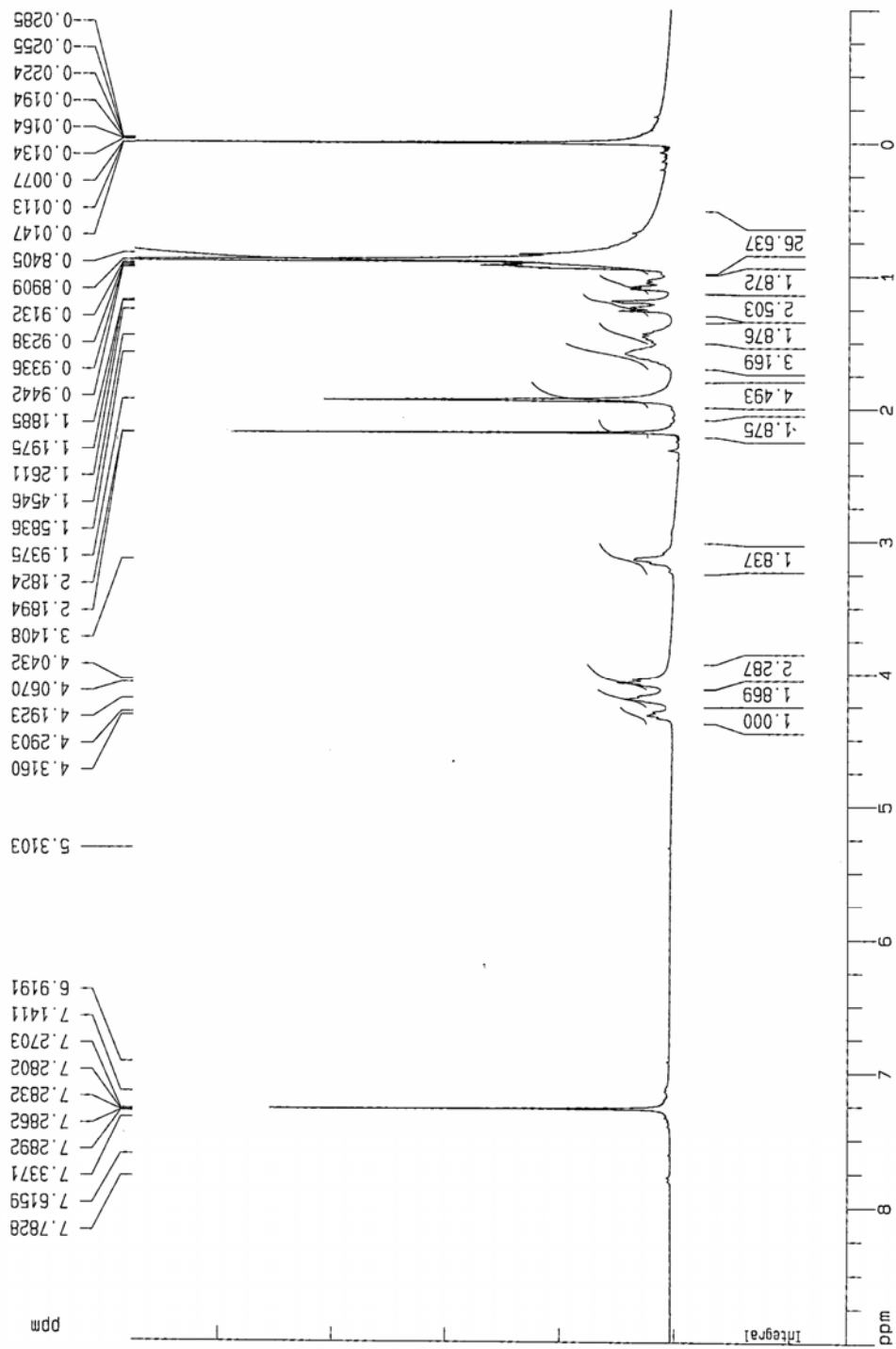


Figure B.3. ¹H-NMR spectrum for AOT-TMH

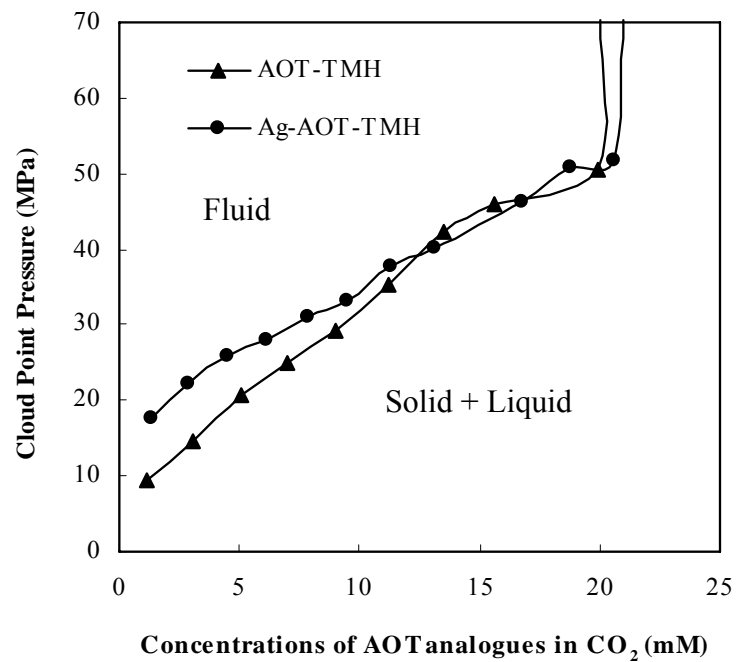


Figure B.4. Phase behavior of AOT-TMH and Ag-AOT-TMH at 40 °C. (Surfactant concentration in mM).

Table B.1. Soil analysis results of Ag-AOT-TMH

original dissolved Ag-AOT-TMH	0.0154	g
AOT dissolved in volume H ₂ O	10	mL
moles Ag-AOT-TMH=	3.343E-05	moles
moles H ₂ O=	0.5555556	moles
original ppm AOT in solution=	60.178749	
assuming all sodium not present exchanged to silver=	85.237314	% exchange

-- ppm in solution --						
Ca	K	Mg	P	Al	B	Cd
8.2	10.0	7.9	7.8	5.4	2.1	<0.1
-- ppm in solution --						
Cr	Cu	Fe	Mn	Na	Ni	Pb
<0.1	0.1	8.2	<0.1	8.9	0.5	2.4

BIBLIOGRAPHY

1. Panza, J.L. and E.J. Beckman, *Surfactants in Supercritical Fluids*, in *Supercritical Fluid Technology in Materials Science and Engineering: Syntheses, Properties, and Applications*, Y.P. Sun, Editor. 2002, Marcel Dekker: New York. p. 255-284.
2. Eastoe, J., et al., *Design and Performance of Surfactants for Carbon Dioxide*, in *Supercritical Carbon Dioxide: Separation and Processes*, A.S. Gopalan, C.M. Wai, and H.K. Jacobs, Editors. 2003, ACS Symposium Series 860; American Chemical Society: Washington, DC. p. 285-309.
3. Desimone, J.M., et al., *Dispersion Polymerizations in Supercritical Carbon-Dioxide*. *Science*, 1994. **265**(5170): p. 356-359.
4. Shaffer, K.A., et al., *Dispersion Polymerizations in Carbon Dioxide Using Siloxane-Based Stabilizers*. *Macromolecules*, 1996. **29**(7): p. 2704-2706.
5. Yazdi, A.V. and E.J. Beckman, *Design, Synthesis, and Evaluation of Novel, Highly CO₂-Soluble Chelating Agents for Removal of Metals*. *Industrial & Engineering Chemistry Research*, 1996. **35**(10): p. 3644-3652.
6. Yazdi, A.V. and E.J. Beckman, *Design of Highly CO₂-Soluble Chelating Agents .2. Effect of Chelate Structure and Process Parameters on Extraction Efficiency*. *Industrial & Engineering Chemistry Research*, 1997. **36**(6): p. 2368-2374.
7. Xu, J.H., A. Wlaschin, and R.M. Enick, *Thickening Carbon Dioxide with the Fluoroacrylate-Styrene Copolymer*. *SPE Journal*, 2003. **8**(2): p. 85-91.
8. Mistele, C.D., H.H. Thorp, and J.M. Desimone, *Ring-Opening Metathesis Polymerizations in Carbon Dioxide*. *Journal of Macromolecular Science-Pure and Applied Chemistry*, 1996. **A33**(7): p. 953-960.

9. Consani, K.A. and R.D. Smith, *Observations on the Solubility of Surfactants and Related Molecules in Carbon Dioxide at 50°C*. Journal of Supercritical Fluids, 1990. **3**(2): p. 51-65.
10. Hoefling, T.A., R.M. Enick, and E.J. Beckman, *Microemulsions in Near-Critical and Supercritical CO₂*. J. Phys. Chem., 1991. **95**: p. 7127.
11. Newman, D.A., et al., *Phase-Behavior of Fluoroether-Functional Amphiphiles in Supercritical Carbon-Dioxide*. Journal of Supercritical Fluids, 1993. **6**(4): p. 205-210.
12. Desimone, J.M., Z. Guan, and C.S. Elsbernd, *Synthesis of Fluoropolymers in Supercritical Carbon-Dioxide*. Science, 1992. **257**(5072): p. 945-947.
13. Hoefling, T.A., et al., *Effect of Structure on the Cloud-Point Curves of Silicone-Based Amphiphiles in Supercritical Carbon-Dioxide*. Journal of Supercritical Fluids, 1993. **6**(3): p. 165-171.
14. Hoefling, T.A., et al., *Design and Synthesis of Highly CO₂-Soluble Surfactants and Chelating-Agents*. Fluid Phase Equilibria, 1993. **83**: p. 203-212.
15. Eastoe, J., A. Paul, and A. Downer, *Effects of Fluorocarbon Surfactant Chain Structure on Stability of Water-in-Carbon Dioxide Microemulsions. Links between Aqueous Surface Tension and Microemulsion Stability*. Langmuir, 2002. **18**(8): p. 3014-3017.
16. Fink, R. and E.J. Beckman, *Phase Behavior of Siloxane-based Amphiphiles in Supercritical Carbon Dioxide*. Journal of Supercritical Fluids, 2000. **18**(2): p. 101-110.
17. Psathas, P.A., et al., *Water-in-Carbon Dioxide Emulsions with Poly(dimethylsiloxane)-based Block Copolymer Ionomers*. Industrial & Engineering Chemistry Research, 2000. **39**(8): p. 2655-2664.
18. McNally, M.P. and F.V. Bright, *"Supercritical Fluid Technology"*. ACS Symposium Series, 1992. **488**.

19. Kumar, S.K. and K.P. Johnston, *Modelling the Solubility of Solids in Supercritical Fluids with Density as the Independent Variable*. Journal of Supercritical Fluids, 1988. **1**(1): p. 15-22.
20. Technical Insights, I., *Supercritical Fluids Processing: Emerging Opportunities*. Emerging Technologies. Vol. no. 15. 1985, Fort Lee, N.J.
21. McHugh, M.A. and V.J. Krukonis, *Supercritical Fluid Extraction: Principles and Practice, 2nd Edition*, ed. H. Brenner. 1994, Stoneham, MA: Butterworth-Heinemann.
22. Schneider, G.M., *Physiochemical Principles of Extraction with Supercritical Gases*. Angew. Chem. Int. Ed. Engl., 1978. **17**: p. 716.
23. Hyatt, J.A., *Liquid and Supercritical Carbon Dioxide as Organic Solvents*. Journal of Organic Chemistry, 1984. **49**(26): p. 5097-5101.
24. Mcfann, G.J., et al., *Carbon-Dioxide Regeneration of Block-Copolymer Micelles Used for Extraction and Concentration of Trace Organics*. Industrial & Engineering Chemistry Research, 1993. **32**(10): p. 2336-2344.
25. Mcfann, G.J., K.P. Johnston, and S.M. Howdle, *Solubilization in Nonionic Reverse Micelles in Carbon-Dioxide*. AIChE Journal, 1994. **40**(3): p. 543-555.
26. Kazarian, S.G., et al., *Specific Intermolecular Interaction of Carbon Dioxide with Polymers*. Journal of the American Chemical Society, 1996. **118**(7): p. 1729-1736.
27. Meredith, J.C., et al., *Quantitative Equilibrium Constants between CO₂ and Lewis bases from FTIR Spectroscopy*. Journal of Physical Chemistry, 1996. **100**(26): p. 10837-10848.
28. Mertdogan, C.A., T.P. DiNoia, and M.A. McHugh, *Impact of Backbone Architecture on the Solubility of Fluorocopolymers in Supercritical CO₂ and Halogenated Supercritical Solvents: Comparison of Poly(vinylidene fluoride-co-22 mol % hexafluoropropylene) and Poly(tetrafluoroethylene-co-19 mol % hexafluoropropylene)*. Macromolecules, 1997. **30**(24): p. 7511-7515.

29. Rindfleisch, F., T.P. DiNoia, and M.A. McHugh, *Solubility of Polymers and Copolymers in Supercritical CO₂*. Journal of Physical Chemistry, 1996. **100**(38): p. 15581-15587.
30. O'Neill, M.L., et al., *Solubility of Homopolymers and Copolymers in Carbon Dioxide*. Industrial & Engineering Chemistry Research, 1998. **37**(8): p. 3067-3079.
31. Jacobson, G.B., et al., *Organic Synthesis in Water/Carbon Dioxide Emulsions*. Journal of Organic Chemistry, 1999. **64**: p. 1207-1210.
32. Jacobson, G.B., et al., *Enhanced Catalyst Reactivity and Separations Using Water/Carbon Dioxide Emulsions*. Journal of the American Chemical Society, 1999. **121**: p. 11902-11903.
33. Ohde, H., F. Hunt, and C.M. Wai, *Synthesis of Silver and Copper Nanoparticles in a Water-in-Supercritical Carbon Dioxide Microemulsion*. Chemistry of Materials, 2001. **13**(11): p. 4130-4135.
34. Ohde, H., et al., *Hydrogenation of Olefins in Supercritical CO₂ Catalyzed by Palladium Nanoparticles in a Water-in-CO₂ Microemulsion*. Journal of the American Chemical Society, 2002. **124**(17): p. 4540-4541.
35. Iezzi, A., *Supercritical Fluid Science and Technology*, in ACS Symposium Series 406, J.M.L.P. Keith P. Johnson, Editor. 1989, American Chemical Society: Washington DC. p. 122.
36. Harrison, K., et al., *Water-in-Carbon Dioxide Microemulsions with a Fluorocarbon-Hydrocarbon Hybrid Surfactant*. Langmuir, 1994. **10**(10): p. 3536-3541.
37. Eastoe, J., et al., *Fluoro-Surfactants at Air/Water and Water/CO₂ Interfaces*. Physical Chemistry Chemical Physics, 2000. **2**(22): p. 5235-5242.
38. Heitz, M.P., et al., *Water Core within Perfluoropolyether-based Microemulsions formed in Supercritical Carbon Dioxide*. J. Phys. Chem. B, 1997. **101**: p. 6707.

39. Chillura-Martino, D., et al., *Neutron Scattering Characterization of Homopolymer and Graft-Copolymer Micelles in Supercritical Carbon Dioxide*. J. Mol. Struct., 1997. **383**: p. 3.
40. McClain, J.B., et al., *Design of Nonionic Surfactants for Supercritical Carbon Dioxide*. Science, 1996. **274**(5295): p. 2049-2052.
41. Fulton, J.L., et al., *Aggregation of Amphiphilic Molecules in Supercritical Carbon-Dioxide - a Small-Angle X-Ray-Scattering Study*. Langmuir, 1995. **11**(11): p. 4241-4249.
42. Heller, J.P., D.K. Dandge, and R.J. Card, *Direct Thickeners for Mobility Control of CO₂ Floods*. Society of Petroleum Engineers Journal, 1985. **25**(5): p. 679-686.
43. Kirby, C.F. and M.A. McHugh, *Phase Behavior of Polymers in Supercritical Fluid Solvents*. Chemical Reviews, 1999. **99**(2): p. 565-602.
44. Stone, M.T., et al., *Molecular Differences between Hydrocarbon and Fluorocarbon Surfactants at the CO₂/Water Interface*. Journal of Physical Chemistry B, 2003. **107**(37): p. 10185-10192.
45. Stone, M.T., et al., *Low interfacial free volume of Stubby surfactants stabilizes water-in-carbon dioxide microemulsions*. Journal of Physical Chemistry B, 2004. **108**(6): p. 1962-1966.
46. Ryoo, W., S.E. Webber, and K.P. Johnston, *Water-in-Carbon Dioxide Microemulsions with Methylated Branched Hydrocarbon Surfactants*. Industrial & Engineering Chemistry Research, 2003. **42**(25): p. 6348-6358.
47. Raveendran, P. and S.L. Wallen, *Sugar Acetates as Novel, Renewable CO₂-Philes*. Journal of the American Chemical Society, 2002. **124**(25): p. 7274-7275.
48. Potluri, V.K., et al., *Peracetylated Sugar Derivatives Show High Solubility in Liquid and Supercritical Carbon Dioxide*. Organic Letters, 2002. **4**(14): p. 2333-2335.
49. Hong, L., M.C. Thies, and R.M. Enick, *Global Phase Behavior for CO₂-philic Solids: the CO₂ + β -D-Maltose Octaacetate System*. Journal of Supercritical Fluids, 2005. **34**(1): p. 11-16.

50. Potluri, V.K., et al., *The High CO₂-Solubility of per-Acetylated Alpha-, Beta-, and Gamma-Cyclodextrin*. *Fluid Phase Equilibria*, 2003. **211**(2): p. 211-217.
51. Raveendran, P. and S.L. Wallen, *Cooperative C-H...O Hydrogen Bonding in CO₂-Lewis Base Complexes: Implications for Solvation in Supercritical CO₂*. *Journal of the American Chemical Society*, 2002. **124**(42): p. 12590-12599.
52. Blatchford, M.A., P. Raveendran, and S.L. Wallen, *Spectroscopic Studies of Model Carbonyl Compounds in CO₂: Evidence for Cooperative C-H Center dot center dot center dot O interactions*. *Journal of Physical Chemistry A*, 2003. **107**(48): p. 10311-10323.
53. Shen, Z., et al., *CO₂-Solubility of Oligomers and Polymers that Contain the Carbonyl Group*. *Polymer*, 2003. **44**(5): p. 1491-1498.
54. Kilic, S., et al., *Effect of Grafted Lewis Base Groups on the Phase Behavior of Model Poly(dimethyl siloxanes) in CO₂*. *Industrial & Engineering Chemistry Research*, 2003. **42**(25): p. 6415-6424.
55. da Rocha, S.R.P., K.L. Harrison, and K.P. Johnston, *Effect of Surfactants on the Interfacial Tension and Emulsion Formation between Water and Carbon Dioxide*. *Langmuir*, 1999. **15**(2): p. 419-428.
56. Sarbu, T., T. Styranec, and E.J. Beckman, *Non-Fluorous Polymers with very High Solubility in Supercritical CO₂ down to Low Pressures*. *Nature*, 2000. **405**(6783): p. 165-168.
57. Liu, J.C., et al., *Solubility of Ls-36 and Ls-45 Surfactants in Supercritical CO₂ and Loading Water in the CO₂/Water/Surfactant Systems*. *Langmuir*, 2002. **18**(8): p. 3086-3089.
58. Liu, J.C., et al., *Formation of Water-in-CO₂ Microemulsions with Non-Fluorous Surfactant Ls-54 and Solubilization of Biomacromolecules*. *Chemistry-A European Journal*, 2002. **8**(6): p. 1356-1360.

59. Drohmann, C. and E.J. Beckman, *Phase Behavior of Polymers Containing Ether Groups in Carbon Dioxide*. Journal of Supercritical Fluids, 2002. **22**(2): p. 103-110.
60. Nave, S., J. Eastoe, and J. Penfold, *What is So Special about Aerosol-OT? I. Aqueous Systems*. Langmuir, 2000. **16**(23): p. 8733-8740.
61. Eastoe, J., et al., *Micellization of Hydrocarbon Surfactants in Supercritical Carbon Dioxide*. Journal of the American Chemical Society, 2001. **123**(5): p. 988-989.
62. Johnston, K.P., et al., *Water in Carbon Dioxide Macroemulsions and Miniemulsions with a Hydrocarbon Surfactant*. Langmuir, 2001. **17**(23): p. 7191-7193.
63. Gale, R.W., J.L. Fulton, and R.D. Smith, *Organized Molecular Assemblies in the Gas Phase: Reverse Micelles and Microemulsions in Supercritical Fluids*. Journal of the American Chemical Society, 1987. **109**(3): p. 920-921.
64. Bartscherer, K.A., M. Minier, and H. Renon, *Microemulsions in Compressible Fluids*. Fluid Phase Equilibria, 1995. **107**(93-150).
65. Johnston, K.P., G.J. Mcfann, and D.G. Peck, *Design and Characterization of the Molecular Environment in Supercritical Fluids*. Fluid Phase Equilibria, 1989. **52**: p. 337-346.
66. Johnston, K.P., et al., *Water-in-Carbon Dioxide Microemulsions: An Environment for Hydrophiles Including Proteins*. Science, 1996. **271**: p. 624-626.
67. Heitz, M.P., et al., *Water Core within Perfluoropolyether-Based Microemulsions Formed in Supercritical Carbon Dioxide*. Journal of Physical Chemistry B, 1997. **101**(34): p. 6707-6714.
68. Clarke, M.J., et al., *Water in Supercritical Carbon Dioxide Microemulsions: Spectroscopic Investigation of a New Environment for Aqueous Inorganic Chemistry*. Journal of the American Chemical Society, 1997. **119**(27): p. 6399-6406.

69. Johnston, K.P., et al., *Water-in-Carbon Dioxide Microemulsions: an Environment for Hydrophiles including Proteins*. Science (Washington, D. C.), 1996. **271**(5249): p. 624-6.
70. Lee, C.T., et al., *Droplet interactions in Water-in-Carbon Dioxide Microemulsions Near the Critical Ppoint: A Small-Angle Neutron Scattering Study*. Journal of Physical Chemistry B, 2001. **105**(17): p. 3540-3548.
71. Zielinski, R.G., et al., *A small-angle neutron scattering study of water in carbon dioxide microemulsions*. Langmuir, 1997. **13**(15): p. 3934-3937.
72. Sun, Y.P., P. Atorngitjawat, and M.J. Meziani, *Preparation of Silver Nanoparticles via Rapid Expansion of Water in Carbon Dioxide Microemulsion into Reductant Solution*. Langmuir, 2001. **17**(19): p. 5707-5710.
73. McLeod, M.C., et al., *Synthesis and Stabilization of Silver Metallic Nanoparticles and Premetallic Intermediates in Perfluoropolyether/CO₂ Reverse Micelle Systems*. Journal of Physical Chemistry B, 2003. **107**(12): p. 2693-2700.
74. Ji, M., et al., *Synthesizing and Dispersing Silver Nanoparticles in a Water-in-Supercritical Carbon Dioxide Microemulsion*. Journal of the American Chemical Society, 1999. **121**(11): p. 2631-2632.
75. McLeod, M.C., W.F. Gale, and C.B. Roberts, *Metallic nanoparticle production utilizing a supercritical carbon dioxide flow process*. Langmuir, 2004. **20**(17): p. 7078-7082.
76. Esumi, K., S. Sarashina, and T. Yoshimura, *Synthesis of Gold Nanoparticles from an Organometallic Compound in Supercritical Carbon Dioxide*. Langmuir, 2004. **20**(13): p. 5189-5191.
77. Morley, K.S., et al., *Clean Preparation of Nanoparticulate Metals in Porous Supports: a Supercritical Route*. Journal of Materials Chemistry, 2002. **12**(6): p. 1898-1905.

78. Ohade, H., M. Ohde, and C.M. Wai, *Swelled Plastics in Supercritical CO₂ as Media for Stabilization of Metal Nanoparticles and for Catalytic Hydrogenation*. Chemical Communications, 2004(8): p. 930-931.
79. Watkins, J.J., J.M. Blackburn, and T.J. McCarthy, *Chemical Fluid Deposition: Reactive Deposition of Platinum Metal from Carbon Dioxide Solution*. Chemistry of Materials, 1999. **11**(2): p. 213-215.
80. Blackburn, J.M., et al., *Deposition of Conformal Copper and Nickel Films from Supercritical Carbon Dioxide*. Science, 2001. **294**(5540): p. 141-5.
81. Shah, P.S., et al., *Nanocrystal Arrested Precipitation in Supercritical Carbon Dioxide*. Journal of Physical Chemistry B, 2001. **105**(39): p. 9433-9440.
82. Shah, P.S., et al., *Role of Steric Stabilization on the Arrested Growth of Silver Nanocrystals in Supercritical Carbon Dioxide*. Journal of Physical Chemistry B, 2002. **106**(47): p. 12178-12185.
83. Taber, J.J., F.D. Martin, and R.S. Seright, *EOR Screening Criteria Revisited .I. Introduction to Screening Criteria and Enhanced Recovery Field Projects*. SPE Reservoir Engineering, 1997. **12**(3): p. 189-198.
84. Enick, R., G. Holder, and B. Morsi, *A Thermodynamic Correlation for the Minimum Miscibility Pressure in CO₂ Flooding of Petroleum Reservoirs*. SPE Reservoir Engineering, 1988.
85. Carcoana, A., *Applied Enhanced Oil Recovery*. 1992: Prentice Hall.
86. Xu, J., *Carbon Dioxide Thickening Agents for Reducing CO₂ Mobility*, in *Department of Chemical and Petroleum Engineering*. 2003, University of Pittsburgh: Pittsburgh.
87. Caudle, B.H. and A.B. Dyes, *Improving Miscible Displacement by Gas-Water Injection*. Trans AIME, 1958. **213**: p. 281-284.
88. Lee, H.O. and J.P. Heller, *Laboratory Measurements of CO₂-Foam Mobility*. SPE Reservoir Engineering, 1990. **5**(2).

89. Lee, H.O., J.P. Heller, and A. Hofer, *Change in Apparent Viscosity of CO₂ Foam with Rock Permeability*. SPE Reservoir Engineering, 1991. **6**(4): p. 421-428.
90. Schramm, L.L., ed. *Foams: Fundamentals and Applications in the Petroleum Industry*. Chapter 5. CO₂ Foams in Enhanced Oil Recovery, ed. J.P. Heller. 1994, American Chemical Society, Advances in Chemistry Series: Washington, DC.
91. Wellington, S.L., *Reservoir-Tailored CO₂-Aided Oil Recovery Process*. 1983, Shell Oil Company (Houston, TX): United States.
92. Wellington, S.L., et al., *Polyalkoxy Sulfonate, CO₂ and Brine Drive Process for Oil Recovery*. 1985, Shell Oil Company: United States.
93. McClain, J.B., et al., *Solution Properties of a CO₂-Soluble Fluoropolymer via Small Angle Neutron Scattering*. Journal of the American Chemical Society, 1996. **118**(4): p. 917-918.
94. Huang, Z.H., et al., *Enhancement of the Viscosity of Carbon Dioxide using Styrene/Fluoroacrylate Copolymers*. Macromolecules, 2000. **33**(15): p. 5437-5442.
95. Fan, X., et al., *Oxygenated Hydrocarbon Ionic Surfactants Exhibit CO₂ Solubility*. Journal of the American Chemical Society, 2005. **Web Released**(35).
96. Span, R. and W. Wagner, *A New Equation of State for Carbon Dioxide Covering the Fluid Region from the Triple-Point Temperature to 1100 K at Pressures up to 800 MPa*. Journal of Physical and Chemical Reference Data, 1996. **25**(6): p. 1509-1596.
97. Panagiotopoulos, A.Z. and R.C. Reid, *New Mixing Rule for Cubic Equations of State for Highly Polar, Asymmetric System*, in *Equations of State: Theories and Applications*, K.C. Chao and R.L. Robinson, Editors. 1986, ACS symposium series 300; American Chemical Society: Washington, D.C. p. 577.
98. Hutton, B.H., et al., *Investigation of AOT Reverse Microemulsions in Supercritical Carbon Dioxide*. Colloids and Surfaces, A: Physicochemical and Engineering Aspects, 1999. **146**(1-3): p. 227-241.

99. Lee, C.T., Jr., et al., *Formation of Water-in-Carbon Dioxide Microemulsions with a Cationic Surfactant: A Small-Angle Neutron Scattering Study*. Journal of Physical Chemistry B, 2000. **104**(47): p. 11094-11102.
100. Maury, E.E., et al., *Graft Copolymer Surfactants for Supercritical Carbon Dioxide Applications*. Polymer Preprints (American Chemical Society, Division of Polymer Chemistry), 1993. **34**(2): p. 664-5.
101. Zhu, D.M. and Z.A. Schelly, *Investigation of the Microenvironment in Triton X-100 Reverse Micelles in Cyclohexane, using Methyl Orange as a Probe*. Langmuir, 1992. **8**(1): p. 48-50.
102. McFann, G.J., *Ph.D. Dissertation Thesis*. 1993, The University of Texas at Austin.
103. Liu, J., et al., *Investigation of Nonionic Surfactant Dynol-604 Based Reverse Microemulsions Formed in Supercritical Carbon Dioxide*. Langmuir, 2001. **17**(26): p. 8040 - 8043.
104. Baczko, K., X. Chasseray, and C. Larpent, *Synthesis and Surfactant Properties of Symmetric and Unsymmetric Sulfosuccinic Diesters, Aerosol-OT Homologues*. Journal of the Chemical Society-Perkin Transactions 2, 2001(11): p. 2179-2188.
105. Zimmermann, J., A. Sunder, and R. Mulhaupt, *Preparation of Partially Hydrolyzed Oligo(vinylacetate) as Polyol for Polyurethane Formation*. Journal of Polymer Science Part a-Polymer Chemistry, 2002. **40**(12): p. 2085-2092.
106. Murphy, A. and G. Taggart, *Synthesis and Characterisation of a Novel Surfactant, Sodium Geranyl Sulphate*. Colloids and Surfaces a-Physicochemical and Engineering Aspects, 2001. **180**(3): p. 295-299.
107. Feller, D., *Application of Systematic Sequences of Wave-Functions to the Water Dimer*. Journal of Chemical Physics, 1992. **96**(8): p. 6104-6114.
108. Fan, X., et al., *Preparation of Silver Nanoparticles via Reduction of a Highly CO₂-Soluble Hydrocarbon-based Metal Precursor*. Industrial & Engineering Chemistry Research, 2005. **In print**.

109. Liu, J., et al., *Synthesis of Ag and AgI Quantum Dots in AOT-stabilized Water-in-CO₂ Microemulsions*. Chemistry--A European Journal, 2005. **11**(6): p. 1854-1860.
110. Ohde, H., et al., *Synthesizing Silver Halide Nanoparticles in Supercritical Carbon Dioxide Utilizing a Water-in-CO₂ Microemulsion*. Chemical Communications (Cambridge), 2000(23): p. 2353-2354.
111. McLeod, M.C., et al., *Synthesis and Stabilization of Metallic Nanoparticles and Pre-metallic Intermediates in PFPE/CO₂ Reverse Micelle Systems*. Phys. Chem. B, 2003. **107**(12): p. 2693.
112. Ji, M., et al., *Synthesizing and Dispersing Silver Nanoparticles in a Water-in-Supercritical Carbon Dioxide Microemulsion*. Journal of the American Chemical Society, 1999. **121**(11): p. 2631-2632.
113. Holmes, J.D., et al., *Synthesis of Cadmium Sulfide Q Particles in Water-in-CO₂ Microemulsions*. Langmuir, 1999. **15**(20): p. 6613-6615.
114. Dong, X., D. Potter, and C. Erkey, *Synthesis of CuS Nanoparticles in Water-in-Carbon Dioxide Microemulsions*. Industrial & Engineering Chemistry Research, 2002. **41**(18): p. 4489-4493.
115. Zhang, R., et al., *Organic Reactions and Nanoparticle Preparation in CO₂-induced Water/P104/p-Xylene Microemulsions*. Chemistry--A European Journal, 2003. **9**(10): p. 2167-2172.
116. Sarbu, T., T.J. Styraneč, and E.J. Beckman, *Non-Fluorous Polymers with Very High Solubility in Supercritical CO₂ Down to Low Pressures*. Nature, 2000. **405**: p. 165.
117. Dimitrov, S., et al., *Predicting the Biodegradation Products of Perfluorinated Chemicals using CATABOL. SAR and QSAR in Environmental Research*, 2004. **15**(1): p. 69-82.
118. Hoefling, T.A., et al., *Design and Synthesis of Highly CO₂-Soluble Surfactants and Chelating Agents*. Fluid Phase Equilibria, 1993. **83**: p. 203.

119. Sarbu, T., T.J. Styraneć, and E.J. Beckman, *Design and Synthesis of Low Cost, Sustainable CO₂-philes*. Ind. Eng. Chem. Res., 2000. **39**(12): p. 4678.
120. Potluri, V.K., et al., *Peracetylated Sugar Derivatives Show High Solubility in Liquid and Supercritical Carbon Dioxide*. Org. Lett., 2002. **4**(14): p. 2333.
121. Rindfleisch, F., T. DiNoia, and M.J. McHugh, *Solubility of Polymers and Copolymers in Supercritical CO₂*. J. Phys. Chem., 1996. **100**: p. 15581.
122. Shen, Z., et al., *CO₂-Solubility of Oligomers and Polymers that Contain the Carbonyl Group*. Polymer, 2003. **44**(5): p. 1491-1498.
123. Lora, M., F. Rindfleisch, and M.A. McHugh, *Influence of the Alkyl Tail on the Solubility of Poly(Alkyl Acrylates) in Ethylene and CO₂ at High Pressures: Experiments and Modeling*. Journal of Applied Polymer Science, 1999. **73**(10): p. 1979-1991.
124. Johnston, K.P., et al., *Water in Carbon Dioxide Macroemulsions and Miniemulsions with a Hydrocarbon Surfactant*. Langmuir, 2001. **17**(23): p. 7191-7193.
125. Raveendran, P. and S.L. Wallen, *Dissolving Carbohydrates in CO₂: Renewable Materials as CO₂-philes*. ACS Symposium Series, 2003. **860**(Supercritical Carbon Dioxide): p. 270-284.
126. Eastoe, J., et al., *Micellization of Economically Viable Surfactants in CO₂*. Journal of Colloid and Interface Science, 2003. **258**(2): p. 367-373.
127. da Rocha, S.R.P., et al., *Surfactants for Stabilization of Water and CO₂ Emulsions: Trisiloxanes*. Langmuir, 2003. **19**(8): p. 3114-3120.
128. Liu, J., et al., *Investigation of Nonionic Surfactant Dynol-604 Based Reverse Microemulsions Formed in Supercritical Carbon Dioxide*. Langmuir, 2001. **17**(26): p. 8040-8043.
129. Dickson, J.L., B.P. Binks, and K.P. Johnston, *Stabilization of Carbon Dioxide-in-Water Emulsions with Silica Nanoparticles*. Langmuir, 2004. **20**(19): p. 7976-7983.

130. Dickson, J.L., et al., *Interfacial Properties of Fluorocarbon and Hydrocarbon Phosphate Surfactants at the Water-CO₂ Interface*. Industrial & Engineering Chemistry Research, 2005. **44**(5): p. 1370-1380.
131. Fan, X., et al., *Oxygenated Hydrocarbon Ionic Surfactants Exhibit CO₂ Solubility*. Journal of the American Chemical Society, 2005. **127**(33): p. 11754-11762.
132. Saunders, A.E., et al., *Solvent Density-Dependent Steric Stabilization of Perfluoropolyether-Coated Nanocrystals in Supercritical Carbon Dioxide*. Journal of Physical Chemistry B, 2004. **108**(41): p. 15969-15975.
133. Shah, P.S., et al., *Steric Stabilization of Nanocrystals in Supercritical CO₂ Using Fluorinated Ligands*. Journal of the American Chemical Society, 2000. **122**(17): p. 4245-4246.
134. Bell, P.W., et al., *Stable Dispersions of Silver Nanoparticles in Carbon Dioxide with Fluorine-Free Ligands*. Langmuir, 2005. **21**(25): p. 11608-11613.
135. Liu, Y., R.B. Grigg, and R.K. Svec, *CO₂ Foam Behavior: Influence of Temperature, Pressure, and Concentration of Surfactant*. SPE 94307, 2005. **SPE Production and Operations Symposium, Oklahoma, OK, 17-19 April, 2005**.
136. Liu, Y., R.B. Grigg, and B. Bai, *Salinity, PH, and Surfactant Concentration Effects on CO₂-Foam*. SPE 93095, 2005. **SPE International Symposium on Oilfield Chemistry, Houston, TX, 2-4 February, 2005**.
137. Yaghoobi, H. and J.P. Heller, *Laboratory Investigation on Parameters Affecting CO₂-Foam Mobility in Sandstone at Reservoir Conditions*. SPE 29168, 1994. **Eastern Regional Conference & Exhibition, Charleston, WV, 8-10 November, 1994**: p. 107-121.
138. Bernard, G.G., L.W. Holm, and C.P. Harvery, *Use of Surfactant to Reduce CO₂ Mobility in Oil Displacement*. SPE Journal, 1980. **20**(4): p. 281-292.
139. Casteel, J.F. and N.F. Djabbarah, *Sweep Improvement in CO₂ Flooding by Use of Foaming Agents*. SPE Reservoir Engineering, 1988. **3**: p. 1186-1192.
140. Holt, T., F. Vassenden, and I. Svorstol, *Effects of Pressure on Foam Stability; Implications for Foam Screening*. SPE 35398, 1996. **SPE/DOE Tenth**

- Symposium on Improved Oil Recovery, Tulsa, OK:** p. 21-24 April, 1996, 543-552.
141. Kuhlman, M.I., H.C. Lau, and A.H. Falls, *Surfactant Criteria for Successful Carbon Dioxide Foam in Sandstone Reservoirs*. SPE Reservoir Evaluation and Engineering, 2000. **3**(1): p. 35-41.
 142. Borchardt, J.K., et al., *Surfactants for CO₂ Foam Flooding*. SPE 14394, 1985. **Annual Technical Conference and Exhibition, 22-26 September, Las Vegas, Nevada.**
 143. Hoefner, M.L. and E.M. Evans, *CO₂ Foam: Results from Four Developmental Field Trials*. SPE Reservoir Engineering, 1995. **10**(4): p. 273-281.

Conclusions and Research Significance

Ionic surfactants with CO₂-philic tails composed of sugar acetate, poly(propylene glycol), or oligo(vinyl acetate) were found to be CO₂ soluble. *This constitutes the first report of highly CO₂-soluble, non-fluorous, ionic surfactants with tails composed solely of carbon, hydrogen and oxygen.* Oligo(vinyl acetate)-functionalized surfactants were particularly promising, with the single tailed surfactants exhibiting CO₂ solubility levels of 2-7 wt%, while the twin tailed surfactant was 3 wt% soluble in CO₂. As water was introduced to these systems, the solubility of all of the (vinyl acetate)-functionalized ionic surfactants decreased to levels of 0.5-1.5%. Although the single tailed surfactants could only attain a single phase at W values less than 10, water loading values of 50 were attained with the twin tailed sodium bis(vinyl acetate)8 sulfosuccinate AOT analog at surfactant concentrations as high as 1 wt%. Further, spectroscopic analysis indicated that only the single tailed oligo(vinyl acetate) ionic surfactants and the AOT analog with twin oligo(vinyl acetate) tails established a polar microenvironment within CO₂ comparable in polarity to methanol. *Ab initio* modeling was performed to address the question of why the oligo(vinyl acetate) tails form polar microenvironments while the peracetyl (sugar acetate) tails, which are similar, do not. The calculations indicate that the acetate group is very hydrophilic, preferring to bind with H₂O over CO₂. We therefore speculate that the peracetyl-tails do not have a sufficiently high hydrophobic driving force to form reverse micelles. In contrast, the oligo(vinyl acetate) tails have both hydrophilic and hydrophobic (methylene backbone) sections, which provide the correct balance of forces necessary to drive water out of the bulk phase into reverse micelles.

These results may enable CO₂ mobility reduction to be achieved via the injection of a CO₂-based surfactant solution that generates mobility-reducing foams *in situ* as it mixes with brine already present in the reservoir. Prior lab and pilot-scale CO₂ foam floods were always generated via the injection of an aqueous surfactant solution prior to the CO₂ slug. This work opens the door for the possible injection of a CO₂ surfactant solution instead, greatly reducing or possibly eliminating the need for alternating aqueous slugs of surfactant solution. Although single phase solutions of the surfactants in CO₂ were achieved at concentrations as high as several weight percent, the pressure required for attaining a single phase was maintaining these small ionic surfactants in solution at 0.1 - 1.0 wt% was high relative to typical MMP values at the same temperature. Therefore these surfactants' structures must be further modified in an attempt to achieve even greater miscibility with CO₂. Although the synthesis of CO₂-soluble surfactants is a promising step toward the development of a new means of diminishing CO₂ mobility during EOR, further testing is required. The ability of these surfactants to generate a stable foam at the MMP must be assessed, and the capacity of that foam to reduce mobility in porous media evaluated. Nonetheless, these results have provided us with another possible avenue for the mobility reduction of CO₂ in EOR projects.

Plans for the Next Reporting Period

We will present our results for CO₂-soluble polymers, hydrogen bonding compounds, and dendrimers. Specifically, results will be presented for poly(acetoxy oxetane), poly(methoxy methyl ether), poly(ethoxy methyl ether), poly(lactic acid), and oligomers of cellulose triacetate. Experiments at pressures up to 10000 psi will be conducted at the University of Pittsburgh. If pressures of 10000-20000 psi are required, Dr. Thies of Clemson University has generously offered us the use of his equipment. (Obviously data in this range are well above the MMP for CO₂ floods, yet this data can still help us to determine which polymers are “better” than others if both are not soluble at 10000 psi and at least one dissolves in the 10000 – 20000 psi range.)

Milestones, Decision Points

Our original proposal lists the following decision points and milestones. A review of our progress is provided after each goal.

Decision point for CO₂-CO₂ philic monomer molecular modeling: If the CO₂-novel monomer interactions are weaker than those exhibited by CO₂-vinyl acetate monomer, the monomer will not be considered a viable monomer for polymerization or inclusion in the hydrogen bonding compounds.

To date, we have identified several monomers that exhibit stronger interactions with CO₂ – based on ab initio calculations – than vinyl acetate. These include acetoxy oxetane, methoxy methyl ether, methoxy ethyl ether.

Decision point for CO₂ philic polymers: If a polymer less CO₂ soluble than PVAc, it will no longer be considered as a successful advance or a viable candidate.

To date, we have synthesized the monomers and polymers, and have begun testing the solubility of these polymers in CO₂. We anticipate reporting on these during the next period (see Plans for Next Reporting Period above).

Decision point for CO₂ thickeners: If the co-polymeric thickener or small hydrogen bonding compound cannot increase the viscosity of CO₂ at pressures by a factor of 2-3 at concentrations below 0.5wt%, it will not be considered a success

To date, we have not performed solubility tests, therefore we have not completed the subsequent viscosity tests. We are currently measuring the mobility of foams flowing through sandstone; the foams being generated in-situ by surfactants dissolved in CO₂ mixing with brine.

Milestone 1: The identification of oxygenated hydrocarbon monomers that interact more favorably with CO₂ (according to molecular modeling) than vinyl acetate

We have successfully attained this target and have begun the synthesis of novel polymers based on these modeling results.

Milestone 2: The synthesis of novel oxygenated hydrocarbon polymers that are more CO₂ soluble than poly(vinyl acetate).

We will report on this during the next reporting period, but can inform you that preliminary results indicate that the current candidates appear to be comparably soluble or less soluble in CO₂ than PVAc.

Milestone 3: The synthesis of novel oxygenated hydrocarbons that can dissolve in CO₂ at pressures at or below the MMP

We are not yet at this milestone (milestone 2 must be successfully achieved prior to approaching this milestone)

Milestone 4: The synthesis of novel oxygenated hydrocarbon thickeners (copolymers or small H-bonding compounds) that can dramatically increase the viscosity of CO₂ by a factor of 2-20 at a concentration of 0.1-0.25wt% at pressures at or below the MMP

Yale University has begun the synthesis of four small, hydrogen bonding compounds with oligo(vinyl acetate) arms, and their CO₂ solubility will be reported during the next reporting period. No copolymeric thickeners have been synthesized yet, nor can they be until milestones 2 and 3 are successfully reached. This progress report details the results of a possible new type of CO₂ thickener; CO₂ soluble ionic surfactants that may be capable of generating CO₂ foams in-situ.

Significant Accomplishments

In our last report, we detailed the design and synthesis of the first non-fluorous, highly CO₂-soluble ionic surfactants. *This report documents the first observations of CO₂ foams stability in a high pressure view cell obtained via the mixing of CO₂, water and a CO₂-soluble surfactant.* Specific tails include oligo(vinyl acetate), sugar acetates, and oligo(propylene oxide). The surfactants with vinyl acetate tails were particularly promising.

Technology Transfer

These results were just published in the country's most prestigious chemistry journal, JACS. The reference is provided below.

Oxygenated Hydrocarbon Ionic Surfactants Exhibit CO₂ Solubility, Fan, X.; Potluri, V. K.; McLeod, M. C.; Wang, Y.; Liu, J.; Enick, R. M.; Hamilton, A. D.; Roberts, C. B.; Johnson, J. K.; Beckman, E. J.; *Journal of the American Chemical Society*; (Article); 2005; 127(33); 11754-11762